One-electron and many-body effects in x-ray absorption and emission edges of Li, Na, Mg, and Al metals

P. H. Citrin, G. K. Wertheim, and M. Schlüter
Bell Laboratories, Murray Hill, New Jersey 07974
(Received 18 April 1979)

A formalism is developed for the analysis of x-ray absorption and emission edges of simple metals in terms of one-electron and many-body effects. These include the transition density of states, the core-hole lifetime, the Franck-Condon lattice excitations, the Fermi function, the Mahan–Nozières–De Dominicis (MND) many-body response of the conduction electrons, the Onodera spin-orbit exchange, and the instrumental response function. Our formalism is applied to the available edge data from the metals Li, Na, Mg, and Al. The basic findings are that the Li K edge is rounded by phonon excitations, the $L_{2,3}$ edges of Na, Mg, and Al are peaked primarily by the many-body effects, and the K edges are rounded solely by the $1s$ hole lifetime. Transition-density-of-states structure makes a significant contribution only in the $L_{2,3}$ emission edges of Mg and Al, spin-orbit exchange only in the $L_{2,3}$ absorption edge of Na. Present theories do not account quantitatively for the minimal effect of many-body screening on the Li K absorption edge because of direct exchange scattering. For Al it is shown that a unique set of Friedel phase shifts accounts in detail for the x-ray photoemission (XPS) singularity index as well as for the many-body effects in the K and $L_{2,3}$ emission and absorption edges. For Mg, the XPS and $L_{2,3}$ edge data predict a small positive K-edge exponent, while for Na a small negative one is predicted. Detailed comparisons with all known earlier experimental and theoretical work are made. The essential conclusion from this study is that irrespective of other factors, many-body effects make significant contributions to all the x-ray edges of the simple metals and that such effects are extremely well described by the MND theory.

I. INTRODUCTION

Considerable controversy exists over the interpretation of the x-ray absorption and emission edges in the simple metals Li, Na, Mg, and Al. In its most basic form, the debate centers on two questions. The first is qualitative in nature and asks what factor or factors are responsible for the unusually peaked or rounded shapes of the observed x-ray edges. Is it predominantly a many-body phenomenon, or are other factors, such as the transition-density-of-states structure, lifetime broadening, or phonons equally or more important? The second question is more quantitative and deals with the ability of the current many-body theory to explain in detail the nature of the many-body response. Is the present theory correct, too simplistic, quantitatively predictive, or just too restrictive to be experimentally tested? The purpose of this work is to clarify and resolve both questions, which together define the so-called "x-ray edge problem." We begin with a brief review of how this problem has evolved.

Prior to 1967 virtually all x-ray absorption and emission data were interpreted solely in terms of one-electron theories.[1-4] Their failure to explain the anomalous $L_{2,3}$ x-ray edge "spikes" observed in the data of some simple metals posed a conspicuous problem. The foundation for a new approach in understanding x-ray threshold phenomena was provided by Mahan,[5] whose theory predicted an enhanced absorption or emission over and above that of the one-electron theory near an edge. A physical understanding of the phenomenon underlying his theory is not difficult. In absorption, a core hole attracts a localized screening cloud of conduction electrons which come from filled states near E_F and get excited into unoccupied states above E_F. This locally enhances the number of empty states at E_F into which core electrons of proper symmetry can be optically excited, and thus increases the density of excitations above threshold. This is similar to the production of excitons in semiconductors, but in metals there is no true bound state and the number of excitations at threshold has the form of an integrable infinity, much like an infrared divergence.[6] The symmetry of the screening electrons is generally s-like, so that dipole selection rules predict that transitions to unoccupied s-like states from p-like core levels should be enhanced, while transitions from s-like core levels will not. Similar arguments apply to x-ray emission at threshold, only now it is the probability of filling a core hole from screening electrons already piled up (relaxed) at E_F that is or is not enhanced.

Anderson[7] pointed out an additional effect that must be considered when a screening cloud forms in a metal. Since the core hole slightly distorts the wave function of each electron in the conduc-

tion band, the transition matrix element in absorption must contain not only the overlap of the initial and final state of the core electron that is excited into the empty conduction band, but also the overlap of initial and final states of all the other wave functions as well. Consequently, the transition strength is severely reduced because the overlap of each of the many electron states is slightly less than unity and the product of very many of them quickly approaches zero. This "orthogonality catastrophe" between initial and final states is clearly insensitive to the symmetry of the core hole and therefore always suppresses transitions to states near threshold.

An exact solution (for a free-electron gas) containing the competing Mahan enhancement and the Anderson suppression effects at threshold was given in 1969 by Nozières and De Dominicis.[8] They showed that near threshold, $\hbar\omega_0$, the shape of the spectrum, $I(\omega)$, has the frequency dependence

$$I(\omega) \propto \sum_{l=0}^{\infty} |A_l(\omega)|^2 \left(\frac{\xi}{\hbar(\omega-\omega_0)}\right)^{\alpha_l}, \tag{1.1}$$

where ξ is a cutoff energy of the order of the width of the filled conduction band[9] and $|A_l(\omega)|^2$ is the usual one-electron dipole transition probability to the states of l symmetry. The many-body effects are contained in the threshold exponents α_l, given by

$$\alpha_l = 2\delta_l/\pi - \alpha, \tag{1.2}$$

$$\alpha = \sum_l 2(2l+1)\left(\frac{\delta_l}{\pi}\right)^2, \tag{1.3}$$

where the scattering of the conduction electrons by the core hole is expressed in terms of the Friedel phase shifts, δ_l. The first term in Eq. (1.2) corresponds to Mahan's enhancement, while the second, defined in Eq. (1.3) and referred to as the singularity index, represents Anderson's suppression. Equations (1.1) and (1.2) show that edges at threshold can be either peaked or rounded depending on whether α_l is positive or negative, respectively. The sign of α_l depends on the relative magnitudes of the scattering phase shifts, which are constrained[10] by the Friedel sum rule,[11]

$$Z = \sum_l 2(2l+1)\frac{\delta_l}{\pi}, \tag{1.4}$$

where Z is the charge to be screened. For x-ray absorption, emission, and photoemission $Z=1$.

The main result of the Mahan, Nozières, and De Dominicis (MND) theory for x-ray edges, Eq. (1.2), has since been rederived in a number of ways, ranging from heuristic to diagrammatic.[6,9,12-16] The success of the theory in quantitatively accounting for complicated phenomena initially led to a great deal of enthusiasm. Simple arguments led to correct predictions. For example, in a hypothetical free-electron metal with only s-wave scattering, Eqs. (1.2), (1.3), and (1.4) predict that for excitation from p core levels $\alpha_0 = \frac{1}{2}$, while from s core levels $\alpha_1 = -\frac{1}{2}$. Thus $L_{2,3}$ edges should be peaked and K edges rounded, in agreement with the observed shapes of such edges in simple metals like Li, Na, and Al. Even phase shifts calculated from simple screening models predicted the same results.[17-19]

It was understandably disappointing, then, when more detailed studies by Dow and co-workers of newer and more precise edge data seemed to show that the phase shifts obtained from analysis of one edge in a given material were inconsistent with the phase shifts obtained from analysis of another edge in the same material.[20-23] Such inconsistencies raised serious doubts about the ability of the MND theory to quantitatively or, it was argued,[20-26] even qualitatively explain the x-ray edge data. Furthermore, it was pointed out by a number of workers that more conventional effects associated with edge spectra such as phonons,[27,28] hole-state lifetimes,[25,29-31] and one-electron transition-density-of-states (TDOS) structure[32-34] may be partly or wholly responsible for the structure in the data and that many-body effects may not even be at all significant. Up to this point it is fair to state that, based on the available edge analyses, there existed little if any definitive experimental evidence to support the validity of (and possibly even the need for invoking) the MND theory.

Fortunately, the theories of MND and Anderson resulted in the suggestion of two alternate experimental testing grounds. In 1971 Doniach, Platzman, and Yue[35] proposed that absorption edges be investigated by energy loss of high-energy electrons transmitted through thin films as a function of scattering angle. This removes the restriction to dipole-allowed transitions implicit in the use of photons. The usefulness of this technique will be discussed more fully in Sec. V D. The second experimental test, suggested by Doniach and Šunjić in 1970,[36] involves the study of the shape of x-ray emission and x-ray photoemission *line* spectra. Both these latter experiments involve a deep core hole, but now the final state does not contain an additional electron (or hole) in the conduction band as it does in *edge* measurements. As a result, the Mahan term in Eq. (1.2) does not contribute and only the Anderson term, α in Eq. (1.3), applies. It has been shown in a previous paper,[37] hereafter referred to as I, that it is possible to deduce α directly from the x-ray photo-

emission spectroscopy (XPS) line shape. For x-ray emission *lines* the situation is more complicated since both the initial and final states contain holes and only the difference in the screening charges between the two states contributes to the singularity. The analysis of x-ray lines has therefore not been particularly useful and will not be discussed further.

Given the fact that α can be obtained from an XPS measurement, it is then possible under certain conditions to determine the scattering phase shifts and thus *predict* the shapes of the absorption and emission edges.[38,39] This should be particularly true for the simple *sp* metals Na, Mg, and Al for which the free-electron approximation, and thus the applicability of the many-body theories, is most appropriate. Assuming that *s* and *p* phase shifts dominate the screening process in these metals, i.e., $\delta_l = 0$ for $l \geq 2$, a measurement of α along with Eq. (1.4) determines δ_0 and δ_1 uniquely. Once the phase shifts are known, Eq. (1.2) determines the edge exponents α_0 and α_1.

It is clear, then, that in order to test the MND theory, reliable experimental threshold exponents of x-ray edge data must be available for comparison with those values predicted from XPS line-shape measurements. Previous determination of α_l's by Dow and co-workers[20-23] have already been stated to be incompatible with both the MND theory and the Friedel sum rule, so it would seem pointless to test for compatibility between the XPS predictions of α_l's and those actually found in x-ray edge data. Ironically, in spite of numerous publications which pointed out the importance of the well-known effects of phonons,[27,28] lifetime,[25,29-31] and one-electron TDOS structure[32-34] in the interpretation of edges, such effects in not only those but in subsequent edge analyses[27,31,32,40-43] have so far been either treated incorrectly or completely ignored. In addition, Onodera[44] has recently shown that in the analysis of $L_{2,3}$ absorption edges, spin-orbit mixing must be taken into account. This effect has also either been excluded or inappropriately corrected for in even the most recent edge analyses.[45,46] In the light of these facts it would seem presumptuous to claim that inconsistencies with MND threshold exponents determined from existing edge analyses represent inadequacies of the MND theory.

In this work we have taken the following steps toward a complete analysis of one- and many-electron effects in x-ray absorption and emission edge spectra of simple metals.[39,47-49] First, one-electron TDOS calculations have been performed for both the $L_{2,3}$ and K edges of Na, Mg, and Al using a combined pseudopotential–orthogonalized-plane-wave (OPW) formalism. This step proved necessary because a complete and consistent set of calculations for these edges was not available. The methodology and results of our calculations, along with comparisons with previously published results where available, are presented in Sec. III. To this one-electron structure we have systematically added the broadening or structure due to the other known effects: the finite temperature of the metal, the lifetime of the core hole, the hole-phonon coupling, the spin-orbit exchange, and the many-body edge peaking or rounding as described by the MND theory. A general description of how these effects manifest themselves in x-ray absorption and emission edge measurements is given in Sec. II, and a description of the procedure used to incorporate them in our analysis is given in Sec. IV. The results of our edge analyses are then discussed in Sec. V, with particular emphasis on (a) self-consistency between the absorption and emission results, (b) compatibility of both of these results with the Friedel sum rule, (c) comparison with theoretical calculations, and (d) comparison with results predicted on the basis of the XPS measurements reported in I.[37] Comparisons with electron energy loss results are also discussed. Conclusions and implications of the present study are summarized in Sec. VI.

Because of the scope of this work we have kept the individual sections as self-contained as possible. Cross references are given.

II. FACTORS INFLUENCING X-RAY ABSORPTION-EDGE SHAPES: GENERAL CONSIDERATIONS

To the reader unfamiliar with the debate over the validity of the MND theory, it may not be obvious why the contributions from other factors affecting x-ray absorption and emission edges need be so carefully considered. The primary reason is that the results of the MND theory, Eqs. (1.1)–(1.3), are asymptotic solutions whose validity is assumed only very close to threshold. The extension of the MND theory to energies removed from threshold is a subject currently under debate[42,50-54] and will be briefly discussed in Secs. IV and V. The point to be emphasized here is that the range of energy over which the MND theory is expected to be valid is also the region in which other sources of broadening or structure will have their most significant effect.

There are five physical phenomena to be considered, including the many-body peaking or rounding. Earlier analyses have assumed that only one or two of these phenomena play a de-

cisive role in influencing the shape of an edge. However, one does not know *a priori* which one might dominate and which can be ignored. Therefore, for a meaningful assessment it is imperative that *all* effects are included in the analysis of the data.

We now describe the way in which each of these effects manifests itself in a measured x-ray edge spectrum. Recent results and current philosophies are stressed. We will assume here that each effect acts independently of all the others. Deviations from this simplifying assumption will be pointed out.

A. Transition density of states

The probability for transitions from core level to metal valence states can be described by the usual golden rule and dipole approximation,

$$M^2 = |\langle \Psi_{\text{core}} | \vec{A} \cdot \vec{p} | \Psi_{\text{val}} \rangle|^2 . \tag{2.1}$$

The first question to ask at this point is: what Hamiltonian produces the eigenstates Ψ_{core} and Ψ_{val} ? Is it the "initial"-state Hamiltonian with the crystal in its ground state and no core hole, or is it the "final"-state Hamiltonian with the crystal in its excited state and a core hole? In the initial-state picture we have, for emission,

$$M^2 = |\langle \hat{\Psi}_{\text{core}} | \vec{A} \cdot \vec{p} | \hat{\Psi}_{\text{val}} \rangle|^2 \tag{2.1a}$$

and for absorption,

$$M^2 = |\langle \Psi_{\text{core}} | \vec{A} \cdot \vec{p} | \Psi_{\text{val}} \rangle|^2 , \tag{2.1a'}$$

where $\hat{\Psi}$ denotes an eigenstate in the presence of a core hole. In the final-state picture we have, for emission,

$$M^2 = |\langle \hat{\Psi}_{\text{core}} | \vec{A} \cdot \vec{p} | \Psi_{\text{val}} \rangle|^2 \tag{2.1b}$$

and for absorption,

$$M^2 = |\langle \Psi_{\text{core}} | \vec{A} \cdot \vec{p} | \hat{\Psi}_{\text{val}} \rangle|^2 . \tag{2.1b'}$$

If the initial-state is regarded as energy zero and if experiments are believed to measure final-state energies (i.e., neglecting the dynamics of the excitation process), the correct Hamiltonian to use should be the final-state Hamiltonian.[55-57] This means that in emission Ψ_{val} could be calculated in the absence of a core hole, as is the usual procedure for band-structure calculations. The only assumption that need be invoked in obtaining M^2, then, is that $\hat{\Psi}_{\text{core}} \approx \Psi_{\text{core}}$, which is certainly expected to be valid since Ψ_{core} is essentially structureless. For absorption, on the other hand, the final-state picture means that $\hat{\Psi}_{\text{val}}$ would have to be calculated in the presence of a core hole, with the valence electrons being *simultaneously* scattered off the core hole and the periodic crystal potential. Such band-structure calculations with a localized hole are, like deep level impurity calculations, rather difficult. Only recently has a first "supercell" calculation been attempted by von Barth and Grossman for Na metal.[56] Bryant and Mahan[57] have also recently examined the difference in the transition density of states calculated in the initial- and final-state pictures for Na, Mg, and Al metals but without considering the effect of band structure, i.e., using a jellium model.

It is important to note that even though the final-state calculations are more appropriate for describing the absorption or emission processes, they still require the addition of the many-body effects at threshold (Eq. 1.1). It is these latter effects that are the dominant source of structure *at the edge*. We have, therefore, chosen to use the initial-state picture for absorption, Eqs. (2.1a) and (2.1a'), and the final-state picture for emission, Eqs. (2.1b) and (2.1b'). The various band-structure effects, i.e., scattering off the crystal potential, and *all* the many-body corrections, i.e., scattering off the core hole *and* its exponential behavior at E_F, are thus treated here as *separate* processes which are then combined by convolution to produce the final-state result. In this approximation Ψ_{core} and Ψ_{val} are solutions of the initial-state Hamiltonian and are accessible by standard band-structure calculations. For emission this approximation is, as we have said, quite valid. For absorption the advantages of this approach more than offset the errors it must introduce because, ultimately, we are interested only in the narrow energy region very near the edge. This is also the approximation that has been used in all previous comparisons of absorption experiments with theory so that our results provide a measure for comparison with earlier work.

With Ψ_{core} and Ψ_{val} determined from the initial-state Hamiltonian, the structure in the transition-matrix element that is mirrored in an x-ray spectrum is determined by two factors. First, dipole selection rules dictate the symmetry of the empty conduction-band states into which a core electron of given symmetry can be optically excited. Accordingly, K edges reflect the p-like bands while $L_{2,3}$ edges reflect the bands of s- and d-like symmetry. The second is introduced by the periodic potential of the crystal, i.e., the band-structure.

The most important point to make here concerns the relative magnitudes of these two effects over the entire energy range of the absorption or emission spectrum. The *overall* shape of the spectrum is clearly influenced by selec-

tion rule and band-structure effects, but so far as the structure in the *edge* region is concerned, the importance of these two effects can hardly be assessed by casual inspection. It is for this reason that a calculation of the TDOS must be particularly accurate near the Fermi level. The criteria used to insure that this goal be realized are that the valence band structure and valence wave functions are reliable and that the calculation itself be precise, i.e., contain highly resolved k-space integration.

The details of the TDOS calculations performed in this work are given in Sec. III. It will be shown that they fulfill these criteria for reliability near the Fermi edge. In Sec. III we also show that some previous TDOS calculations failed to meet such criteria and resulted in erroneous conclusions regarding the importance of TDOS structure.

B. Core-hole lifetimes

The lifetime of a core hole introduces an indeterminancy which is represented in energy space by a Lorentzian line shape. The energy of the core-hole state created (destroyed) in the absorption (emission) process would otherwise be sharply defined. Consequently, the edge spectrum is Lorentzian broadened. We emphasize this obvious fact here to establish that the correct analysis of an experimental edge spectrum must take this type of broadening into account. It cannot be ignored or approximated by a Gaussian broadening as has been done in several previous analyses.

The magnitude of core-hole lifetimes can be evaluated by either theoretical or empirical procedures. The theoretical approach involves standard techniques that have been reviewed elsewhere[58] and discussed in particular for the metals Li, Na, Mg, and Al.[37] One direct, empirical approach involves the measurement of the Lorentzian contribution to XPS line shapes. Another is to measure the Lorentzian contribution in the x-ray absorption edges. Comparison between these two approaches is given in Sec. V A.

C. Phonons and other temperature-related effects

The principal temperature-related effects appearing in x-ray spectra are those dealing with the production of phonons and the thermal excitation of electrons at the Fermi level. As with lifetime broadening, these well-known effects have also been neglected or incorrectly considered in earlier analyses.

The effects of TDOS structure and lifetime broadening in an x-ray edge spectrum are, to a good approximation, temperature independent. TDOS may be indirectly affected by temperature modification of the band structure due to anharmonic lattice distortions. These and other[59,60] processes could also indirectly distort the lifetime of those core-hole states that involve the valence wave functions.

The occupation of states at the Fermi level is given by the usual Fermi-Dirac expression, $(e^{(E-E_F)/kT}+1)^{-1}$. The transition at E_F is sharp at low T, but, as we shall see in Sec. IV, at $T=300$ K it is generally comparable to the $L_{2,3}$ hole lifetimes of Na, Mg, and Al metals and cannot be ignored. Its contribution is particularly significant in Li K-edge spectra at elevated temperatures and must be specifically considered to determine accurate hole-state lifetime and hole-phonon broadening values.

The sudden appearance of a core hole in a metal produces phonons due to the electronic contraction of the hole-state atom. The statistical distribution of phonons at $T=0$ K is strictly Poisson.[61,62] In the classical limit, which is usually applicable, the phonon envelope approaches a Gaussian.[61-64] At finite temperatures the zero-point phonon spectrum is multiplied by a Bose-Einstein factor for a thermal ensemble in a Debye solid. The additional production of phonons by the recoil of the hole-state atom,[65] important in photoemission where an electron is ejected at high kinetic energies, is unimportant in x-ray absorption or emission because the momentum transfer is small. The magnitude of the electron-phonon broadening in the simple metals is generally nonnegligible, and in the case of Li is, in fact, unusually large.[37] Its value in the various metals can be calculated by a number of approaches and these will be mentioned and compared with experiment in Sec. V A.

Phonon broadening can be empirically determined from either XPS line shapes or x-ray absorption edges, although the feasibility of doing this has been a subject of recent debate. It has been argued[66] that if the lifetime of the core hole is sufficiently short, then it is no longer possible to think of hole annihilation (lifetime broadening) and hole-phonon coupling (phonon broadening) as separate processes. The concern over phonon-lifetime interference has, however, been recently shown by several authors to be important *only* in x-ray and Auger electron emission, *and only* when the hole-state lifetime and the effective phonon period are comparable.[67-70] Under such conditions, i.e., when the hole disappears before the lattice has adjusted to it completely, there is an additional broadening of either the emission edge or Auger line.

Mahan[69] and Almbladh[70] have independently formulated theories for calculating the extent of this "incomplete phonon relaxation" for emission edges, while the phenomenon in Auger electron emission has very recently been considered.[71] In x-ray absorption and photoemission incomplete phonon relaxation is unimportant, a fact which allows core-hole lifetimes to be determined from those techniques by simply measuring the Lorentzian contribution in the (Gaussian) phonon-broadened edge or line. Still another reason for using these techniques (as opposed to x-ray emission edges) for determining phonon and lifetime broadening is that self-absorption effects in emission can distort the leading part of the edge. This point is discussed further in Sec. II F below. For a discussion of incomplete phonon relaxation and why XPS and x-ray absorption spectroscopies contain simple convolutions of lifetime and phonon broadenings the reader is referred to I (Ref. 37) and references therein.

D. MND threshold exponents

The principal results of a peaked or rounded edge described by the MND theory have already been summarized in Sec. I along with the physical explanations underlying their formulation. More detailed considerations regarding the theory's region of applicability in the data, the range of its acceptable (compatible) phase shifts in the simple metals, and its simplifying assumptions, limitations, and implications are discussed in subsequent sections.

E. Spin-dependent exchange effects

The MND theory treats the direct Coulomb interaction between the core hole and the conduction electrons, but neglects any modification in the Coulomb interaction by exchange. The effects of exchange in absorption spectra had been considered some years ago,[72,73] but only recently have their magnitudes been shown to be appreciable in some cases. We briefly review here the essential features of how exchange modifies the MND theory and the observed x-ray spectra.

For the electron-hole system in the *LS* coupling limit, i.e., the case of vanishing spin-orbit coupling as for core holes of *s symmetry*, the diagonal part of exchange can be treated in a straightforward way. Girvin and Hopfield[74] (GH) showed that exchange makes the scattering phase shifts spin dependent, modifying them by an amount μ_l according to

$$\delta_l^+ = \delta_l + \mu_l, \quad \delta_l^- = \delta_l - \mu_l, \tag{2.2}$$

where (+) or (−) denotes the orientation of the conduction electron spin. Since treatment of the off-diagonal part of the exchange is considerably less straightforward, GH assumed that, to lowest order, the total (diagonal plus off-diagonal) exchange correction to the singularity index, α, was simply three times the diagonal correction alone, i.e.,

$$\alpha^{\mathrm{GH}} = \alpha + \mu^{\mathrm{GH}}, \tag{2.3}$$

where

$$\mu^{\mathrm{GH}} = 3\mu, \tag{2.4}$$

and

$$\mu = 2\sum_l (2l+1)(\mu_l/\pi)^2. \tag{2.5}$$

This allowed GH to express the spin-dependent threshold exponent in the same inverse power form as the MND theory, Eq. (1.1), simply as (assuming a spin-down core hole)

$$\alpha_l^{\mathrm{GH}} = 2\delta_l^+/\pi - \alpha^{\mathrm{GH}}. \tag{2.6}$$

The validity of GH's approach, particularly Eq. (2.4), has recently been questioned by several workers.[75,76] Kaga showed,[75] as had Kato *et al.*[73] previously, that in the presence of exchange and using the most divergent term approximation, the MND inverse power form is multiplied by an additional logarithmic factor $(1 - 4|\mu/\pi|\ln|\hbar\omega/\xi|)^{-3/2}$. Kaga also found a different threshold exponent than that of GH in Eq. (2.3), but one that still differed from Eq. (1.2). Yoshimori and Okiji[76] disagree with this latter result, maintaining that only the logarithmic factor should multiply Eq. (1.1), i.e., the threshold exponent is unaffected by exchange and thus its effect is not so dramatic as GH (and Kaga) would suggest. It is not clear at this point to what degree it is appropriate to treat the potential scattering to all orders but the exchange scattering only to logarithmic orders as Yoshimori and Okiji have done, nor is it obvious just how either to calculate or to assess empirically the effects of exchange as proposed by these latest workers.[75,76] Certainly the logarithmic factor has a much weaker singularity than the potential scattering term in Eq. (1.1), but near threshold this modification would be difficult to distinguish experimentally from simply using Eq. (1.1) with a reduced threshold exponent.

Despite the known inaccuracies of GH's approach, their results are intuitively plausible, heuristically simple, and amenable to calculation (see Sec. V B). For these reasons we use Eqs. (2.2)–(2.6) in addressing the two *practical* questions of this section. These are (a) what is the

effect of such exchange in an experimental spectrum, and (b) in what materials should it be important? Since exchange reduces the attractive potential (i.e., the scattering phase shift) between core hole and electron in the optically produced singlet state, e.g., for a spin-down core hole $\delta_l^+ < \delta_l$, and since the spin-dependent singularity index must increase according to Eqs. (1.4) and (2.3), i.e., $\alpha^{GH} > \alpha$, then the threshold exponent with exchange must be reduced, i.e., $\alpha_l^{GH} < \alpha_l$. Among the alkali metals, Li is unique in that it contains no p core levels to screen out the s-like conduction electrons. Therefore $1s$-$2(s,p)$ exchange is expected to be comparitively large in Li. In Sec. V B we discuss in more detail the calculations of and the possible experimental evidence for spin-dependent exchange effects of this type.

So far we have assumed the *LS* coupling limit for the electron-hole system. In the presence of spin-orbit coupling, as for core levels of *p symmetry*, the *LS* limit and its symmetries are destroyed and additional off-diagonal exchange (spin-flip scattering) can occur. Since only singlet components are affected by exchange and are accessible by optical transitions, intensity branching ratios predicted on the basis of spin-orbit splitting alone can be considerably modified. An example of such spin-orbit mixing is found in the $L_{2,3}$ absorption edge spectra of Na metal.[44]

To understand this effect in Na metal, consider first the free Na^+ ion, for which a spin-orbit splitting of $\lambda = 0.17$ eV and an exchange energy of $\Delta = 0.43$ eV is reported for the $2p^5 3s$ configuration.[77] (Here Δ is the singlet-triplet splitting in the absence of spin-orbit coupling, which, in the notation of Eqs. (2.2)–(2.5), equals $-4\mu/\pi$.) The ratio $\Delta/\lambda = 2.53$ gives an intensity ratio of the L_3 ($j = \frac{3}{2}$) to the L_2 ($j = \frac{1}{2}$) components of ~0.05 : 1, according to $(\Delta E - \Delta + \frac{1}{3}\lambda)/(\Delta E + \Delta - \frac{1}{3}\lambda)$, where $\Delta E = [(\Delta - \frac{1}{3}\lambda)^2 + \frac{8}{9}\lambda^2]^{1/2}$.[72] This ratio is considerably smaller than the *jj* coupling limit value of 2 : 1 and thus indicates that for the free Na^+ ion the *LS* limit is more appropriate. In *metallic* Na, however, the exchange interaction is screened by the conduction electrons and is thus reduced by about 50% (Ref. 44) with respect to the free-ion value. This, in turn, reduces the ratio Δ/λ and mixes the states.

Onodera[44] has considered these simplified ideas and developed a line-shape treatment of the spin-orbit (A-B) doublet in the presence of exchange, obtaining

$$I(\omega) = \frac{1}{\pi} \operatorname{Im} \frac{2R_A(\omega) + R_B(\omega)}{3 - \Delta[2R_A(\omega) + R_B(\omega)]}, \tag{2.7}$$

where

$$\begin{aligned} R_A &= -(3/4E_F)\Gamma(\alpha)\cos^2\delta_0[(\xi/-z)^{\alpha_l} - 1], \\ R_B &= R_A(z - \lambda), \\ z &= \hbar\omega - \tfrac{1}{2}i\Gamma_n. \end{aligned} \tag{2.8}$$

Here Γ_{n_l} is the lifetime of the n_l hole state measured at full width at half-maximum (FWHM), $\Gamma(\alpha)$ is the gamma function, and α_l is the MND threshold exponent according to Eq. (1.2).

There are several features of Eqs. (2.7) and (2.8) that require mention. First, note that the prefactor in Eq. (2.8) tacitly implies that the TDOS from a p-like core state can be approximated by a constant density of states (DOS) of s-character only. Under such conditions, only the α_0 term in Eq. (2.8) is considered. For a structureless and predominantly s-like TDOS, like that of Na, this approximation should be quite valid, but for Mg and Al it could conceivably break down. The potential errors introduced by this approximation are discussed in Sec. IV. Second, note that Eq. (2.7) automatically considers the result of interchannel mixing between the A and B components by considering them as one unified line shape. Only when $\Delta = 0$ is the spectrum reduced to the superposition of two spin-orbit split components. Thirdly, note that only spin-orbit exchange is considered here, i.e., the spin-dependent threshold exponent of Eq. (2.6) is not used. In Sec. V B we will see that this approximation is valid for Na.

Finally, it is appropriate to ask in what materials is spin-orbit exchange most likely to be important, i.e., when is Δ non-negligible? Since the exchange interaction is of short range, being limited by the extension of the p core wave function, it should increase with the amount of s-like valence character in the vicinity of E_F. On the other hand, this increase will be partially compensated by the enhanced screening (reduction) of Δ. Therefore, the ratio of s/p valence wave function character at E_F should be a guiding parameter for estimating the importance of spin-orbit exchange. In Sec. III we present calculations which show the s/p ratio to be considerably larger in Na than in Mg and Al, and in Sec. IV show this supposition to be borne out by experiment. In Sec. V A *a priori* calculations of Δ in Na metal will be compared with our empirical determination.

F. Experimental broadening

The five factors discussed so far are all inherent in the x-ray absorption or emission spectrum. There are, however, two additional

sources of broadening that arise from the experimental measurement itself. These are the instrumental resolution and, in x-ray emission, self-absorption. The former results from the angular acceptance of a slit or series of slits or gratings, and/or from the Darwin bandwidth and the mosaic spread of the monochromating crystals.[78] According to the central limit theorem, the net effect of these contributions are generally well approximated by a Gaussian. Their effects are taken into account by an additional Gaussian convolution.

Self-absorption presents a more difficult problem. The phenomenon arises from x rays being absorbed in the solid before they are detected externally. The most obvious example of this is seen in $L_{2,3}$ edge emission spectra where the more energetic L_2 x-rays are absorbed by the less energetic L_3 electrons. The result is a suppression of the L_2 edge. Consequently, when treating $L_{2,3}$ emission spectra only the L_3 edge can be fit. Furthermore, the *leading* part of the L_3 edge, which overlaps the unknown intensity of the L_2 component, obviously cannot be fit. This means that phonon and lifetime broadening must be known from other experiments, such as XPS or x-ray absorption. In K-emission spectra, the leading part of the edge which overlaps the K-absorption spectrum can also be affected by self-absorption. The importance of such effects can usually be assessed by monitoring the K-edge shape as a function of either the incident primary electron energy,[79] its incident angle,[80] or the detection angle of x-ray emission.[80] Another approach is to compare the emission spectra using electrons (primary excitation) versus photons (secondary excitation).[29,81] Corrections for self-absorption can and have been performed,[81] but only by the experimentalist making the measurement. It is therefore important to choose only those emission data which have been explicitly corrected for or have been shown not to exhibit self-absorption.

III. CALCULATION OF ONE-ELECTRON TRANSITION DENSITY OF STATES

To investigate the one-electron band-structure contributions to the shape of x-ray absorption and emission spectra we have calculated the imaginary part $\epsilon_2(\omega)$ of the complex dielectric function in the random-phase approximation:

$$\epsilon_2(\omega)=\frac{e^2\hbar^2}{3\pi m^2\omega^2}\sum_n\int_{BZ}d\vec{k}\,|\langle\psi_{\text{core}}(\vec{k},\vec{r})|\nabla|\psi_n(\vec{k},\vec{r})\rangle|^2\delta(E_{\text{core}}-E_n(\vec{k})+\hbar\omega)\begin{cases}[1-n(E,E_F,T)] \text{ for absorption},\\ n(E,E_F,T) \text{ for emission}.\end{cases} \tag{3.1}$$

Equation (3.1) contains the usual dipole transition intensity, summed over all one-electron states in the solid accessible from $\psi_{\text{core}}(\vec{k},\vec{r})$, which describes the core wave function with energy E_{core}. In the cases of $L_{2,3}$ spectra this state is the $2p$ state; in the case of K spectra it is the $1s$ state. The final states are Bloch states $\psi_n(\vec{k},\vec{r})$ of wave vector $\vec{k}$, band index n, and energy $E_n(\vec{k})$. The δ function in Eq. (3.1) assures energy conservation, and the Fermi function $n(E,E_F,T)$ restricts the final states to unoccupied conduction states for absorption and to occupied valence states for emission. Since the core states $\psi_{\text{core}}(\vec{r})$ may be approximated to be dispersionless, the integral is taken over constant energy surfaces in the valence electron system.

If the transition-matrix elements $\langle\psi_{\text{core}}(\vec{r})|\nabla|\psi_n(\vec{k},\vec{r})\rangle$ in Eq. (3.1) were assumed to be constant, structures in the density of states (DOS), rather than in the joint density of states as in optical transitions, would determine the spectra. This constant matrix element approximation would lead to the usual parabolic shape $\sim(\hbar\omega-E_{\text{core}})^{1/2}$ of the emission (or absorption) spectra for free-electron metals. (The bottom of the conduction band is set to $E=0$.) In this approximation two important types of band-structure effects are neglected. (i) In realistic solids the periodic lattice potential modulates the valence electron charge density. Deviations from the parabolic free-electron DOS appear for energies high enough to allow for Bragg reflections of the electronic wave functions. (ii) Strong dipole selection rules influence the transition-matrix elements. Due to the localized character of the involved core states these selection rules are atomiclike, i.e., $\Delta l=\pm1$. Thus for $L_{2,3}$ spectra, only transitions into the s- or d-like part of the Bloch wave functions $\psi_n(\vec{k},\vec{r})$ contribute to the integral of Eq. (3.1), whereas K spectra sample the p-like part. Evaluation of the dielectric function according to Eq. (3.1), however, necessarily accounts for effects (i) and (ii) and does indeed yield an accurate TDOS. As mentioned in Sec. II A above, this statement is true only within the approximation that ψ_{core} and ψ_n are eigenstates of the initial-state Hamiltonian.

The valence electron band structure $E_n(\vec{k})$ and the associated Bloch wave functions are calculated on the basis of the empirical pseudopoten-

tial method.[82] This method involves the solution of a Schrödinger equation of the form

$$[-\nabla^2 + V_{ps}(\vec{r})]\phi_n(\vec{k},\vec{r}) = E_n(\vec{k})\phi_n(\vec{k},\vec{r}) . \quad (3.2)$$

The empirical pseudopotential $V_{ps}(\vec{r})$, which replaces the exact one-electron crystal potential, is a weakly varying function and does not allow for any core states. Consequently, the Bloch wave functions $\phi_n(\vec{k},\vec{r})$ are "pseudo"-wave functions and are inaccurate in the vicinity of the ion cores. The lack of orthogonality to the core states is relatively unimportant if optical spectra involving valence-to-conduction band transitions are considered. Errors in $\epsilon_2(\omega)$ for optical spectra are typically of the order of 10%.[83] If transitions from or to core states are involved, however, $\phi_n(\vec{k},\vec{r})$ is inappropriate because it is nodeless. To obtain approximate wave functions with the correct nodal structure, $\phi_n(\vec{k},\vec{r})$ can be orthogonalized to the core states. The orthogonalized wave function[84] $\psi_n(\vec{k},\vec{r})$ is then expressed in terms of pseudo-wave-functions $\phi_n(\vec{k},\vec{r})$ and core wave functions $\psi_{\text{core}}(\vec{k},\vec{r}) = b_t^\alpha(\vec{k},\vec{r})$ as

$$|\psi_n(\vec{k},\vec{r})\rangle = |\phi_n(\vec{k},\vec{r})\rangle - \sum_{t,\alpha} \langle b_t^\alpha(\vec{k},\vec{r})|\phi_n(\vec{k},\vec{r})\rangle |b_t^\alpha(\vec{k},\vec{r})\rangle . \quad (3.3)$$

Here $|b_t^\alpha(\vec{k},\vec{r})\rangle$ is a core wave function with t denoting the quantum numbers n, l, m and corresponding to atom α; it can be written

$$|b_t^\alpha(\vec{k},\vec{r})\rangle = \frac{1}{N}\sum_{\nu,\alpha} \exp[i\vec{k}\cdot(\vec{R}_\nu + \vec{\tau}_\alpha)] a_t(\vec{r} - \vec{R}_\nu - \vec{\tau}_\alpha) , \quad (3.4)$$

where a_t stands for a core orbital, $\vec{R}_\nu$ is a primitive translation vector, $\vec{\tau}_\alpha$ describes the position of atom α in the unit cell, and N is the number of cells in the crystal. The orthogonalization of the pseudo-wave-functions requires renormalization, i.e., the evaluation of

$$\langle\psi_n(\vec{k},\vec{r})|\psi_n(\vec{k},\vec{r})\rangle = 1 - \sum_{t,\alpha} |\langle b_t^\alpha(\vec{k},\vec{r})|\phi_n(\vec{k},\vec{r})\rangle|^2 . \quad (3.5)$$

At this point it becomes clear that the *post hoc* orthogonalized wave function $\psi_n(\vec{k},\vec{r})$ is only an approximate solution since the renormalization also affects the crystal wave function outside the core region. In practice, however, the renormalization is small, ~5%, for the pseudopotentials used in the present calculations. Optical dipole matrix elements between a particular core state $|b_{t_0}^{\alpha_0}(\vec{k},\vec{r})\rangle$ and any valence function are in turn given by

$$\langle b_{t_0}^{\alpha_0}|\nabla|\psi_n\rangle = \langle b_{t_0}^{\alpha_0}|\nabla|\phi_n\rangle - \sum_t \langle b_{t_0}^{\alpha_0}|\nabla|b_t^{\alpha_0}\rangle\langle b_t^{\alpha_0}|\phi_n\rangle . \quad (3.6)$$

Here the first term represents contributions from core-pseudo-wave-transitions, which are usually rather small. The second term accounts for the oscillatory part in the valence and conduction wave functions. Because of atomic selection rules, the sum over core states t may be restricted to states with $l = l_0 \pm 1$ and $m = m_0, m_0 \pm 1$.

Let us examine the case of a $L_{2,3}$ spectrum for any of the third row metals like Na, Mg, or Al. The chosen core state is a $2p$ state, which generally limits the sum in Eq. (3.6) to $t = s$- and d-like contributions. Since no d-core states exist for third row elements, only p-to-s contributions are picked up by the second term in Eq. (3.6). Due to the absence of any d-core states, the d part of the valence wave function is fully described by the pseudo-wave-function $\phi_n(\vec{k},\vec{r})$, and p-to-d contributions are contained in the first term in Eq. (3.6).

It is apparent from the form of Eq. (3.6) that structure in the dielectric function related to matrix-element effects results mainly from the variation of the "atomic" projections $|\langle b_t^{\alpha_0}|\phi_n\rangle|^2$ of pseudo-valence-functions onto core states. In particular, if the pseudo-wave-functions are expanded into plane waves,

$$|\phi_n(\vec{k},\vec{r})\rangle = \frac{1}{\sqrt{\Omega}}\sum_{\vec{G}} c_{\vec{G}}^n(\vec{k}) \exp[i(\vec{k}+\vec{G})\cdot\vec{r}] , \quad (3.7)$$

and the core orbitals are written as

$$a_t(r) = R_{n,l}(r) Y_l^m(\theta,\phi) , \quad (3.8)$$

one finds for the "atomic" projection,

$$\langle b_t^{\alpha_0}(\vec{k},\vec{r})|\phi_n(\vec{k},\vec{r})\rangle = \frac{4\pi}{\sqrt{\Omega_0}} i^l \sum_{\vec{G}} c_{\vec{G}}^n(\vec{k}) Y_l^{m*}(\hat{k}+\hat{G}) S^{\alpha_0}(\vec{G}) \times \int_0^\infty dr\, r^2 R_{n,l}(r) j_l(|\vec{k}+\vec{G}|\, r) . \quad (3.9)$$

Here Ω_0 is the volume of the unit cell, $j_l(kr)$ the spherical Bessel function of order l, and $S^{\alpha_0}(\vec{G})$ the structure factor for the atom α_0. $Y_l^{m*}(\hat{k}+\hat{G})$ is a spherical harmonic with its argument given by the direction of $\vec{k}+\vec{G}$. The radial integrals may be evaluated using atomic wave functions as given by Herman and Skillman.[85] The form of Eq. (3.9) illustrates that the angular character of the valence wave function, represented by

the $j_l(|\vec{k}+\vec{G}|r)$ terms, enters the overlap integral only in the vicinity of the cores, i.e., where $R_l(r) \neq 0$. However, their relative weights are determined by the plane summations and thus by the crystal potential. Calculations of core-to-conduction band transitions have been successfully performed along these lines for PbSe and PbTe,[83] and are also used for the present problem.

A slightly different and instructive approach for estimating the importance of one-electron band-structure effects in x-ray spectra can be described as follows. Rather than projecting on *particular* core states, transition intensities may be approximated by considering the *general* l-character of the valence Bloch states. The transition matrix-elements are then replaced by

$$|\langle b_{t_0}^{\alpha 0}|\nabla|\psi\rangle| \approx \sum_l M_{t_0,l}\langle\psi|l\rangle\langle l|\psi\rangle\,. \tag{3.10}$$

Here $M_{t_0,l}$ is a constant, which obeys the correct atomic selection rules between a core state of quantum number t_0 and the lth angular momentum component in the valence-band wave functions. The nonlocal operator $|l\rangle\langle l|$ projects out the lth component of the wave function ψ_n. Since this projection is not limited by the radial decay of any core wave function, it explicitly contains some cutoff radius R. It is clear that for localized wave functions this radius is naturally given by the spatial extent of ψ_n. For free-electron-like wave functions, however, R has to be specified in accordance with the physics of the problem.

The dependence of relative s-, p-, and d-character on R may be seen by examining $\langle\vec{k}|l\rangle\langle l|\vec{k}\rangle$ for a nonorthogonalized plane wave. This simple example should represent a reasonable approximation to the l-character decomposition and its energy dependence of the free-electron valence states at the bottom part of the valence bands of the isochoric series Na, Mg, and Al.

In Fig. 1 we show the $l=0, 1, 2$ character in the wave function of a free-electron metal (one plane wave with $|\vec{k}| = \sqrt{E}$) for various cutoff radii R. While partial densities of states may be defined for any radius R [e.g., the muffin-tin radius used in augmented-plane-wave (APW) or Korringa-Kohn-Rastoker (KKR) calculations], an adequate cutoff prescription for core-to-valence band transitions may be determined by the spatial extent of the core wave functions, i.e., by the shape of $r^2R_l^2(r)$. For the cases of 2s and 2p functions for Na, Mg, and Al, the maxima of these functions fall between 0.5 and 0.6 a.u. At $R=1$ a.u. the functions decay to about $\frac{1}{10}$ of their maximal value. It can also be seen from Fig. 1 that with

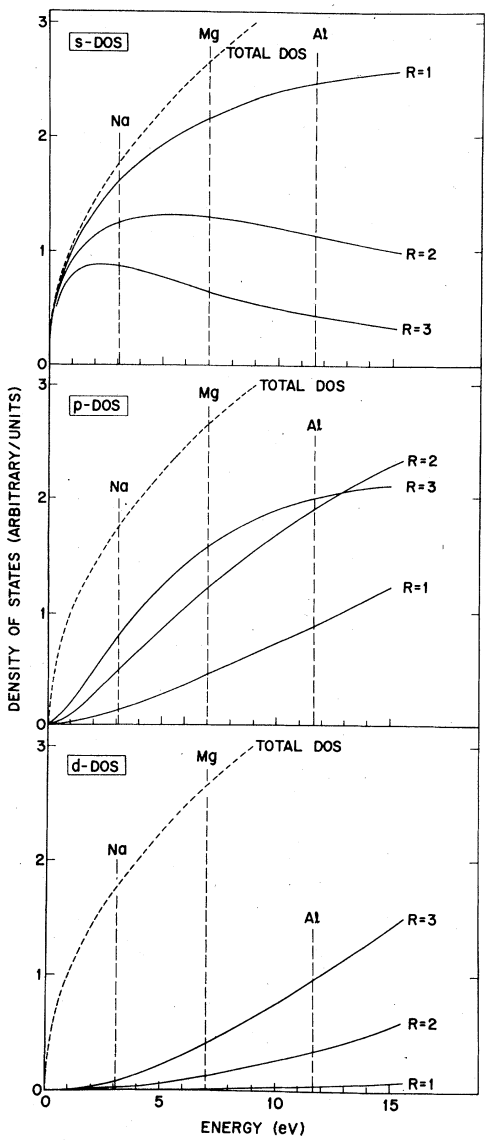

FIG. 1. Partial density of states for a hypothetical free-electron metal containing one nonorthogonalized plane wave and different cutoff radii, $R=1$, 2, and 3 a.u. The Fermi energies of Na, Mg, and Al are also indicated.

increasing kinetic energy $|\vec{k}|^2 = E$, higher angular momenta contributions increase relative to their low l values.

While this simple picture does not contain any band-structure, orthogonality, or crystal potential effects, it nicely demonstrates some general trends in the one-electron contribution to the shape of x-ray edges. For the series Na, Mg, and Al it predicts decreasing s-like and increasing p-like character at the Fermi level in going from Na to Al. As discussed in Sec. II E, this observation explains the relative importance of

spin-orbit exchange contributions to the x-ray edge for Na and its minor importance for Mg and Al. Due to the absence of any d cores in this series, the relative amount of d-like character in Fig. 1 is certainly an underestimation and is affected by orthogonality corrections to s and p contributions.

For a more quantitative analysis, band-structure effects are included by using nonorthogonalized pseudopotential wave functions rather than the simple plane waves as above. Schrödinger's equation is solved for a large number of $\vec{k}$ points in the irreducible parts of the respective Brillouin zones (~170 points for Na, ~225 points for Mg, and ~200 points for Al). The employed empirical pseudopotentials are taken from detailed Fermi surface studies (i.e., Ref. 86 for Na, Ref. 87 for Mg, and Ref. 88 for Al) and

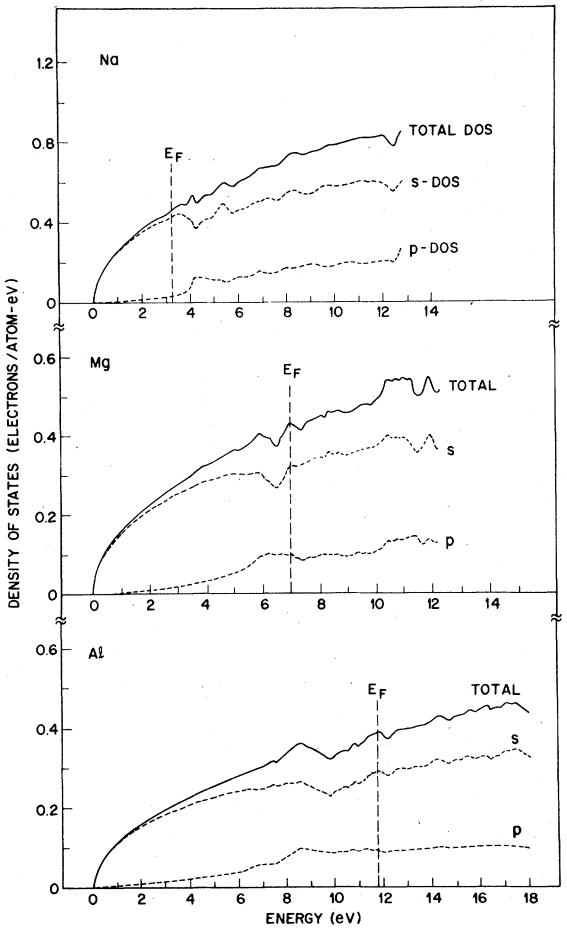

FIG. 2. Partial density of states (DOS) for Na, Mg, and Al using nonorthogonalized pseudopotential wave functions and cutoff radii of $R=1$ a.u. Compare with DOS in Fig. 1, which do not contain band-structure effects. The very weak d DOS, underestimated because of their nonorthogonality, are not shown.

should give very accurate band structures within several eV of the respective Fermi energies. The integration in $\vec{k}$ space necessary to evaluate Eq. (3.1) is done using the Gilat-Raubenheimer[89] technique. This semianalytical method uses energy derivatives calculated by $\vec{k}\cdot\vec{p}$ interpolation and is believed to yield accurate results if carried out for a very fine $\vec{k}$-space sampling grid such as that chosen here.

Results for the conduction-electron DOS are shown in Fig. 2 along with their decomposition into partial s and p densities (using unorthoganalized pseudopotential wave functions). Cutoff radii of $R=1$ a.u. are chosen for the partial densities. One readily recognizes here the general shapes that were also obtained in the free-electron model in Fig. 1. Superimposed on these shapes are the band-structure and crystal potential modulation effects. Their main features appear around 4.2 eV for Na, 6.5 eV for Mg, and 10 eV for Al. At approximately these energies electrons possess enough kinetic energy to undergo a first Bragg reflection induced by the weak crystal pseudopotential. Standing waves are formed by mixing relatively large amounts of higher angular momenta into the predominantly s-like conduction bands. At energies above these thresholds, mixing continues in a more complicated manner, resulting in the spectra shown in Fig. 2.

The most quantitative calculations are the $\epsilon_2(\omega)$ spectra calculated according to Eq. (3.1), which contain both band-structure and orthogonality effects. The results are shown in Fig. 3 for transitions from 1s and 2p core states.

The TDOS spectra calculated here can be compared with calculations carried out independently by others. Gupta and Freeman have calculated one-electron x-ray $L_{2,3}$ spectra for Na[34] and for Mg[33] in a similar manner as done here but using the APW band-structure scheme. A direct comparison is shown in Figs. 4 and 5 for Na and Mg, respectively. For Na our results are in overall good agreement with theirs, including the region around E_F. This should be contrasted with that region in Mg shown in Fig. 5, where sharp structures at and just above the Fermi level are seen. It has been claimed by Gupta and Freeman[33] that these peaks may to a large extent explain the $L_{2,3}$ x-ray edge shapes of Mg. In Sec. IV we show that even if the peak just above E_F were real the experimental absorption spectrum at E_F would not be affected by it. It is our belief that this peak is in fact not real, but is rather a spurious result in the density of states originating from a slightly incorrect band structure at E_F. We base this on the fact

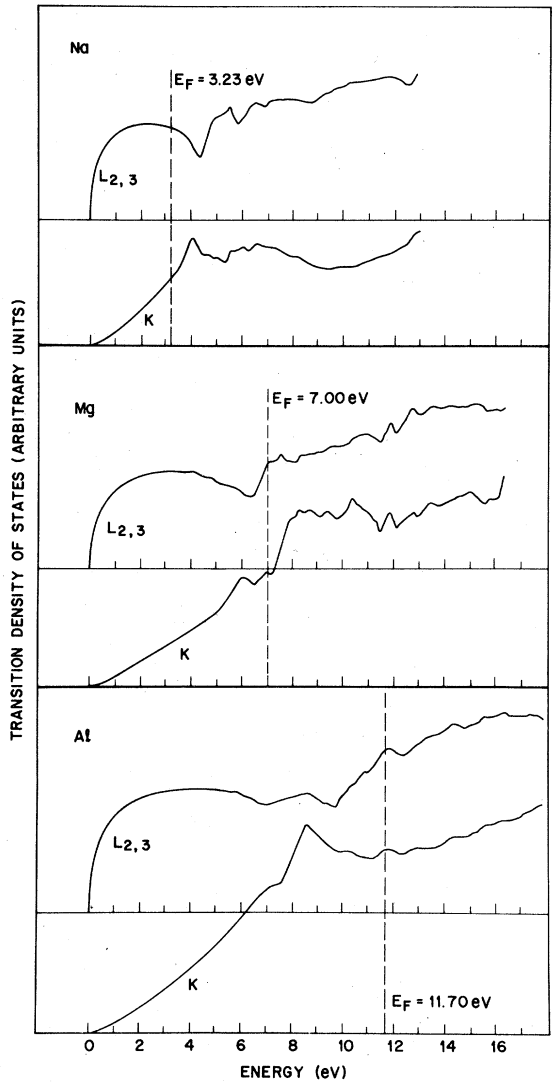

FIG. 3. Calculated transition density of states (TDOS) for Na, Mg, and Al K and $L_{2,3}$ edges using orthogonalized pseudopotential wave functions. The $L_{2,3}$ TDOS contain contributions from both s- and d-like states.

that if we slightly altered the empirical pseudopotential used here from the value determined from the Fermi-surface de Haas–van Alfen data,[87] we were able to reproduce that same peak at E_F. Also, in Sec. IV we show that their calculated structure at about 1 eV above E_F is exaggerated when compared with experiment. The peak at and just below E_F, which is relevant to the Mg $L_{2,3}$-emission edge, does indeed contribute structure to the experimental spectrum. However, as we shall also show in Sec. IV, such structure cannot by itself account for the observed edge shape.

One-electron x-ray emission spectra for Al

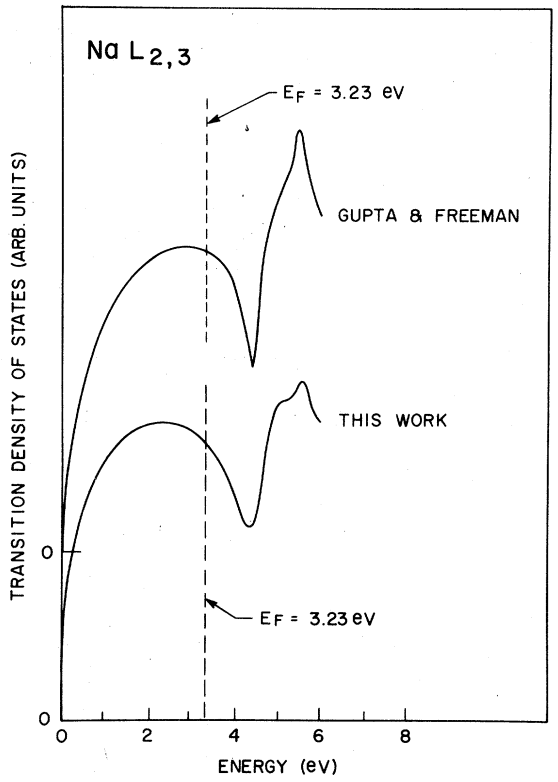

FIG. 4. Comparison between our calculated TDOS for the Na $L_{2,3}$ edge and that of Gupta and Freeman, Ref. 34.

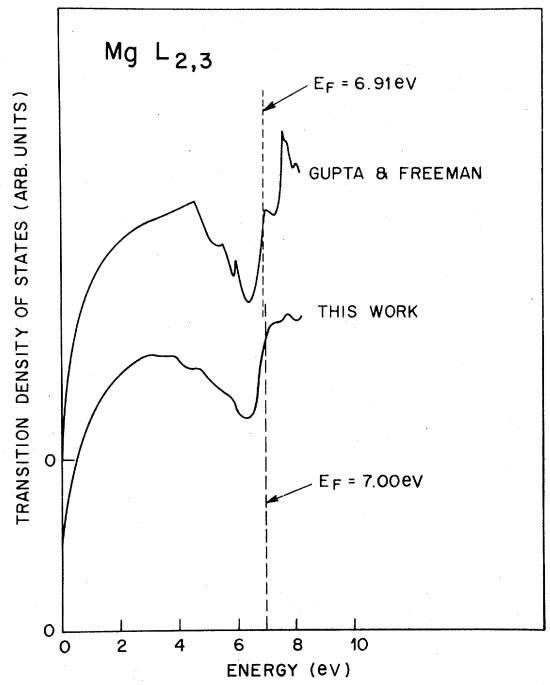

FIG. 5. Comparison between our calculated TDOS for the Mg $L_{2,3}$ edge and that of Gupta and Freeman, Ref. 33.

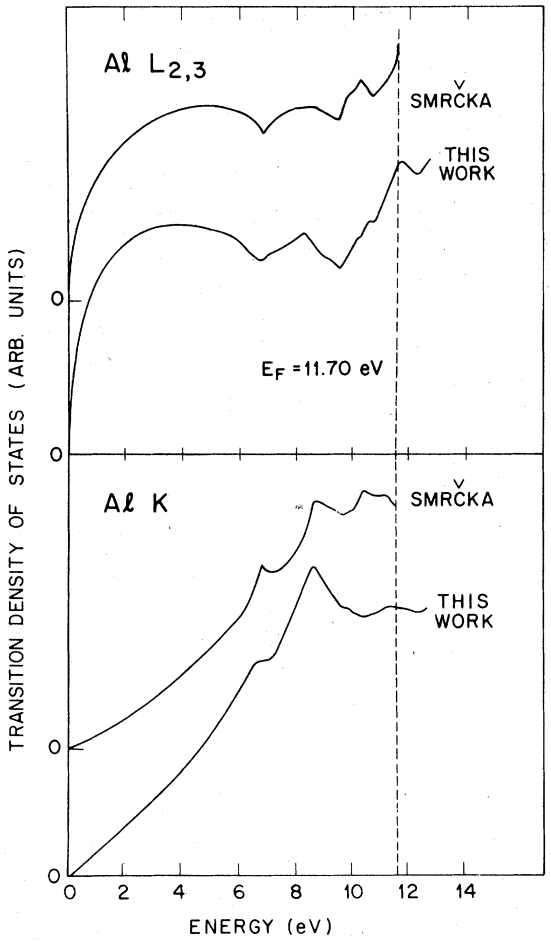

FIG. 6. Comparison between our calculated TDOS for the Al K and $L_{2,3}$ edges and those of Smrčka, Ref. 90.

have been calculated by Smrčka[90] using the APW scheme. In Fig. 6 we compare his results, calculated only for states below E_F, with ours for the K and $L_{2,3}$ edges. In general, the agreement is good. Another derivation of Al x-ray emission spectra has been given by Rooke[91] based on a band-structure calculation by Segall.[92] Calculations of the one-electron band-structure contributions to the x-ray absorption and emission spectra of Li have not been carried out here because of the existence of virtually identical results obtained by McAlister,[27] by Shaw and Smith,[93] by Mahan,[94] and by Gupta *et al.*[95]

A final comparison of our calculations with those of other authors concerns the relative weightings of the s and d character in the TDOS for the $L_{2,3}$ core states. These quantities are simply the transition probabilities $|A_0|^2$ and $|A_2|^2$ in Eq. (1.1) (the K spectra involve only $|A_1|^2$). The partial densities of states (Figs. 1 and 2) in principle contain the required decomposition

TABLE I. Comparison of calculated percentage of d intensity at $L_{2,3}$-absorption edge.

Na	Mg	Al	Reference
		40	90
32	62	73	42
10		34	96
7	31		33 and 34
1	4	7	51
4	14	28	97

of angular-momentum dependence but, as already mentioned, the lack of d core levels in Na, Mg, and Al combined with the use of *non*orthogonalized pseudo-wave-functions produce considerably underestimated d-like DOS. The more reliable TDOS (Figs. 3–6), which use orthogonalized core states, unfortunately cannot separate out the s- and d-like components. Therefore, to assess the importance of $|A_2|^2$ we must rely on the calculations of other workers (Refs. 34, 42, 51, 90, 96, and 97). A variety of such calculations are listed in Table I. With the exception of Mahan's results,[42] all show $|A_2|^2/(|A_0|^2+|A_2|^2)$ to be less than 0.5. In Sec. IV we will show that the effect of including the $|A_2|^2$ term in our analysis of the $L_{2,3}$ spectra is, in fact, not large.

IV. ANALYSIS OF EDGE DATA: PROCEDURES AND RESULTS

In this section we describe the analysis of the x-ray absorption and emission edge data using a theoretical model that incorporates all of the factors discussed in Sec. II. To our knowledge it is the most complete and unified treatment to date. In order to delineate its distinctions, as well as its limitations, we consider first the principles that underlie our approach.[39,47-49]

All phenomena known to contribute to the shape of the edge are considered in the analysis. The importance of this fact cannot be overstated because, while the magnitude of some of these effects may in some cases appear to be small on an absolute energy scale, they will be seen to be quite significant in determining the detailed shape. While we have treated all the effects known to us, the possibility remains that additional factors will be discovered.

Although the deviation of the power-law singularity of the MND theory is valid only in the limit of small excitation energy, there are various indications, both experimental and theoretical, that this functional form provides a good representation of the many-body phenomenon over a finite range of energy. The experimental

evidence comes from XPS data for the simple metals, which are well fitted by this form over at least 2 eV.[37] This is a particularly good test because the XPS line shape is not complicated by a TDOS and is only minimally affected by background. From a theoretical point of view one can show, using Hopfield's perturbation theory formalism,[6] that the power law remains exact so long as the e-h pair excitation matrix element remains equal to that at E_F, and the density of states for e-h pair creation increases proportionately with the excitation energy.[48] Using a more realistic model, Minnhagen[98] has shown that the power-law exponent changes little over an energy equal to a sizeable fraction of the bandwidth, generally up to the point where the plasmon tail starts to make an appreciable contribution. For our present purposes we conservatively define the "near-threshold" region in which the MND theory should be meaningfully tested to be *within* ~0.5 eV from the (L_3 or K) edge in Al and Mg, and ~0.3 eV in Na. Taking ξ in Eq. (1.1) to be ~E_F,[9] therefore implies a near-threshold region of ~0.1 E_F in Na to ~0.04 E_F in Al. From a theoretical point of view these limits are arbitrary. Deviations between fitted and measured spectra outside this region (particularly for the L_2 edge) are not regarded as significant, in part because of our lack of confidence in the (unspecified) background subtraction in the data, and in part from the realization that the calculated TDOS may introduce some uncertainty as well (see Sec. II A).

No existing many-body theory incorporates all the effects that must be considered in an accurate analysis of a measured x-ray absorption edge spectrum. Consequently, an *ad hoc* means for doing so must be devised. For a purely one-electron system the procedure is clear, namely, convolute the appropriate TDOS (see Sec. II A) with the standard line shapes of the other known effects. In a many-electron system we assume that the power-law line shape of the MND theory extends sufficiently far beyond the edge to be tested. The theoretical edge shapes are generated as prescribed by Eq. (1.1). The density of states is cut off at the Fermi energy and multiplied by the power-law term. The various broadening mechanisms are then introduced by successive convolutions with (i) the derivative of the Fermi function, (ii) a Lorentzian corresponding to the lifetime width, and (iii) a Gaussian corresponding to the combined width of the instrumental response function and phonon broadening. For $L_{2,3}$ edges the second spin-orbit component is introduced by adding the original line with half intensity, displaced by the spin-orbit splitting.

For K edges it is sufficient to use only the $|A_1|^2$ term in Eq. (1.1). For $L_{2,3}$ edges it is, in general, necessary to consider both the $|A_0|^2$ and $|A_2|^2$ terms. Even though the ratio of d- to s-transition probability is not necessarily small in the simple metals (see Table I), other factors serve to make the effect of the $|A_2|^2$ term on the edge shape relatively weak. This comes about through the following set of circumstances. Since d phase shifts are comparitively small in the simple metals, α_2 is well approximated by $-\alpha$, i.e., it is negative and results in a rounding of the d part of the edge. On the other hand, α_0 will be positive and results in a peaking. The power-law shapes corresponding to these cases are illustrated in Fig. 7(a), in which the energy from threshold, $\hbar\omega_0$, is expressed as a fraction of ξ, taken as the width of the occupied band. For illustrative purposes we use the α_0 and α_2 values for Al determined later on in this section. While Fig. 7(a) appears to indicate that the d contribution is quite significant, it is actually misleading because the validity of the power law (and hence the analysis) is assumed valid only within the immediate vicinity of the edge, i.e., within only a small fraction of the bandwidth. In Fig. 7(b) we show the same functions for Al in the near-threshold region of interest ($\hbar(\omega-\omega_0) \lesssim 0.5$ eV), defined by the dashed vertical line. We also include the corresponding

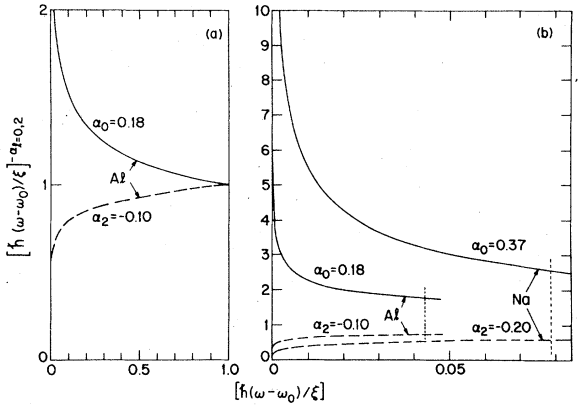

FIG. 7. Relative contributions of s- and d-threshold exponents, α_0 and α_2, according to Eq. (1.1) and assuming $|A_0|^2 = |A_2|^2$. Contributions for Al and Na $L_{2,3}$ edges are plotted as a function of fractional cutoff energy ξ, taken to be E_F, with energy $\hbar\omega$ measured from threshold $\hbar\omega_0$. Note different scales in (a) and (b). Dashed vertical lines indicate limits of the near-threshold energy regions within which edge data are fit. α_0 and α_2 values are taken from fits (see text). Actual d contributions in the data are even smaller than shown here because $|A_0|^2 > |A_2|^2$ (see text).

functions for Na using the α_0 and α_2 values determined from our analysis in this section.

Focusing first on Al we find that, qualitatively, the α_2 term is small and relatively constant, while the α_0 term is enhanced and significantly peaked. The ratio of d to s transition probability in Al, $|A_2/A_0|^2$, is taken from Table I to be 0.52 (Ref. 96) [intermediate between the values of 0.39 (Ref. 97) and 0.66 (Ref. 90)], so that the d contribution is attenuated still further by this additional factor. The net result of considering both the d and the s terms, then, is mainly to add a small slowly varying function to a larger and more rapidly varying one. To evaluate the actual contribution of the α_2 part to the edge shape more quantitatively, Fig. 7(b) shows that at $\hbar(\omega-\omega_0)/\xi=0.025$ (corresponding to ~0.3 eV above threshold) the many-body enhancement of the s- relative to the d-transition probability is ~3. Since $|A_2/A_0|^2$ is actually ~0.5, the real total fractional d content $[d/(d+s)]$ of the experimental edge width is only $\sim\frac{1}{7}$, i.e., the shape is not grossly affected by the d contribution. This is borne out empirically by our observation that α_0 decreased from 0.18 to 0.155, i.e., ~15%, if the d contribution is left out entirely.

The rounding due to the α_2 contribution is so small that there is no possibility to determine α_2 experimentally. What we have done in our fitting procedure, therefore, is to use an iterative approach whereby the α_2 values are initially approximated by $-\alpha$. More accurate values for α_2 are then obtained (see Sec. V B) from the phase shifts calculated from our empirically determined threshold exponents α_1 and α_0. Once α_2 is known, it is incorporated into the fit through multiplication of the $|A_0|^2$ and $|A_2|^2$ terms by the total calculated TDOS for the $L_{2,3}$ edge. As pointed out in Sec. III, our TDOS contains both s and d contributions which cannot be separated. This procedure introduces little error, however, not only because of the small magnitude of the d correction but also because the d-TDOS structure near threshold is very similar to the s-TDOS.[33,90] The above discussion shows that the $|A_2|^2$ term is an essential ingredient for a quantitative analysis of the edge data, but is not needed for a qualitative understanding.

When the Onodera spin-orbit exchange mechanism[44] is to be included in the analysis of the $L_{2,3}$ absorption edges the above procedure has to be modified (for $L_{2,3}$ emission edges such exchange effects are small). Recall from Sec. II E that the Onodera formalism, Eqs. (2.7) and (2.8), directly yields a spin-orbit doublet. The effects of thermal, instrumental, and phonon broadenings are introduced by convolution as above, but because only p-s exchange is considered in these equations (i.e., p-d exchange is ignored) there is no opportunity to separate the individual $|A_0|^2$ and $|A_2|^2$ terms in Eq. (1.1). If Mg and Al had significant spin-orbit exchange this would pose a serious obstacle in the data analysis. As we will see, however, it is only in Na that spin-orbit exchange is important and, fortunately, it is only in Na that the $|A_2|^2$ is almost completely negligible. We demonstrate this latter assertion in Fig. 7(b), where we have indicated the approximate limit of the near-threshold region in Na by the dashed vertical line (corresponding to $\hbar(\omega-\omega_0)\sim 0.2$ eV; it is smaller in Na than in Al because of the smaller bandwidth). Even at this outer limit the enhancement of the s- relative to the d-transition probability (assuming $|A_2/A_0|^2=1$) is ~4; with an estimated upper limit of $|A_2/A_0|^2=0.1$ from Table I this reduces the total fractional d content of the Na $L_{2,3}$ edge to $\sim\frac{1}{40}$, i.e., a negligible amount. This value is even smaller midway in the near-threshold region and for somewhat smaller estimates of $|A_2/A_0|^2$.

For the case of $L_{2,3}$ emission spectra, the same procedure is applied as for $L_{2,3}$ absorption edges without exchange, only now the intensity of the L_2 component is ignored because of self-absorption (see Sec. II F). In our fits to the $L_{2,3}$ emission data we have simply used the theoretical $L_3:L_2$ intensity ratio of 2.

The computer generated net result is overlaid with the experimental data in a video display. This mode of sequential interactive data analysis is particularly helpful for elucidating the relative importance of the various adjustable parameters. The spectrometer function and the Fermi-Dirac function are well known and are not considered adjustable. The calculated TDOS are also not adjustable. To assess their relative importance and to provide a basis for comparison with earlier analyses we have made fits using a constant (unphysical) TDOS. Of the adjustable parameters there are six, namely, intensity, position, α_l, Γ_{n_l}, $\Gamma_{\rm ph}$, and (for $L_{2,3}$ absorption) Δ. The first two are trivial, while the distinctive line shapes associated with the remaining parameters allows their effects to be well monitored. For example, Γ_{n_l} and $\Gamma_{\rm ph}$ are determined from the leading edge of the data and are virtually insensitive to the choice of α_l or Δ. It is therefore straightforward to assess whether it is a single phenomenon or a particular combination of them that is responsible for the overall shape of an absorption or emission edge. In our presentation of the analysis, we will incorporate the various factors in the most logical sequence to illustrate the predominate one(s).

TABLE II. Summary of parameters used in absorption-edge data analysis.

Edge	Fig.	Curve (temp., K)	TDOS[a]	Γ_{n_l}[b] (eV)	Γ_{sp}[c] (eV)	Γ_{ph}[d] (eV)	α_0[e]	α_1[e]	α_2[e]	Δ[f] (eV)
	8(a)	*a* (77)	const. or Ref. 27	0	0	0		0		
		b (77)	const. or Ref. 27	0	0.11	0		0		
		c (77)	const. or Ref. 27	0.04	0.11	0		0		
Li K[g]		*d* (77)	const. or Ref. 27	0.04	0.11	0.21 or 0.23		0		
	8(b)	−(4)	Ref. 27	0.04	0.03	0.18		0		
		−(293)	Ref. 27	0.04	0.11	0.33		0		
		−(443)	Ref. 27	0.04	0.11	0.38		0		
	8(c)	−(300)	Ref. 27	0.04	0.08	0.35		0		
		a(300)	const.	0	0	0		0		
	9(a)	*b*(300)	const.	0.47	0	0		0		
		c(300)	const.	0.47	0.14	0.07		0		
Al K[h]	9(b)	*d*(300)	const.	0.47	0.14	0.07		0.04		
		e(300)	this work	0.47	0.14	0.07		0		
	9(c)	*f*(300)	this work	0.47	0.14	0.07		0.06		
		g(300)	this work	0.47	0.14	0.07		0.095		
		a (77)	const.	0	0	0	0		0	0
	10(a)	*b* (77)	const.	0	0	0	0.26		0	0
		c (77)	const.	0.06	0.012	0	0.26		0	0
		d (77)	const.	0.01	0.012	0.09	0.26		0	0
Na $L_{2,3}$[i]	10(b)	*e* (77)	const.	0.01	0.012	0.09	0.37		0	0
		f (77)	const.	0.01	0.012	0.09	0.32		0	0
	10(c)	*g* (77)	const.	0.01	0.012	0.09	0.37		0	0.21
	10(d)	*h* (77)	const.	0.01	0.012	0.09	0.26		0	0.21
	10(e)	*i* (77)	this work	0.01	0.012	0.09	0.37		0	0.21
	10(f)	*j* (77)	this work	0.01	0.012	0.09	0.37		0	0.29
	11(a)	*a* (77)	const.	0.04	0.026	0.07	0		−0.10	0
		b (77)	const.	0.04	0.026	0.07	0.20		−0.10	0
Al $L_{2,3}$[i]	11(b)	*c* (77)	const.	0.04	0.026	0.07	0.17		0	0
		d (77)	const.	0.04	0.026	0.07	0.17		0	0.05
	11(c)	*e* (77)	const.	0.04	0.026	0.07	0.23		−0.10	0
		f (77)	this work	0.04	0.026	0.07	0.18		−0.10	0
	12(a)	*a* (77)	const.	0.02	0.026	0.07	0.23		−0.12	0
		b (77)	const.	0.02	0.026	0.07	0.18		−0.12	0
	12(b)	*c* (77)	const.	0.02	0.026	0.07	0.22		0	0
Mg $L_{2,3}$[i]		*d* (77)	const.	0.02	0.026	0.07	0.22		0	0.09
	12(c)	*e* (77)	this work	0.02	0.026	0.07	0.23		−0.12	0
		f (77)	Ref. 33	0.02	0.026	0.07	0.21		−0.12	0

[a] Transition density of states.
[b] Lorentzian lifetime broadening of n_l hole state at FWHM.
[c] Spectrometer broadening at FWHM, assumed Gaussian.
[d] Gaussian phonon broadening at FWHM.
[e] Threshold exponent from Eq. (1.1).
[f] Spin-orbit exchange parameter from Eq. (2.7).
[g] Data in 8(a) from Ref. 32, in 8(b) from Ref. 40, in 8(c) from Ref. 41.
[h] Data from Ref. 31.
[i] Data from Ref. 103.

A. Absorption edges

The absorption-edge data used in our analyses have been previously published and analyzed by other workers. They were obtained by measuring either x-ray absorption, photoyield, or electron energy loss. The choice of these particular data is primarily governed by their superior energy resolution, typically of the order of 0.1 eV or less. As will be seen, the rather small spin-orbit splitting and the limited range of data that lie within the near-threshold region make energy resolution a particularly important requirement.

The absorption data analyzed are the K edges of Li and Al and the $L_{2,3}$ edges of Na, Mg, and Al. We are unaware of published K-absorption-edge data of Na and Mg. Except where necessary to understand the sequence of data analysis, discussion of the results will be deferred to Sec. V. A summary of our results is presented in Table II below.

1. Li K

The photoyield data taken by Petersen[32] at 77 K are shown twice as dark dashed curves in Fig. 8(a). The way in which the data are fit is the same except that the left-hand spectrum assumes a constant TDOS (i.e., a step-function edge) while the right-hand spectrum uses the TDOS after McAlister.[27] Curve a is a Fermi-Dirac function at $T = 77$ K, curve b is curve a convoluted with a Gaussian spectrometer function with $\Gamma_{sp} = 0.11$ eV,[32] and curve c is curve b convoluted with a Lorentzian 1s lifetime width at FWHM of 0.04 eV. This latter value was determined to within ±0.03 eV from Li-1s XPS lineshape analyses, previously reported in I.[37] Comparison of either of curves c with the data shows that, independent of the TDOS model, additional broadening is required. If we increase the Lorentzian lifetime width to values suggested by several workers[30,42] the fits are decidedly poor. Similarly unsatisfactory results are obtained using negative α_1 values as suggested by several calculations.[17-19,99-101] However, convoluting curves c with a Gaussian phonon broadening at FWHM of $\Gamma_{ph} = 0.21$ eV or 0.23 eV for the left- and right-hand cases, respectively, gives an excellent fit to the data, curves d, and shows that McAlister's calculated TDOS, not surprisingly, is the better choice for the upper part of the Li K edge. Detailed agreement at energies greater than ~0.5 eV past the point of inflection is not expected because it is considered to be outside the near-threshold region.

The above sequence of steps clearly shows that the dominant rounding mechanism of the Li K-absorption edge is phonon broadening. In the fits to Petersen's data we have used $\alpha_1 = 0$. Within our experimental uncertainty of about ±0.03, α_1 is of negligible importance.

In Fig. 8(b) we have analyzed the photoyield and absorption data of Kunz *et al.*[40] taken at various temperatures (shown as dark dashed lines) using the TDOS of McAlister. At the higher temperatures the Fermi-Dirac function plays a significant role in the broadening. The dominant broadening, however, is again due to phonons. The values of Γ_{ph} are 0.18 eV at 4 K, 0.33 eV at 293 K, and 0.38 eV at 443 K. The precision of these values is ±0.02 eV, while the accuracy, which depends on

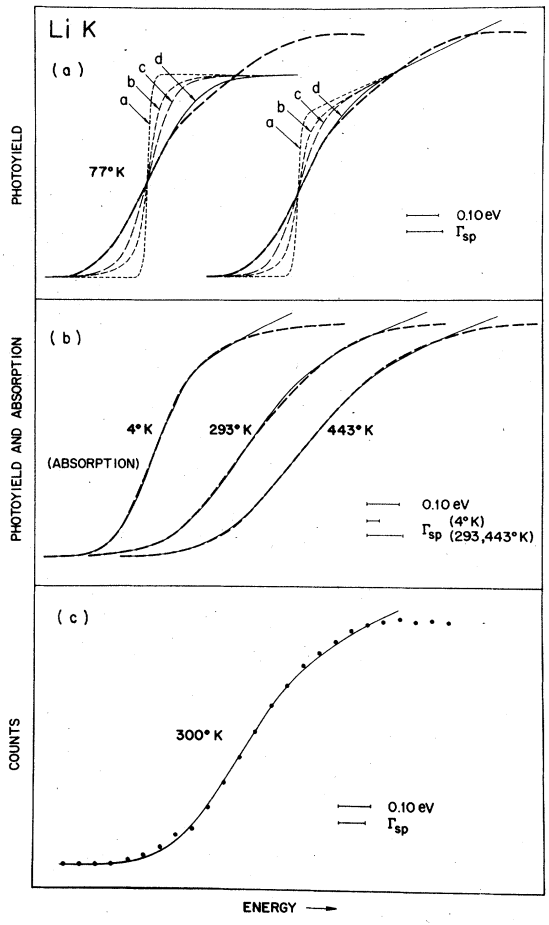

FIG. 8. Analysis of Li K-edge measurements from (a) Petersen, Ref. 32; (b) Kunz, Petersen, and Lynch, Ref. 40; and (c) Ritsko, Schnatterly, and Gibbons, Ref. 41. For full description of fitting curves see Table II. (a) Shows phonon broadening is dominantly responsible for edge shape and that TDOS after McAlister, Ref. 27, (right) is more appropriate than constant TDOS (left). (b) Shows temperature dependence of edge is well described by phonon broadening. (c) Shows electron energy loss data is also well described by phonon broadening.

the unspecified uncertainty of Γ_{sp}, is somewhat larger. The values of Γ_{sp} are 0.03 eV at 4K,[40] and 0.11 eV at 293 and 443 K.[32]

The points in Fig. 8(c) show the electron energy loss data of Ritsko *et al.*[41] taken at 300 K. The same procedures as above were followed in its analysis, giving $\Gamma_{ph} = 0.35 \pm 0.02$ eV. Also as above, α_1 was set equal to zero. The value of Γ_{sp} here is 0.08 eV.[41]

1. Al K

The data of Neddermeyer[31] taken at 300 K are shown as points in Fig. 9. Curve *a* is the Fermi-Dirac function with a constant TDOS and $\alpha_1 = 0$. Curve *b* is curve *a* convoluted with a Lorentzian 1*s* lifetime width of 0.47 eV. While the agreement of curve *b* with the data is not quantitative,

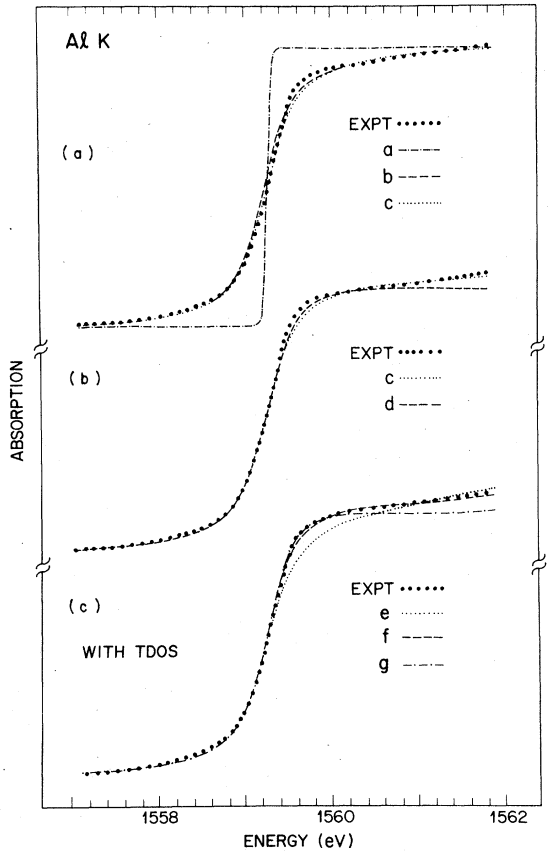

FIG. 9. Analysis of Al *K*-absorption-edge data from Neddermeyer, Ref. 31, taken at 300 K. For full description of fitting curves see Table II. (a) Shows lifetime broadening is dominantly responsible for edge shape, but positive threshold exponent α_1 still required in *near-threshold* region of data. (b) Compares $\alpha_1 = 0$ and $\alpha_1 = 0.04$ (after Dow *et al.*, Ref. 23), indicating latter value is insufficiently positive *near threshold*. (c) Shows that inclusion of calculated TDOS requires a still larger positive α_1 to fit data *near threshold*. Curve *g* is best fit.

it is obvious that qualitatively the overall shape of the edge is dominated by lifetime broadening. Convolution of curve *b* with Gaussian components of $\Gamma_{ph} = 0.07$ eV and $\Gamma_{sp} = 0.14$ eV (Ref. 102) gives a more quantitative fit somewhat past the point of inflection. The individual uncertainties of Γ_{ph} and Γ_{sp} are ±0.02 eV and of Γ_{1s} is ±0.04 eV. Beyond the inflection point but within ~0.5 eV the fit drops below the data. More than ~0.5 eV past the inflection point the agreement between curve *c* and the data is improved, but as in the case of Li, we consider this to be outside the near-threshold region and so not relevant to the assessment of the MND theory.

The fact that the data are more *peaked* than curve *c* within the near-threshold region indicates the need for a *positive* value of α_1. In Fig. 9(b) we show curve *d*, which is identical to curve *c* except that we now use $\alpha_1 = 0.04$, a value used by Dow *et al.*[23] in their analysis of the same Al *K*-edge data. The result is still insufficiently peaked.

Recall that so far we have used a constant (unphysical) TDOS, as in an earlier analysis.[23] If instead we use the calculated TDOS from Fig. 3 and set $\alpha_1 = 0$ (to isolate the effects of the TDOS alone), we obtain curve *e* shown in Fig. 9(c). This should be compared with curve *c*, which also has $\alpha_1 = 0$. Note that the effect of the correct TDOS is to suppress the peaking of the edge still further. This implies that a value of α_1 more positive than 0.04 is required. Curve *f* is curve *e* (with the calculated TDOS) but with $\alpha_1 = 0.06$. Although the fit is improved, it is still inadequate within the near-threshold region (it is quite good beyond). Curve *g* is curve *e* with $\alpha_1 = 0.095$, and it is seen to fit the data very well in the near-threshold region (beyond this point it is unsatisfactory, but this is not significant). The spread in α_1 values which gives satisfactory fits to the data in the near-threshold region is ±0.015.

3. Na $L_{2,3}$

In Fig. 10(a), the data of Kunz *et al.*[103] taken at 77 K are shown as a solid line. In the following sequence of curves we systematically illustrate the effects of each of the various phenomena discussed in Sec. II. For the Mg and Al $L_{2,3}$ spectra below, less detail is presented to show the correlated effects of lifetime and phonon broadening, although it should be noted that the analyses for those spectra are identical to that shown here for Na.

Curve *a* shows two step functions, one superposed on the other, split by 0.16 eV and weighted in the theoretical $L_3 : L_2$ intensity ratio of 2 : 1. The spin-orbit splitting is close to the free ion

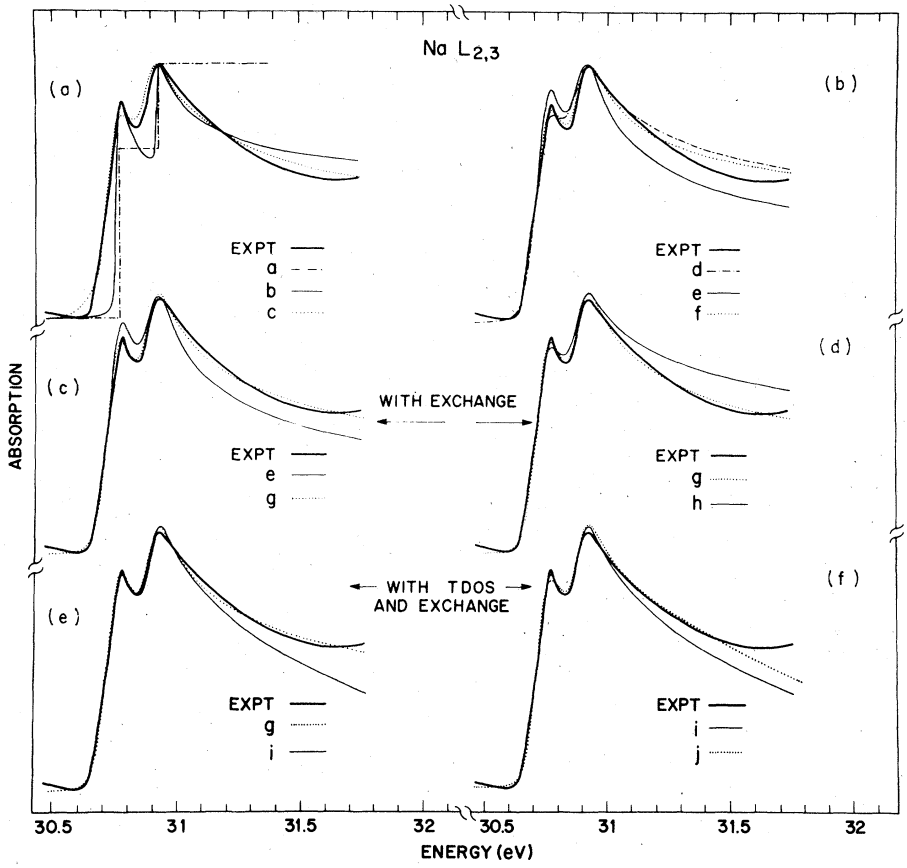

FIG. 10. Analysis of Na $L_{2,3}$-absorption-edge data from Kunz *et al.*, Ref. 103, taken at 77 K. For full description of fitting curves see Table II. (a) Shows need for large positive threshold exponent α_0, inadequacy of $\alpha_0 = 0.26$ (after Dow *et al.*, Ref. 22), and overestimation of $2p$ lifetime of 0.06 eV (after Onodera, Ref. 44). (b) Shows inadequacy of various α_0 values without including exchange. Important disagreement is in *near-threshold* region of data. (c) Shows improved agreement with inclusion of spin-orbit exchange and $\alpha_0 = 0.37$. (d) Shows inadequacy of fit using $\alpha_0 = 0.26$ with exchange included. (e) Shows small effect of including calculated TDOS. (f) Shows effect of varying spin-orbit exchange energy. Curve *i* is best fit as judged by agreement with *near-threshold* region of data.

value of 0.17 eV (Ref. 77) and has a precision of ±0.01 eV (determined below from the more complete fits). Curve *b* consists of two Fermi-Dirac functions at $T = 77$ K split by 0.16 eV, weighted 2:1, and with $\alpha_0 = 0.26$ for each component following Eq. (1.1). The choice of α_0 comes from the value suggested in an earlier edge analysis of the same data by Dow *et al.*[22] As discussed at the beginning of this section, the $|A_2|^2$ term in Eq. (1.1) is negligible for Na and is thus ignored in the analysis. The need for additional broadening is obvious. Curve *c* is curve *b* convoluted with a Lorentzian lifetime broadening of $\Gamma_{2p} = 0.06$ eV at FWHM and a Gaussian spectrometer broadening of $\Gamma_{sp} = 0.012$ eV.[103] The value of Γ_{2p} was chosen because of its use by Onodera.[44] The overall shape of the spectrum is improved, but it is seen at the "foot" of the spectrum that Γ_{2p} is too large. Quantitative agreement in the peak areas is also lacking.

In Fig. 10(b) we include a Gaussian phonon broadening of $\Gamma_{ph} = 0.09$ eV and reduce the Lorentzian lifetime of Γ_{2p} to 0.01 eV to obtain curve *d*, again with $\alpha_0 = 0.26$.[22] The lower part of the L_3 edge is now seen to agree with the data, and this determines Γ_{ph} and Γ_{2p} to within ±0.02 eV (their effects are correlated). The agreement in the L_2 peak is good but the L_3 peak and valley (between-the-peak) regions are in noticeable disagreement. Increasing α_0 from 0.26 to 0.37, curve *e*, does not improve the agreement, while curve *f* with $\alpha_0 = 0.32$ is a compromise choice that still shows misfit. This procedure shows that another effect must be considered.

In Sec. II E we discussed the effect of spin-orbit exchange in $L_{2,3}$ absorption spectra whereby the $L_3 : L_2$ intensity ratio is modified due to spin-flip scattering.[44] In Figs. 10(c) and 10(d) the effects of such exchange are shown in Na. The parameters of curve *e* (i.e., $\alpha_0 = 0.37$, $\Gamma_{ph} = 0.09$ eV and $\Gamma_{2p} = 0.01$ eV) are used in curve *g*, which is generated from Eq. (2.7) using a finite exchange energy of $\Delta = 0.21$ eV. The agreement with the data in the near-threshold region is considerably improved, particularly the $L_3 : L_2$ intensity ratio and the region between the peaks. The effect of Δ on the value of α_0 is seen in Fig. 10(d) where we compare curves *g* and *h*, each with $\Delta = 0.21$ eV but with *g* having $\alpha_0 = 0.37$ and *h* with $\alpha_0 = 0.26$. The former curve is clearly more satisfactory, especially in the near-threshold region. Changes in Δ for a fixed $\alpha_0 = 0.26$ do not improve the qual-

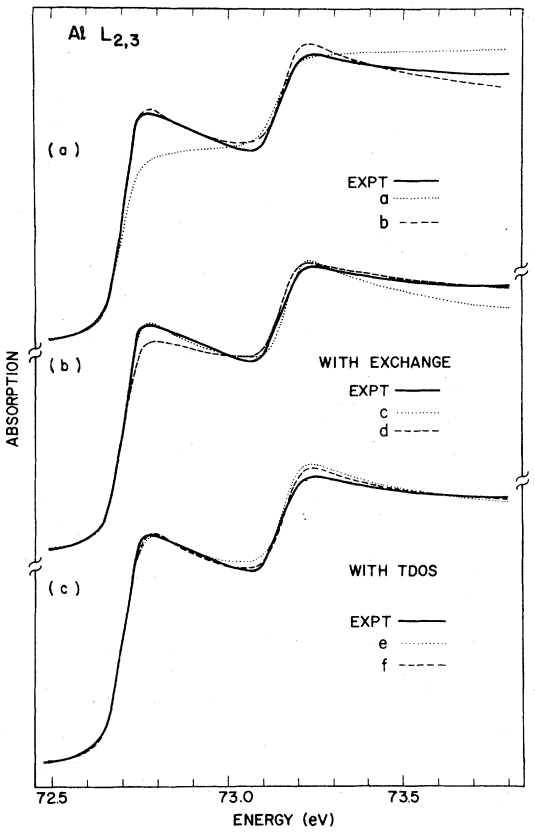

FIG. 11. Analysis of Al $L_{2,3}$-absorption-edge data from Kunz *et al.*, Ref. 103, taken at 77 K. For full description of fitting curves see Table II. (a) Shows need for positive threshold exponent α_0. (b) Shows inclusion of spin-orbit exchange worsens agreement with data. (c) Shows small effect of including calculated TDOS. Agreement is judged only within *near-threshold* region of data.

ity of the fit. These procedures show that spin-orbit exchange is important in Na and that $\alpha_0 = 0.26$ is unacceptable either with exchange (curve *h*) or without it (curve *d*).

All the above analyses have assumed an unrealistic constant TDOS. To assess the effect of using the TDOS from Fig. 3 we have generated curve *i* in Fig. 10(e) from the parameters of curve *g* but using the calculated TDOS for Na. Within ~0.3 eV beyond the L_3 edge curves *g* and *i* are superimposable, while beyond this point curve *i* is in poorer agreement with the data. This procedure shows that while the overall shape of the absorption spectrum is affected by including the calculated TDOS, its effect in the near-threshold region is completely negligible. The agreement ~0.3 eV past the L_3 edge can be improved by increasing Δ to 0.29 eV, curve *j* in Fig. 10(f), but only at the expense of worsening the agreement in the near-threshold region of the edges.

As emphasized at the beginning of this section, it is this latter region that is considered important in evaluating the success of the MND theory and so the misfit beyond the near-threshold region is ignored. It should also be noted that $E_F \sim \xi$ in Eq. (1.1) is considerably smaller in Na than in Mg and Al, so the near-threshold region in Na is expected to be correspondingly smaller. Furthermore, the comparatively smaller spin-orbit splitting in Na makes the fit beyond the L_2-derived component even less reliable since it contains non-negligible contributions from the L_3-derived component. *Therefore, the region considered to be most reliable for quantitatively assessing the effects of the threshold exponent in Na extends immediately from the threshold of the L_3-derived component to and just including the threshold of the L_2-derived edge.* The only reason for considering the L_2 edge at all, in fact, is to determine the effect of spin-orbit exchange. As we have seen, α_0 and Δ are indeed strongly correlated. This fact leads to conservative uncertainty limits of ± 0.03 in α_0 and ± 0.05 eV in Δ.

4. Al $L_{2,3}$

The data of Kunz *et al.*[103] taken at 77 K are shown as a solid line in Fig. 11. Curve *a* consists of two Fermi-Dirac functions split by 0.46 eV weighted in the theoretical ratio of 2:1. To obtain the best values of Γ_{ph} and Γ_{2p}, each component is convoluted with Gaussian factors of $\Gamma_{sp} = 0.026$ eV (Ref. 103) and $\Gamma_{ph} = 0.07$ eV and with a Lorentzian factor of $\Gamma_{2p} = 0.04$ eV. Agreement with the lower (bottom) part of the spectrum is apparent. The precision of the variable spin-orbit splitting is ± 0.02 eV, and its value found here is larger than the free-ion value[77] by 0.02 eV. The precision of Γ_{ph} and Γ_{2p} is better than ± 0.02 eV. The expanded data alone may not reveal the peaking of the edges, but comparison between curve *a* and the data clearly shows the need for a positive threshold exponent. Curve *b* is curve *a* with $\alpha_0 = 0.20$ and $\alpha_2 = -0.10$ and is seen to fit the data moderately well within ~0.2 eV from the L_3 edge and less well beyond. In our fit we have taken $|A_2/A_0|^2 = 0.52$ after the calculations of Almbladh and von Barth.[96] As pointed out in the beginning of this section, α_2 was determined iteratively and does not effect the fit significantly between the limits of ± 0.04 because of its small contribution. Acceptable values of α_0 with a constant (unphysical) TDOS range from 0.18 to 0.22. This range is conservatively determined based on the estimated value of $|A_2/A_0|^2$, which could conceivably vary by as much as $\pm 20\%$.[90,97]

From Sec. II E and the Na $L_{2,3}$ data analysis above we saw that spin-orbit exchange[44] may play

a role in the shape of the $L_{2,3}$-absorption-edge spectra. To test the importance of this effect in Al we have generated curves *c* and *d* in Fig. 11(b) using Eq. (2.7), the broadening parameters from curve *b*, and the value of $\alpha_0 = 0.17$. The α_0 value is somewhat smaller than in curve *b* because of the need imposed by Eq. (2.7), which neglects the *d* contribution in the edge, i.e., $|A_2|^2 = 0$. The effect of including spin-orbit exchange is seen by comparing curve *c*, which does not include exchange, with curve *d*, which does. Even with a small exchange value of $\Delta = 0.05$ eV it is seen that spin-orbit mixing worsens the agreement with the data because of the incorrect adjustment of the $L_3 : L_2$ intensity ratio. No improvement is found by varying either Δ or α_0.

The effect of using the calculated TDOS and the $|A_2|^2$ term is illustrated in Fig. 11(c). Curves *e* and *f* have the same parameters as in curve *b* except that $\alpha_0 = 0.18$ for both and that curve *f* includes the TDOS from Fig. 3. Comparison of these curves with the data shows that while the effect of TDOS is not large, it does cause a slight peaking, which is the reason for our having used a somewhat smaller α_0 value than 0.20. Inclusion of the TDOS also improves the agreement with the data up to ~0.5 eV from the L_3 edge. Beyond the L_2 edge, which is superposed on the tail of the L_3 edge, the agreement is poorer, and to this we attribute much of the problem to being outside the near-threshold region. The precision of α_0 in this fit is again ±0.02 because of the unknown accuracy of $|A_2/A_0|^2$.

5. *Mg* $L_{2,3}$

The data of Kunz *et al.*[103] taken at 77 K are shown as a solid line in Fig. 12. Curve *a* consists of two Fermi-Dirac functions split by 0.28 eV (the same as the free ion value[77]) weighted in the ratio of 2 : 1 with $\alpha_0 = 0.23$ and $\alpha_2 = -0.12$. The components were broadened with Gaussians of $\Gamma_{sp} = 0.026$ eV (Ref. 103) and $\Gamma_{ph} = 0.07$ eV, and with a Lorentzian of $\Gamma_{2p} = 0.02$ eV. The precision of these latter broadening values is the same as for the Al $L_{2,3}$ spectrum. The agreement of curve *a* with the data is fair within ~0.4 eV from the L_3 edge, and deteriorates beyond. Decreasing α_0 to 0.18 in curve *b*, a value used by Slusky *et al.*,[43] results in a noticeably poorer fit. In our fit we take $|A_2/A_0|^2 = 0.33$, a compromise value interpolated from several calculations in Table I.[33,51,97] As was the case for Al, the fit is sensitive neither to this value nor to our choice of α_2. Setting limits as large as ±20% and ±0.04 for these values, respectively, gives uncertainty limits of ±0.02 in α_0.

The effect of including spin-orbit exchange using Eq. (2.7) is seen in Fig. 12(b), where we have taken the broadening parameters of curve *a*, decreased α_0 to 0.22, set $|A_2|^2 = 0$, and generated curves *c* and *d* with zero and finite exchange of $\Delta = 0.09$ eV, respectively. The agreement with the data is worsened primarily in the region between the L_3 and L_2 components. Within the uncertainty of our fitting we therefore determine spin-orbit exchange to be negligible in Mg.

In Fig. 12(c) we have generated curve *e* with the

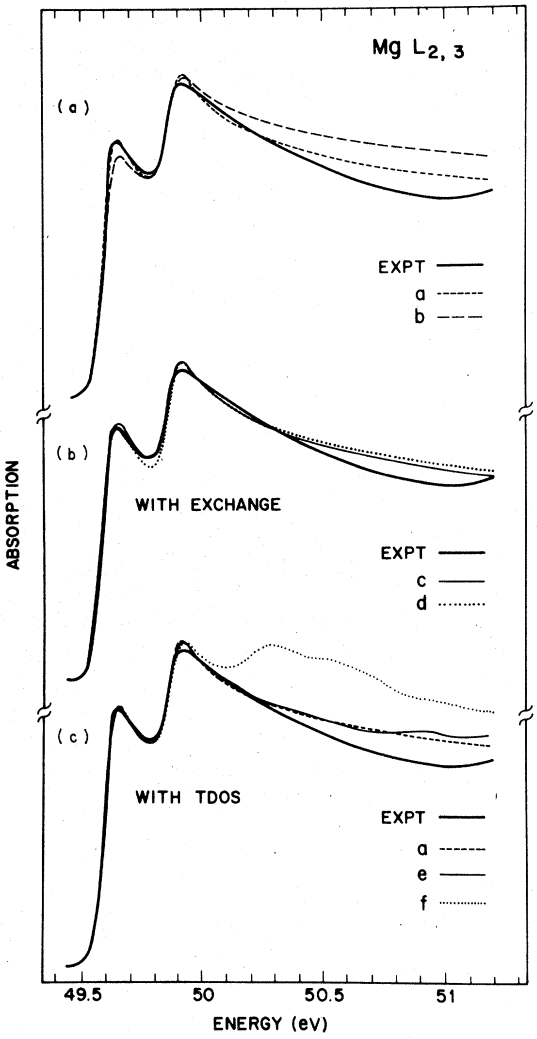

FIG. 12. Analysis of Mg $K\beta$-absorption-edge data from Kunz *et al.*, Ref. 103, taken at 77 K. For full description of fitting curves see Table II. (a) Shows need for positive threshold exponent α_0 and inadequacy of $\alpha_0 = 0.18$ (after Slusky *et al.*, Ref. 43). (b) Shows inclusion of spin-orbit exchange worsens agreement with data. (c) Shows small effect of including calculated TDOS. Agreement is judged only within *near-threshold* region of data. Also shown is poorer agreement with data using TDOS from Gupta and Freeman, Ref. 33.

parameters of curve *b* but using the TDOS from Fig. 3. Comparing curves *a* and *e* directly shows the effect of including the calculated TDOS. The main effect is to improve the agreement slightly with the data in the regions of the L_3 peak. Overall the effect is small. We also show curve *f*, which consists of the same parameters as in curve *b* but using the calculated TDOS of Gupta and Freeman.[33] Also, α_0 was reduced slightly to 0.21 to improve the quality of the fit in the peaks. It is seen that within the near-threshold region the agreement is less good and that from ~0.2 eV and beyond the agreement is poor.

B. Emission edges

The emission-edge data used in our analyses are those of Neddermeyer[31] which he has analyzed previously. For the case of the Mg $L_{2,3}$ data we have checked for and obtained consistency between his results and those recently obtained by Callcott *et al.*[104] These latter authors have determined that incomplete phonon relaxation (see Sec. II C) occurs in the Na $L_{2,3}$- and Li K-emission data, but not in the $L_{2,3}$-emission spectra of Mg and Al.[45,104] For this reason our analyses are limited only to the latter edges. The K-emission edge of Na, to our knowledge, has not been measured, while the Mg K-edge data of Neddermeyer[31] is believed by us (see below) to contain artifactual broadening effects. As emphasized in Sec. II F, self-absorption is a potentially serious limitation and only those data which do not exhibit or which have been corrected for self-absorption can be analyzed with confidence. Only the Al K-edge data of Neddermeyer fall into this category. We have summarized our emission-edge results in Table III below.

1. Al Kβ

The data of Neddermeyer[31] taken at 300 K, which have been corrected for self-absorption,[81] are shown as points in Fig. 13. Curve *a* is a Fermi-Dirac function (constant TDOS and $\alpha_0 = 0$) convoluted with a Lorentzian 1*s* lifetime width of 0.47 eV and Gaussian phonon and spectrometer contributions of 0.14 eV,[102] and 0.05 eV, respectively. These values were obtained from the x-ray *absorption* data,[31] Fig. 9(a). The excellent agreement of curve *a* with the leading part of the edge indicates that self-absorption effects have indeed been effectively removed by Neddermeyer. Curve *b* has the same parameters as *a* except that the calculated TDOS from Fig. 3 is used. The fact that both curves are identical within ~0.8 eV from the edge and that the knee of the data at 1559 eV

TABLE III. Summary of parameters used in emission edge data analysis.

Edge	Fig.	Curve (temp., K)	TDOS[a]	Γ_{n_l}[b] (eV)	Γ_{sp}[c] (eV)	Γ_{ph}[d] (eV)	α_0[e]	α_1[e]	α_2[e]
Al K[f]	13(a)	*a*(300)	const.	0.47	0.14	0.05		0	
		b(300)	this work	0.47	0.14	0.05		0	
	13(b)	*c*(300)	const.	0.47	0.14	0.05		0.11	
		d(300)	const.	0.47	0.14	0.05		0.13	
		e(300)	const.	0.47	0.14	0.05		0.09	
	13(c)	*f*(300)	this work	0.47	0.14	0.05		0.12	
		g(300)	this work	0.47	0.14	0.05		0.14	
		h(300)	this work	0.47	0.14	0.05		0.10	
Al $L_{2,3}$[f]	14(a)	*a*(300)	const.	0.03	0.19	0.05	0.17		−0.10
		b(300)	const.	0.03	0.19	0.05	0.22		−0.10
	14(b)	*c*(300)	this work	0.03	0.19	0.05	0.15		−0.10
		d(300)	this work	0.03	0.19	0.05	0.19		−0.10
		e(300)	this work	0.03	0.19	0.05	0.17		−0.10
Mg $L_{2,3}$[f]	15(a)	*a*(300)	this work	0	0	0	0		0
		b(300)	this work	0.02	0.10	0.11	0		0
	15(b)	*c*(300)	const.	0.02	0.10	0.11	0.32		−0.12
		d(300)	this work	0.02	0.10	0.11	0.18		−0.12

[a] Transition density of states.
[b] Lorentzian lifetime broadening of n_l hole state at FWHM.
[c] Spectrometer broadening at FWHM, assumed Gaussian.
[d] Gaussian phonon broadening at FWHM.
[e] Threshold exponent from Eq. (1.1).
[f] Data from Ref. 31.

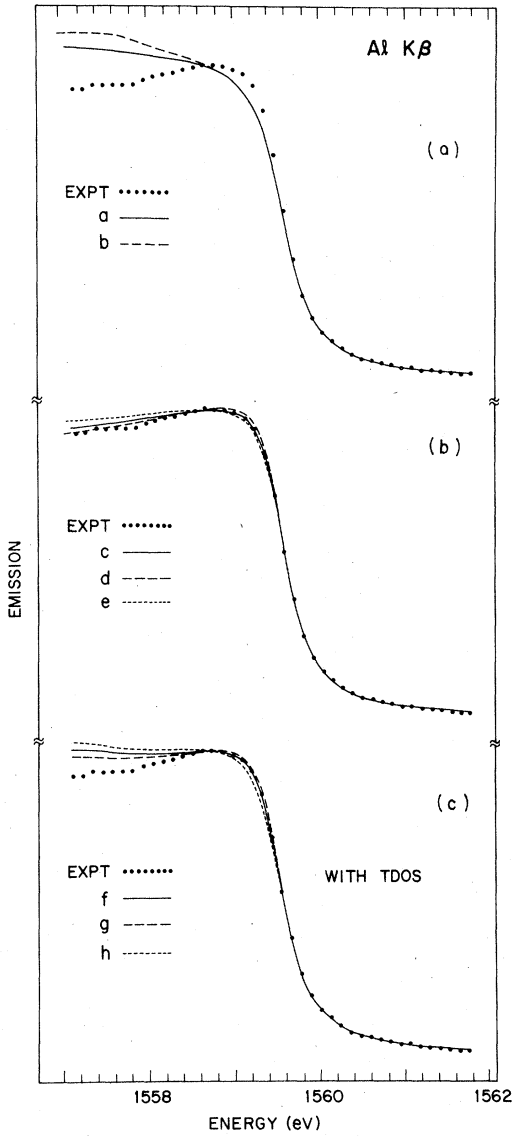

FIG. 13. Analysis of Al $K\beta$-emission data from Neddermeyer, Ref. 31, taken at 300 K. For full description of fitting curves see Table III. (a) Shows need for positive threshold exponent α_1 either including or neglecting calculated TDOS. (b) Shows agreement with data for various α_1 values without TDOS. (c) Shows agreement with *near-threshold* region of data using various α_1 values and including calculated TDOS.

is clearly more peaked than the initial rise at 1560 indicate the relative unimportance of TDOS structure and the need for a positive α_1. In Fig. 13(b) the magnitude and error limits of α_1 are determined assuming a constant (unphysical) TDOS. Curve *c* is the same as curve *a* but with $\alpha_1 = 0.11$. It gives a very satisfactory fit to the data within and even somewhat beyond the near-threshold region. Curves *d* and *e* have α_1 values of 0.13 and 0.09, respectively, and are seen to be unsatisfactory, placing error limits $< \pm 0.02$ in α_1. Fig. 13(c) shows the same series of curves, only now the calculated TDOS is used. Curve *f* is the same as *b*, but with $\alpha_1 = 0.12$, and gives the best fit. Curves *g* and *h*, with α_1 values of 0.14 and 0.10, set precision limits of ± 0.015 on α_1. Inclusion of the TDOS is seen to worsen the agreement with the data more than ~1 eV from the edge, although this is considered outside the near-threshold region.

2. Mg $K\beta$

Neddermeyer[31] has measured the Mg $K\beta$ emission edge at 300 K. In attempting to fit his data we found that in addition to the Gaussian broadening from the spectrometer response and from phonons, a Lorentzian broadening of ~0.6 eV (FWHM) was required. This exceeds the value of 0.35 ± 0.03 eV determined from XPS measurements,[37] a value also consistent with several theoretical calculations.[105-107] We know of no mechanism that could reduce the XPS-derived lifetime and are therefore forced to conclude that some artifactual broadening effects must be present in the Mg $K\beta$ data.

3. Al $L_{2,3}$

The data of Neddermeyer[31] taken at 300 K are shown as a solid line in Fig. 14. Curve *a* consists of two Fermi-Dirac functions split by 0.43 eV, weighted 1:2, with $\alpha_0 = 0.17$ and $\alpha_2 = -0.10$. The TDOS is assumed to be constant, and the same $|A_2/A_0|^2 = 0.52$ value[96] as used in the Al $L_{2,3}$-absorption data is applied. Each component is convoluted with Gaussian factors of $\Gamma_{ph} = 0.05$ eV, $\Gamma_{sp} = 0.19$ eV,[31] and a Lorentzian contribution of $\Gamma_{2p} = 0.03$ eV. The intensity of the L_2 component at higher energy has not been corrected for the self-absorption by the lower energy L_3 edge. The choices of $\alpha_0 = 0.17$ and $\alpha_2 = -0.10$ were based on the similar values used for the Al $L_{2,3}$-absorption-edge data,[103] see Fig. 11(c). The parameters of curve *a* are obviously unsatisfactory for the Al $L_{2,3}$-emission-edge data. This conclusion is based on the disagreement in the near-threshold region of the data, not in the leading part of the edge which is obscured by self-absorption and the residual contribution of the L_2 component. The values of Γ_{ph}, Γ_{sp}, and Γ_{2p} were obtained from the well-defined x-ray absorption edge and the XPS line shape, so that either α_0 or the choice of a constant TDOS must be incorrect. Changing α_0 to 0.22 improves the fit, curve *b*, but it is still not wholly satisfactory.

In Fig. 13(b), curve *e* contains the same parameters as curve *a* except that the calculated

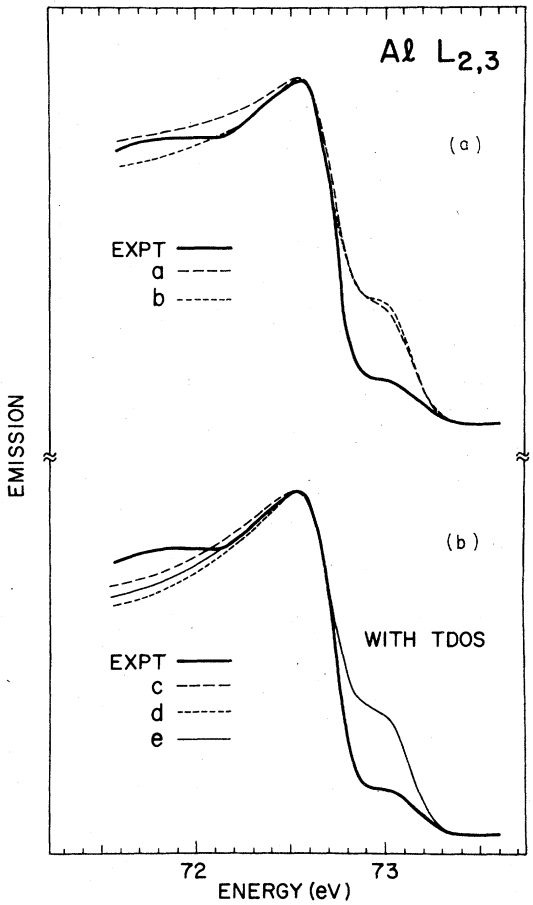

FIG. 14. Analysis of Al $L_{2,3}$-emission data from Neddermeyer, Ref. 31, taken at 300 K. For full description of fitting curves see Table III. (a) Shows positive threshold exponent α_0 is required. (b) Shows improved agreement and smaller α_0 values with inclusion of calculated TDOS. Quality of agreement judged only for *near-threshold* region of L_3 edge data. Disagreement above 72.7 eV for L_2 edge is due to self-absorption.

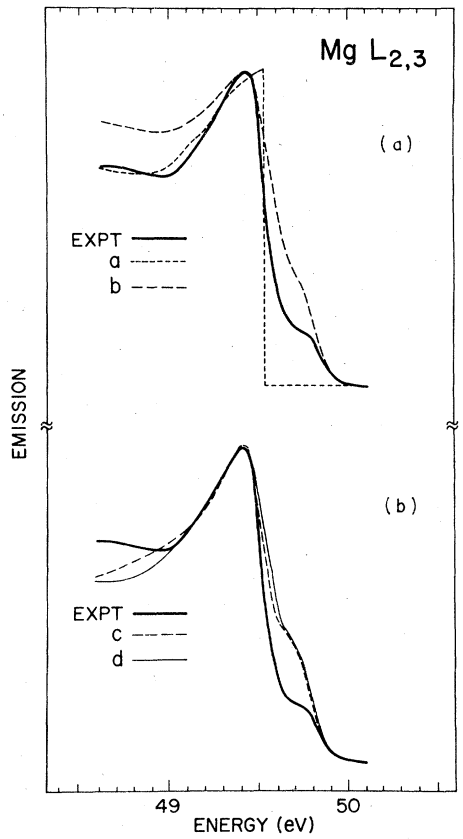

FIG. 15. Analysis of Mg $L_{2,3}$-emission data from Neddermeyer, Ref. 31, taken at 300 K. For full description of fitting curves see Table III. (a) Shows unbroadened calculated TDOS closely resembles data, but with appropriate broadening a positive threshold exponent α_0 is still required. (b) Shows need for both positive α_0 and TDOS. Agreement is judged only for *near-threshold* region of L_3-edge data. Disagreement above 49.4 eV for L_2 edge is due to self-absorption.

TDOS from Fig. 3 is used. The agreement with the data is excellent, indicating that the TDOS structure contributes a significant (but not dominant) fraction of the edge peaking (see Fig. 5). Error limits of ±0.02 for α_0 are determined from curves *c* and *d*, containing $\alpha_0 = 0.15$ and 0.19, respectively.

4. Mg $L_{2,3}$

The data of Neddemeyer[31] taken at 300 K are shown as a solid line in Fig. 15. Curve *a* is the calculated TDOS from Fig. 3 *without* any broadening or many-body peaking. Note the close overall similarity of its shape to the data. Curve *b* is the result of convoluting curve *a* with a Lorentzian lifetime width of 0.02 eV, a Gaussian phonon broadening of 0.11 eV, and a Gaussian spectrometer broadening of 0.10 eV.[31] It also includes the L_2 component at half the intensity of the L_3 component and at higher energy by the spin-orbit splitting of 0.28 eV.[77] Despite the peaked nature of the TDOS, the striking disagreement of curve *b* with the data illustrates the need for invoking a many-body correction.

In Fig. 15(b) we show how important the many-body effects are relative to the TDOS. Curve *c* contains the same broadenings as curve *b* except that it assumes a constant TDOS and requires a threshold exponent of $\alpha_0 = 0.32$ and $\alpha_2 = -0.12$ in order to obtain agreement with the data in the near-threshold region. As with the Mg $L_{2,3}$-absorption data, we take $|A_2/A_0|^2 = 0.33$ and determine α_2 iteratively (its effect is small). Curve *d* is the same as curve *b*, i.e., with the calculated TDOS, but with $\alpha_0 = 0.18$ and $\alpha_2 = -0.12$. Excellent agreement with the data is obtained.

The precision of α_0 for curve d is estimated to be ± 0.02 to allow for the uncertainty in $|A_2/A_0|^2$ and in the position and intensity of the L_3 edge (which are affected by the self-absorbed L_2 component). Comparison of curves c and d graphically illustrate the importance of considering both TDOS and many-body effects: without the former α_0 is very large, and without the latter there is no agreement with the data.

V. DISCUSSION

The primary goal of this work is to test critically the validity of the MND theory[5,8] in quantitatively explaining the shape of x-ray absorption and emission edges in the simple metals Li, Na, Mg, and Al. This statement contains several points which require some elaboration. (a) It is only in the *edge* region of the data that the MND theory can be tested, in part because its solutions are valid only in the limit of small excitations,[50-52] but also because uncertainties in the background and in the TDOS rapidly increase away from the edge. Accordingly, in Sec. IV we defined a "near-threshold" region of $\lesssim 0.5$ eV from the edge in which our analysis of the data was restricted. (b) The simple metals were chosen because of their closest approximation to the free-electron picture in which the MND theory is expected to be most appropriate. Contrary to suggestions in previous works,[22,108,109] the study of alloys and semiconductors involving these simple metals is, in our opinion, either inappropriate (unphysical) or too complicated to analyze meaningfully. (c) Despite the comparative simplicity of these metals, a quantitative evaluation of the many-body effects in the edge data must necessarily include the other effects as well. These have been discussed in Sec. II and include hole-phonon coupling, lifetime broadening, TDOS structure, and spin-dependent exchange. (d) A critical test of the MND theory must demonstrate that the results of these quantitative edge analyses are completely consistent with and supported by other experiments and theoretical calculations. This last point forms the basis of this section and is, ultimately, the essential purpose of this paper.

We have divided this section into four subsections. In V A we compare the one-electron results obtained from our x-ray absorption edge analyses with those obtained from x-ray photoemission measurements and from theory. In V B we perform the same comparison with the many-body x-ray threshold exponents. In V C we compare both our one-electron and many-body edge results with those obtained from other analyses of the same x-ray absorption and emission-edge data. In V D we discuss our results in terms of those obtained from other experiments and other theoretical correlations.

A. Non-MND-related effects: Comparison of x-ray edge results with x-ray photoemission and with theory

Of all the experimental techniques that fall within the domain of the MND theory, x-ray photoemission spectroscopy (XPS) is by far the easiest to interpret. The initial state is the ground state, the final state is one with a high-energy electron which can in general be thought of as noninteracting with the remaining system, and the dipole selection rules governing the excitation do not introduce structure because of the continuum nature of the final state. In x-ray absorption spectroscopy (XAS), on the other hand, the initial state is the ground state, but the final state contains a very low-energy electron which both interacts with the many-body system and which introduces structure in the measured spectrum by way of the TDOS. The difference in the many-body interactions in the final state between XAS and XPS is discussed more in Sec. V B below, but for this section it is important to realize the absence of two complicating effects in XPS that are present in XAS: spin-orbit exchange (not direct exchange, however) and TDOS structure. This means that XPS offers a direct experimental cross check on the other two effects which are present in both techniques, namely, core-hole lifetime broadening and hole-phonon coupling. The reason for comparing XPS with XAS and not x-ray emission spectroscopy is that the latter generally contains either the inherent effects of incomplete phonon relaxation (see Sec. II C) or the instrumental effects of self-absorption (see Sec. II F).

1. Lifetime and phonon broadening

In a previous XPS line-shape analysis of the core levels in Li, Na, Mg, and Al, Paper I,[37] both of these quantities were determined and compared with existing theoretical calculations. Very good agreement was obtained for the experimental and theoretical $1s$,[105-107,110] and $2p$,[111] lifetimes in all four metals and for the phonon broadening values in Na and Al.[112] (The $2s$ lifetimes, which are not relevant here, were not in good agreement.[111]) No temperature-dependent phonon theory exists for Mg, while all existing theories[27,28,65,112-114] failed to explain quantitatively the phonon broadening magnitudes in Li. Since detailed discussion of the XPS-theory comparison is given in I, we present here only the comparison of lifetime and phonon broadening values determined empirically between XPS and

TABLE IV. Comparison of x-ray photoemission (XPS) and x-ray absorption (XAS) results for phonon broadening, Γ_{ph}, and lifetime broadening, Γ_{n_l} (FWHM values in eV).

	Temp. (K)	Γ_{ph} XPS[a]	Γ_{ph} XAS[b]	Γ_{n_l} XPS[a]	Γ_{n_l} XAS[b]
Li 1s	4		0.18 ± 0.02[d]		
	80[c]	0.23 ± 0.04	0.21 ± 0.02[e]	0.04 ± 0.03	
	300	0.32 ± 0.03	0.33 ± 0.02[d]	0.03 ± 0.03	
	440	0.36 ± 0.03	0.38 ± 0.02[d]	0.03 ± 0.03	
Na 1s	300			0.28 ± 0.03	
2s	300	0.15 ± 0.04		0.28 ± 0.03	
2p	80[c]		0.09 ± 0.02[f]		$0.01^{+0.02}_{-0.01}$[f]
	300	0.17 ± 0.04		0.02 ± 0.02	
Mg 1s	300			0.35 ± 0.03	
2s	300	0.16 ± 0.04		0.46 ± 0.03	
2p	80[c]	0.14 ± 0.04	0.07 ± 0.02[f]	0.03 ± 0.02	0.02 ± 0.02[f]
2p	300	0.16 ± 0.04		0.03 ± 0.02	
Al 1s	300				0.47 ± 0.04[g]
2s	300	0.05 ± 0.05		0.78 ± 0.05	
2p	80[c]		0.07 ± 0.02[f]		0.04 ± 0.02[f]
2p	300	0.05 ± 0.05		0.04 ± 0.02	

[a] From Paper I, Ref. 37. Listed values do not include effects of phonon recoil or instrumental broadening. Quoted errors reflect accuracy (includes all known uncertainties).

[b] This work.

[c] Temperature rounded off. XPS temperature quoted as 90 K, XAS quoted as 77 K.

[d] Data from Ref. 40. Quoted error is precision (instrumental uncertainty unspecified).

[e] Data from Ref. 32. Quoted error is precision (instrumental uncertainty unspecified).

[f] Data from Ref. 103. Instrumental resolution negligible.

[g] Data from Ref. 31. Γ_{1s} obtained using $\Gamma_{ph} = 0.07 \pm 0.02$ eV from Al $L_{2,3}$ data of Ref. 103.

XAS. This is given in Table IV. Wherever comparisons are possible, the agreement is generally very good to excellent (lifetimes of a given core hole measured at different temperatures can be compared). Only in the case of the 80-K Mg-2p data is there not significant overlap in the two determined phonon broadening values. The reader should be aware of the small total uncertainties quoted in Table IV.

The importance of the comparisons shown in Table IV is that they (a) serve to establish good agreement between the XAS values and theory (since the XPS results agree well with theory), and (b) allow the other effects determined from our absorption- and emission-edge analyses, namely, spin-orbit exchange in absorption (see below) and the threshold exponents in absorption and emission (see Sec. V B), to be compared with theory and with other experimental results without concern about the possibility that incorrect lifetime and phonon broadening values may be falsifying those comparisons. The final evaluation of the importance of phonon and lifetime broadening in the x-ray edge data is made in Sec. V B.

2. *Transition density of states*

Comparisons between our calculated TDOS and those of Gupta and Freeman for Na,[34] and Mg,[33] and those of Smrčka for Al,[90] have been made in Sec. III. The disagreement in the case of the Mg TDOS was pointed out there and in Sec. IV, where it was shown that a somewhat inaccurate band-structure[33] led to a spurious peak at E_F and an exaggerated structure at about 1 eV above E_F. Good agreement for Na and Al was obtained. The most important feature of our own band-structure calculations is that they are particularly reliable near the Fermi level where their effects are most important in evaluating the MND theory. This statement remains valid even though initial-state TDOS calculations are used because (a) for x-ray emission these are most appropriate (see Sec. II A), and (b) for x-ray absorption the presence of a core hole should not greatly affect the TDOS within the chosen narrow region of energy near E_F (see Sec. IV). The assessment of the calculated TDOS's contribution in the x-ray edge data are deferred to Sec. V B.

3. *Spin-dependent exchange*

In Sec. II E we discussed two general classes of spin-dependent exchange effects in x-ray absorption spectra, one associated with direct exchange, which affects the magnitude of the threshold ex-

ponents by making the phase shifts spin dependent, and another associated with spin-orbit exchange, which affects the intensity ratio of the L_3 and L_2 spin-orbit components by spin-flip scattering. Since the former deals with the many-body phase shifts described in Sec. V B, we focus here only on the spin-orbit exchange process.

From our analyses of the $L_{2,3}$-absorption-edge data in Sec. IV we found that only Na had a non-negligible spin-orbit exchange energy Δ defined in Eq. (2.7). The reason for this was briefly given in Secs. II E and III: the s-like character of the valence wave functions at E_F which participate in the $2p$-$3s$ exchange is largest in Na according to our TDOS calculations. There are three cross checks of our results on the relative and absolute magnitudes of Δ. (i) Our empirical determination of Δ for Na is 0.21 ± 0.05 eV, and this agrees very favorably with Onodera's empirically determined value of 0.23 eV,[44] using the same data.[103] Kunz *et al.*[103] and Mahan,[15] while not attempting an analysis of Δ, also observed a significant discrepancy in the $L_3 : L_2$ ratio of Na. Similarly, using their own Na $L_{2,3}$-absorption data, Callcott *et al.*[45] reported an appreciable deviation of that ratio from the theoretical 2:1 value. (ii) For Mg and Al we found values of Δ that were significantly smaller than that in Na and which were, in fact, negligible within experimental error. This result for Mg is in agreement with the analysis by Slowik[109] on the same data.[103] (iii) Almbladh and von Barth[101] have made two different *a priori* calculations of the spin-orbit exchange magnitudes in Na, Mg, and Al. First, they expressed the spin-orbit exchange mixing by a dimensionless "Onodera parameter" a which they write as

$$a = \tfrac{2}{3}\, \nu_s(E_F) G_1(2p, E_{Fs}), \tag{5.1}$$

where ν_s is the s-wave density of states and G_1 is the relaxed, Fermi surface value of the Slater exchange integral. In the notation of Onodera's equations, (2.7), a is given by

$$a = (3/4E_F)\Delta . \tag{5.2}$$

Second, these authors[101] extended the formulation of a in terms of spin-dependent s-phase shifts according to Eq. (2.2),

$$a' = (2/\pi)(\delta_0^+ - \delta_0^-), \tag{5.3}$$

where they maintain that a' is equivalent to a to lowest order in the core-valence exchange interaction. These authors have then calculated a and a' for Na (they are, in fact, comparable) and get good agreement with our and Onodera's empirical values determined from Eq. (5.2) ($a_{\text{calc}} = 0.057$, $a'_{\text{calc}} = 0.051$; $a_{\text{expt}} = 0.051 \pm .011$). Also, they have calculated a for Al (0.025) and a' for Mg (0.028) and find that they are comparable with each other and that both are about half as large as that for Na. This result agrees qualitatively with our empirical results.

Summarizing Sec. V A, we have shown that the effects of phonon and lifetime broadening, TDOS, and spin-orbit exchange associated with x-ray edge measurements—which are not at all related to the MND theory but which must be accurately known and properly included in the data analysis in order to assess the MND theory—are consistent with and supported by independent empirical x-ray photoemission results and by independent theoretical calculations.

B. Many-body effects: Comparison of x-ray absorption- and emission-edge results with x-ray photoemission and with theory

The purpose of this section is to discuss the results of our analyses in Sec. IV, with particular emphasis on the x-ray threshold exponents α_l described by the MND theory in Eqs. (1.1)–(1.3). As stated throughout the text, this is only possible *after* having correctly considered the other *non*-MND-related effects in the x-ray absorption or emission process (see Sec. V A).

The organization of this section is as follows. We first show how the x-ray threshold exponents α_0 and α_1 are related to each other and to the singularity index α using the Friedel sum rule, Eq. (1.4). These are the compatibility relations first discussed by Dow[20] for s and p phase shifts only. In our treatment we have extended this to include d phase shifts as well. This inclusion does not have dramatic effects in Na and Mg, but for Al will be seen to be essential for achieving quantitative compatibility. The x-ray threshold results of Sec. IV are then considered separately for each metal and with these three tests of increasing rigor are performed on the MND theory. First, we compare experimental α values (determined from XPS measurements) with theoretical calculations (one known versus theory). Second, the experimental α's plus the Friedel sum rule assuming s and p phase shifts only are used to predict α_0, α_1, δ_0 and δ_1. The threshold exponents are then compared with our experimental values determined from the x-ray edge measurements (one known plus one equation versus a second known). Third, the experimental α's plus the experimental α_0 values plus the Friedel sum rule assuming s, p, and d phase shifts are used to predict α_1, δ_0, δ_1, and δ_2. The phase shifts are then compared with theoretical calculations (two knowns plus one equation versus

theory) and with the phase shifts predicted from only α alone (i.e., assuming two phase shifts). For Na and Mg we cannot compare α_1 with experiment because their K edges have not been measured; we can only compare the α_1 values predicted from either a two or three phase shift analysis. For Al, however, we can compare the α_1 values predicted from both analyses with those values empirically determined from the absorption and emission K edges. This is the most rigorous test possible (two knowns plus one equation versus a third known). Furthermore, we can use all three experimental values of α, α_0, and α_1 plus the Friedel sum rule to predict δ_0, δ_1, δ_2, *and* δ_3. The f-phase shift must be positive due to the attractive nature of the electron-hole scattering, and must also be small due to the nature of the Al conduction band. These physical constraints on δ_3 will be seen to provide an extremely sensitive test on the compatibility of α, α_0, and α_1.

1. Compatibility relationships

An important simplification in the study of the free-electron-like metals Li, Na, Mg, and Al is that their conduction bands are predominantly composed of s- and p-like wave functions. This means that the dominant scattering phase shifts in these metals are also of this symmetry. With δ_0 and δ_1 as the only unknown quantities, an XPS measurement of the singularity index α and the Friedel sum rule, Eq. (1.4), uniquely determine the threshold exponents α_0 and α_1.[38,39] An important qualification, however, is that this correlation is only possible provided the measured α is not smaller than the minimum value $\alpha_{\min}$ defined by

$$\alpha_{\min} = 1/m\,, \tag{5.4}$$

where

$$m = \sum_{l=0}^{l_{\max}} 2(2l+1)\,.$$

For s- and p-type screening ($l_{\max}=1$, $\alpha_{\min}=\frac{1}{8}$; if d-type screening is also involved ($l_{\max}=2$), $\alpha_{\min}=\frac{1}{18}$. The role of δ_2 becomes clear in a plot of α_0 and α_1 as a function of α for given fractions of δ_2 contributions (we will see below that $\delta_l \ll 1$ for $l>2$).

In Fig. 16 we show a plot of α_0 and α_1 vs α for different δ_2/δ_1 ratios. The α_0 vs α curves are shown as solid lines, and the α_1 vs α curves are shown as dot dashed. For clarity, the curves are terminated where α_0 and α_1 become of comparable magnitude, and we show only the region described by δ_0 and $\delta_1>0$ (corresponding to the attractive potential between core hole and screening electron). The horizontal bars give the range of α values determined from the XPS measurements reported in I.[37]

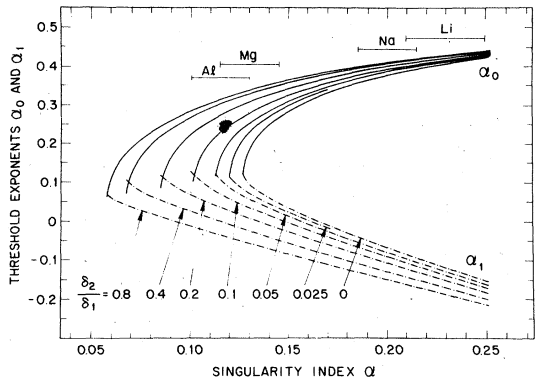

FIG. 16. X-ray threshold exponents α_0 and α_1 as a function of x-ray photoemission singularity index α. Compatibility curves calculated with all positive s, p, and d phase shifts. Two phase shift analysis indicated by $\delta_2/\delta_1=0$ contours. For clarity, curves are terminated where α_0 and α_1 are of comparable magnitude for given δ_2/δ_1 ratio. Experimental range of α values from Ref. 37 are indicated by horizontal bars for Li, Na, Mg, and Al.

Although a detailed comparison of α with α_l's will be given below for each metal, Fig. 16 shows several qualitative features which are worth mentioning here. For Li and Na the measured α values determine α_0 and α_1 rather unambiguously because of the relatively small contributions of δ_2. Both metals are predicted to have fairly large positive α_0's and only small negative α_1's. For Mg and Al, on the other hand, the threshold exponents are not well defined by this approach. Despite the uncertainties in α_l, however, it is evident that the α_1 values are predicted to be close to zero. This, of course, does not imply that the δ_l's themselves are zero (as has been suggested in several works[23,38]), but rather that the two competing Mahan enhancement and Anderson suppression terms in Eq. (1.2) are of comparable magnitude.

An alternate way of relating threshold exponents to singularity indices is obtained by plotting fixed α curves as a function of both α_0 and α_1. This is shown in Fig. 17, where we have divided the region of $\frac{1}{18}\leq\alpha\leq\frac{1}{8}$ and $\frac{1}{8}\leq\alpha\leq\frac{1}{2}$ in the top and bottom halves, respectively.[115] These compatibility plots include δ_0, δ_1, and δ_2 phase shifts of both positive and negative sign. In the following discussions, we show expanded sections of these plots that are relevant to the metal under question (except for Li where there is incompatibility).

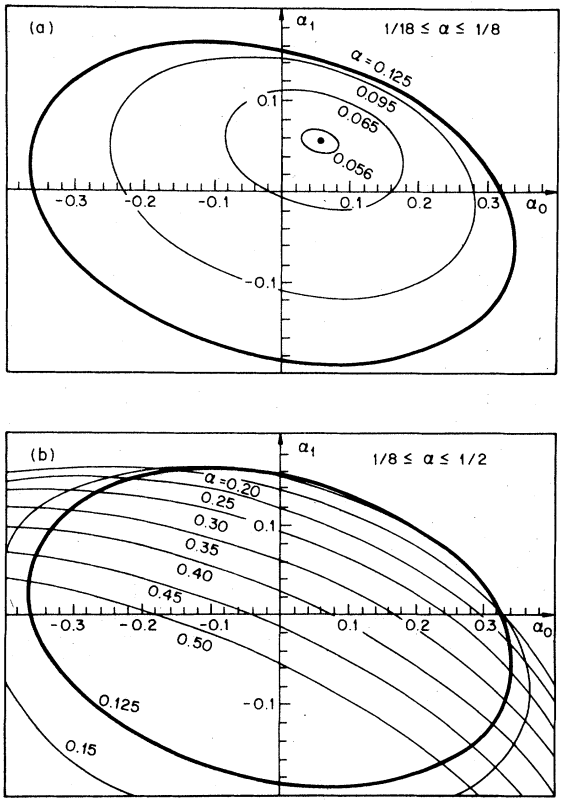

FIG. 17. General compatibility plots relating x-ray threshold exponents α_0 and α_1 with contours of given x-ray photoemission singularity index α. Curves are calculated using s, p, and d phase shifts of both positive and negative sign. Note from separate α regions shown in (a) and (b) that a point in the (α_0, α_1) plane corresponds to two values of α.

2. *Lithium*

In Sec. IV we found that very satisfactory fits to the Li K-edge data were obtained with $\alpha_1 \sim 0$. Significant deviations from this result assuming other values for Γ_{ph} or Γ_{1s} were unacceptable. On the other hand, it is also found from Fig. 16 that using the experimentally determined value of $\alpha = 0.23 \pm 0.02$ from XPS measurements[37] plus Eq. (1.4) assuming only s and p phase shifts predicts a value of $\alpha_1 = -0.11 \pm 0.03$. Inclusion of d phase shifts only makes α_1 more negative. This result directly demonstrates the incompatibility between the experimental and predicted α_1 values. Since it is not possible to predict δ_l's based on the empirical α and α_1 values plus the sum rule, we can only predict the δ_l's based on α alone. These, along with the experimental α and α_1 values, are compared with various theoretical calculations (Refs. 17, 18, 42, 57, 74, 96, 98–101) in Table V. The point of this comparison is simply to confirm the incompatibility of the experimental results with those of all the theories except the last two, which attempt to include the effects of direct spin-dependent exchange.

The inability of the MND theory to explain the Li K-edge data was first demonstrated by the electron energy loss experiments of Ritsko *et al.*[41] By looking at nonzero electron momentum transfer they were able to measure non-dipole-allowed transitions into conduction bands of s symmetry and thus measure α_0 as well as α_1. The difference between the α_0 and α_1 values determined from their data was very close to zero, whereas all the calculations up to that time, see Table V, predicted $|\alpha_1 - \alpha_0| > 0.4$. It was this result that stimulated Girvin and Hopfield (GH)[74] to reconsider the earlier suggestion by Kato *et al.*[73] of the possible importance of direct spin-dependent exchange.

The qualitative features of GH's approach were discussed in Sec. II E. In Table V we list the results of their calculations. Note that $|\alpha_0 - \alpha_1|$ is now considerably reduced to only about 0.2 and that α_1 is itself close to zero. The importance of this result is that is suggests that direct spin-dependent exchange could have a significant effect on the MND threshold exponents in Li. From this result it would follow that conclusions about the values of these exponents of the MND theory itself without exchange must be viewed as inappropriate.

The theme of this work is to test the quantitative predictiveness of the MND theory, and in this regard the success of GH's approach in reconciling the validity of the MND theory for Li must be judged as being only qualitative for two reasons. First, although $|\alpha_0 - \alpha_1|$ is reduced, it still is not sufficiently close to zero. Second, although GH's calculated value of $\alpha = 0.16$ is larger than that calculated in the absence of exchange, 0.11, it still is substantially below the measured XPS value of 0.23 ± 0.02.[37] These difficulties have been recently considered by Almbladh and von Barth,[101] who recalculated the spin-dependent phase shifts within GH's formalism using their own spherical-solid model.[96] Their results are listed in Table V below those of GH. Their calculated $\alpha = 0.25$ is now in very good agreement with the experimental value, but the threshold exponents are somewhat less successful. The quantity $|\alpha_0 - \alpha_1|$ is 0.13 and α_0 is only -0.02, both significant improvements, but $\alpha_1 = -0.15$ is too large and negative. This remaining discrepancy is *not* due to inaccuracies in the calculated phase shifts, because these authors have not only calculated a value of α for Li which agrees very well with experiment[37] but they have calculated α for Na—where direct exchange is not a complication—which also agrees

TABLE V. Comparison between (1) empirically determined, (2) predicted, and (3) theoretically calculated values of singularity indicates α, threshold exponents α_l, and phase shifts δ_l.

	α	α_0	α_1	δ_0	δ_1	δ_2	Reference
Lithium							
(1) Expt.[b]	0.23		~0(Abs)				
(2) Predicted[c]		0.42	−0.11	1.02	0.18		
(3) Theory	0.20	0.41	−0.10	0.95	0.15	0.03	17
	0.18	0.39	−0.08	0.90	0.15	0.03	18(Thomas-Fermi)
	0.15		−0.06		0.14		18(OPW)
	0.33	−0.01	−0.3	0.51	0.05		99
	0.22	0.42	−0.13	1.02	0.14	0.03	42
	0.24	0.43	−0.14	1.07	0.17	0.01	98 and private communication
	0.16	0.27	0.05	0.67	0.33	−0.02	96
	0.20	0.41	−0.11	0.96	0.15	0.02	100
	0.16	0.23	0.08	0.61	0.37	−0.02	57
	0.11	0.06	0.14	0.26	0.39	0.03	74
	0.16	−0.16	0.04	0.02	0.33	0.03	74[e]
	0.25	−0.02	−0.15	0.35	0.16	−0.02	101[c]
Sodium							
(1) Expt.[b]	0.20	0.37(Abs)					
(2) Predicted[c]		0.39	−0.06	0.92	0.22		
Predicted[d]			−0.04(Abs)	0.90	0.25	~0	
(3) Theory	0.19	0.40	−0.09	0.92	0.16	0.02	17
	0.20	0.41	−0.11	0.96	0.15	0.03	18
	0.12	0.33		0.70			18
	0.14	0.34	−0.02	0.76	0.20	0.04	42
	0.21	0.39	−0.07	0.93	0.22	0.00	98
	0.20	0.38	−0.05	0.90	0.23	0.00	96[f]
	0.14	0.34	−0.02	0.75	0.19	0.04	100[f]
	0.17	0.38	−0.06	0.87	0.17	0.03	100[g]
	0.54	0.10	−0.10	−2.13	0.68	0.18	57
	0.12	0.28	0.04	0.62	0.25	0.04	74[e]
	0.20						101[e]
Magnesium							
(1) Expt.[b]	0.13	0.23(Abs)					
		0.18(Em)					
(2) Predicted[c]		0.21	0.09	0.53	0.35		
Predicted[d]			0.08(Abs)	0.57	0.34	~0	
			0.10(Em)	0.49	0.36	~0	
(3) Theory	0.10	0.25	0.06	0.55	0.25	0.06	42
	0.13	0.28	0.05	0.63	0.27	0.03	98 and private communication
	0.10	0.27	0.04	0.56	0.20	0.05	100[f]
	0.12	0.32	0.00	0.70	0.19	0.04	100[g]
	0.12	0.19	0.10	0.47	0.34	0.02	57
	0.12	0.17	0.13	0.46	0.36	0.01	101
	0.12	0.15	0.11	0.44	0.33	0.01	101[e]
Aluminum							
(1) Expt.[b]	0.12	0.18(Abs)	0.10(Abs)				
		0.17(Em)	0.12(Em)				
(2) Predicted[c]		[h]	[h]	[h]	[h]	[h]	
Predicted[d]			0.10(Abs)	0.46	0.34	0.02	
			0.11(Em)	0.45	0.34	0.02	

TABLE V. (*Continued*)

	α	α_0	α_1	δ_0	δ_1	δ_2	Reference
(3) Theory	0.09	0.24	0.05	0.53	0.23	0.07	42
	0.11	0.25	0.06	0.56	0.26	0.03	98 and private communication
	0.13	0.06	0.14	0.30	0.43	0.01	96[f]
	0.16	0.05	0.14	0.32	0.47	−0.01	96[g]
	0.08	0.22	0.06	0.46	0.21	0.06	100[f]
	0.10	0.28	0.03	0.59	0.20	0.05	100[g]
	0.10	0.13	0.12	0.36	0.35	0.03	57

[a] All values rounded off to nearest hundredth.

[b] Singularity indices α from Paper I (Ref. 37), threshold exponents α_l from this work.

[c] Predicted threshold exponents α_0 and α_1 and phase shifts δ_0 and δ_1 determined from empirical singularity indices α and Friedel's sum rule, Eq. (1.4), assuming $\delta_l = 0$ for $l > 1$.

[d] Predicted threshold exponent α_1 and phase shifts δ_0, δ_1, and δ_2 determined from empirical singularity index α, empirical (absorption or emission) threshold exponent α_0, and Friedel's sum rule, Eq. (1.4), assuming $\delta_l = 0$ for $l > 2$ and $\delta_2 \geq 0$.

[e] Quoted values are those corresponding to singlet state containing spin-dependent phase shifts.

[f] Quoted values are those obtained for $L_{2,3}$ holes.

[g] Quoted values and those obtained for K holes.

[h] α_l and δ_l cannot be predicted because α_{expt} is smaller than $\alpha_{\text{min}} = 0.125$ determined from a two-phase shift analysis [see Eq. (5.4)].

extremely well with experiment. These calculated α results should be contrasted with those of GH for Li and Na (see Table V).

Summarizing our discussion of Li, we conclude that the lack of quantitative agreement between the theoretical and experimental threshold exponents lies in the fact that the formalism of GH for describing direct exchange requires additional refinements. This has already been pointed out most recently by Kaga,[75] by Andereck and Iche,[76] and by Yoshimori and Okiji.[76] The importance of direct exchange in Li is still suggestive[41,74,75,101] in spite of the present lack of quantitive theoretical results for describing it. The same statement applies to phonon broadening in Li: no theory has as yet accurately accounted for its magnitude.[37] Overriding the details of the exchange corrections to the MND theory, however, is the following message. It is only in Li (as we shall see below) in which the MND theory is not quantitatively successful. The reason for this is at least partially due to the existence of direct exchange.

3. *Sodium*

In Sec. IV we saw that a value of $\alpha_0 = 0.37 \pm 0.03$ gave an excellent fit to the Na $L_{2,3}$ data[103] in the near-threshold region—provided spin-orbit exchange[44] was considered. Without such exchange, it was possible to fit only an unacceptably small (~0.2 eV) region of the L_3 edge, and the $L_3 : L_2$ intensity ratio was seen to be fit very poorly. The need for including spin-orbit exchange was clearly demonstrated in Sec. IV by the observation that the $L_3 : L_2$ intensity ratio does not equal the theoretical value of 2. The magnitude of the exchange energy determined from our analysis was shown in Sec. V A to be in accord with other independent cross checks. The neglect of the $|A_2|^2$ term in Eq. (1.1) in our analysis of the Na data and its negligible effect in determining the magnitude of α_0 and the exchange energy were already discussed in the beginning of Sec. IV. Phonon and lifetime broadenings and TDOS structure were shown to be necessary ingredients in the quantitative analysis of the data, but of only secondary importance in qualitatively determining the shape of the edge. Efforts were made to adjust these other parameters such that a value of $\alpha_0 = 0.26$,[22] would be acceptable, but without success (see Sec. V C below).

The XPS measurements of $\alpha = 0.20 \pm 0.015$ (Ref. 37) along with the sum rule using only δ_0 and δ_1, see Fig. 16, predicts a value of $\alpha_0 = 0.385^{+0.022}_{-0.028}$. The excellent agreement of this result with our experimental determination of $\alpha = 0.37 \pm 0.03$ is a striking confirmation of the MND theory in Na. The small margin of uncertainty allowed in the predicted α_0 value due to the negligible d phase shift contribution makes this comparison particularly reliable.

Comparison of the experimental α from XPS[37] with the results from a variety of theories (Refs. 17, 18, 42, 57, 74, 96, 98, 100, and 101), see Table V, shows overall good agreement, especially with those models assuming a point charge in a free-electron medium. A detailed discussion of the various theories and their results is beyond our scope here, but one point worth mentioning is that the results of Girvin and Hopfield[74] and of Almbladh and von Barth,[101] while differing from

each other, both show that inclusion of direct exchange is of negligible importance in Na. This result is significant because it allows Onodera's Eq. (2.7),[44] which considers only spin-orbit exchange, to be used with confidence [for further discussion on the validity of Eq. (2.7) in Na, see Secs. IV and V A].

From Fig. 16 and assuming $\delta_2 = 0$, a value of $\alpha_1 = -0.062^{+0.027}_{-0.025}$ is predicted from the experimentally determined α. Since no measurements of the Na K-absorption or emission edges have been made, we cannot test this prediction at this time. We can, however, determine more realistic and stringent bounds on the acceptable (i.e., compatible) values of α_1 that should be measured based on our experimental values of α and α_0. In Fig. 18 we show an expanded view of Fig. 17(b), where we have indicated the range of predicted α_1 values by the lightly shaded region. A value of $\alpha_1 = -0.042^{+0.034}_{-0.055}$ is predicted. We note that this analysis includes d as well as s and p phase shifts, but with either positive or negative sign. The fact that the potential between the core hole and the screening conduction electrons is attractive places the additional compatibility constraint that δ_0, δ_1, and δ_2 all be $\gtrsim 0$. (Although overscreening by s and/or p electrons is possible, which would require the d phase shift to be negative, such a situation is unlikely in the simple sp metals.) In Fig. 18 we have indicated the limiting contour of $\delta_2 = 0$ (the only one of concern in this region) by a solid line. For combinations of α_0 and α_1 above that contour (i.e., in the upper right-hand region of the figure), there are no solutions with real phase shifts. The error limits of α_0 and α, along with the constraint that $\delta_2 \gtrsim 0$, define the overlapping (dark) shaded region of compatibility. It is therefore clear that using either a two or three phase shift analysis, our values of α or (α, α_0) predict the Na K edge to exhibit a very slight rounding due to a many-body effect, with the overall rounding arising predominantly from the Na 1s lifetime width of 0.28 eV (see Table IV).

We have also used our three phase shift analysis to predict values of δ_0, δ_1, and δ_2 (with the constraint that they be positive) and have compared them with theory in Table V. Listed are the δ_l's corresponding to the $(\alpha, \alpha_0, \alpha_1)$ values of $(0.19, 0.37, -0.042)$. It should be borne in mind that these are merely representative. Equally acceptable values can be obtained from the cor-

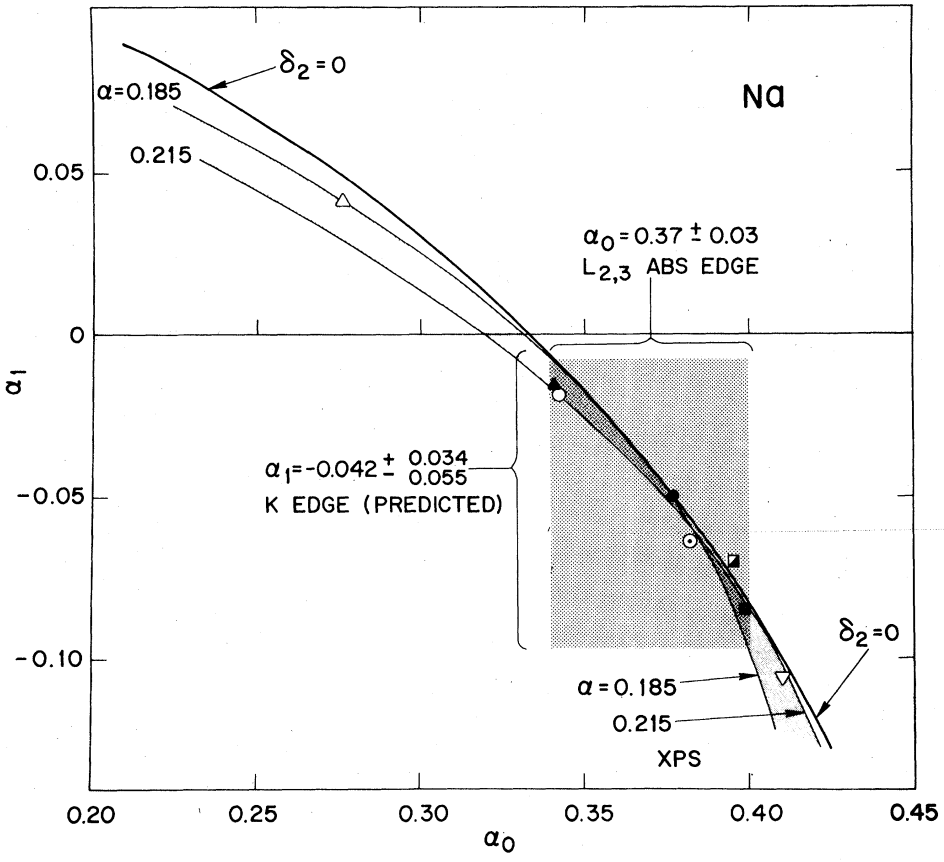

FIG. 18. Compatibility plot using three phase shift analysis for Na relating x-ray threshold exponents α_0 and α_1 with singularity index α. Range of compatibility indicated by intersection of α_0 values (this work) and α values (Ref. 37). Solutions above $\delta_2 = 0$ contour are unphysical, corresponding to imginary δ_2's. Based on this analysis, a range of negative α_1 values are predicted for the K edge. Solid circle corresponds to calculations of Almbladh and von Barth, Ref. 96; solid square to Ausman and Glick, Ref. 17; open triangle to Girvin and Hopfield, Ref. 74; inverted open triangle to Longe, Ref. 18; solid triangle to Mahan, Ref. 42; half-filled square to Minnhagen, Ref. 98; open and dotted circles to Ohmura and Sano, Ref. 100, for L and K holes, respectively. ABS: absorption.

responding (α, α_0, α_1) values that fulfill the condition of compatibility, i.e., that lie within the dark shaded region in Fig. 18. To facilitate comparison of these results with theory we have also included the calculated threshold exponents in Fig. 18. It is seen that the calculations of Almbladh and von Barth[96] are in particularly good agreement with our experimental and predicted results, although those of Ausman and Glick,[17] of Longe[18] (using a Thomas-Fermi potential), and of Minnhagen[98] give very good agreement as well. Only for those calculations which show sizeable d phase shift scattering is there significant discrepancy with experiment.

Summarizing our discussion for Na, its $L_{2,3}$ absorption edge is peaked solely from the many-body effect, which is quantitatively described by the MND theory. This conclusion is based on the excellent agreement obtained between the empirical value of the threshold exponent determined here and that predicted both from independent XPS measurements and from a variety of theoretical calculations. TDOS structure, phonons, and lifetime broadening are negligible. Spin-orbit exchange,[44] however, is definitely important and must be included to obtain a quantitative fit. From our analysis the Na K-emission and -absorption edges are *predicted* to be rounded due to lifetime broadening, with an additional small *rounding* due to the many-body effect. Experimentally observed rounding of this nature would be the first of its kind. As pointed out by Callcott *et al.*[45] the Na $L_{2,3}$-emission edge is complicated by incomplete phonon relaxation.[69,70]

4. Magnesium

In Sec. IV we found that the most acceptable fit to the $L_{2,3}$ data of Mg in the near-threshold region was $\alpha_0 = 0.23 \pm 0.02$ for the absorption edge[103] and 0.18 ± 0.02 for the emission edge.[31] The s-threshold exponents α_0 were determined with the inclusion of the d-threshold exponent $\alpha_2 = -0.12$. The contribution of d-transition probability relative to the s-transition probability, $|A_2/A_0|^2$, was taken to be 0.33, intermediate between the various calculated values[33,51,97] in Table I. The inclusion of the $|A_2|^2$ term made about a 10% correction to the value of α_0, and this correction was neither sensitive to small changes in α_2 or $|A_2|^2$ (see Sec. IV for further details). Lifetime, phonon, exchange, and TDOS contributions were all included in the data analysis. The first three were seen to have a negligible effect on the qualitative shape of both edges; the

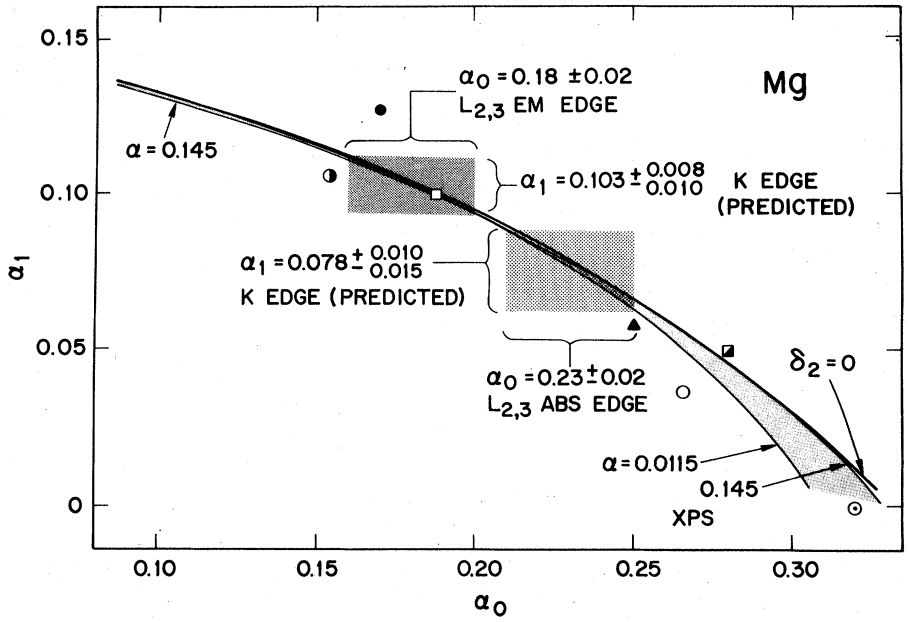

FIG. 19. Compatibility plot using three phase shifts for Mg relating threshold exponents α_0 and α_1 with singularity index α. Ranges of compatibility indicated by intersection of α_0 values (this work) and α values (Ref. 37). Solutions above $\delta_2 = 0$ contour are unphysical. Based on this analysis, narrow range of positive α_1 values are predicted for the K edge. Solid and half-filled circles correspond to calculations of Almbladh and von Barth, Ref. 101, for $L_{2,3}$ holes with and without spin-orbit exchange, respectively; open square to calculations of Bryant and Mahan, Ref. 57; solid triangle to Mahan, Ref. 42; half-filled square to Minnhagen, Ref. 98; open and dotted circles to Ohmura and Sano, Ref. 100, for L and K holes, respectively. EM: emission, ABS: absorption.

first two were important in obtaining a quantitatively meaningful fit.

The TDOS structure in the $L_{2,3}$-absorption-edge data was seen to be very small, but in the $L_{2,3}$-emission-edge data was actually quite significant. This fact highlights the importance of having an accurate calculated TDOS, since a small exaggeration of the peaking at E_F (see Figs. 3 and 5) could affect the determination of α_0. Recall (Sec. II A) that we assumed the same initial-state Hamiltonian for calculating both the absorption and emission TDOS. For a comparitively featureless TDOS *near* E_F (such as in Na and Al) this approximation is expected to be quite valid, but for one as structured as that for the Mg $L_{2,3}$-emission edge it is possible that measureable errors could be introduced. Furthermore, from a purely practical point of view, it is not unreasonable to expect some uncertainty in fitting the $L_{2,3}$-emission edge of any metal because of unavoidable self-absorption effects (see Sec. II F) which necessarily limit the degree of precision in uniquely determining α_0. With these facts in mind, and considering the ease with which our analyses are performed using our calculated TDOS, the difference in the α_0 values for the absorption and emission data, 0.23 ± 0.02 and 0.18 ± 0.02, is regarded as acceptable.

The XPS measurement of $\alpha = 0.13 \pm 0.015$ (Ref. 37) enables α_0 to be predicted using Eq. (1.4) and only δ_0 and δ_1, see Fig. 16. From a two phase shift analysis we predict $\alpha_0 = 0.207^{+0.071}_{-0.082}$, which is almost exactly bracketed by the empirical values from our analysis of the absorption and emission data. We are quick to note that the assumption of $\delta_2 = 0$ in Mg should be less reliable than it is in Na, as seen by the diverging curves in Fig. 16 for even small δ_2 contributions. It would therefore be more meaningful to predict α_0 from an independent measurement of α_1. To our knowledge, however, no x-ray absorption experiment of the Mg K edge has as yet been performed. (In Sec. IV we mentioned our reservations about broadening effects on the published Mg $K\beta$ data.[31]) Until Mg K-absorption-edge data are measured and analyzed, the best available cross check of experimental versus predicted α_0's is to use the two phase shift analysis.

Such an analysis has also been used to predict $\alpha_1 = 0.091^{+0.034}_{-0.044}$. As discussed for Na, the reliability of this predicted value and its limits of compatibility can be increased by a three phase shift analysis. The result of this is shown in Fig. 19. As in Fig. 18, we have indicated the contour of $\delta_2 = 0$ which limits the region of physical (non-imaginary) phase shifts. The indicated shaded region determined from the experimental α and α_0 values predicts $\alpha_1 = 0.078^{+0.010}_{-0.015}$ from the absorption data and $\alpha_1 = 0.103^{+0.008}_{-0.010}$ from the emission data. Considering the spread in α_0 values, the total range over which our predicted α_1 values all fall, 0.088 ± 0.023, is actually quite narrow. Thus, our analyses predict that the Mg K edge should be slightly peaked due to the many-body effect; it will, nonetheless, appear predominantly rounded due to the much larger effect of the 0.35-eV lifetime broadening from the 1s level (see Table IV).

Our analysis also predicts δ_0, δ_1, and δ_2 values, and these are listed in Table V. The experimental and predicted α, α_0, α_1, and δ_l values are compared with the results of several calculations[42,57,98,100,101] in Table V. For easier comparison with experiment the theoretical results are shown in Fig. 19. In Table V we have quoted only those phase shifts compatible with the $(\alpha, \alpha_0, \alpha_1)$ values of (0.13, 0.18, 0.08) for emission and (0.13, 0.23, 0.10) for absorption. Other acceptable phase shifts are, of course, allowed within the overlapping shaded regions in Fig. 19. From Table V and Fig. 19 we see that, in general, all of the various theories predict α values in good agreement with experiment, but only the recent results of Bryant and Mahan[57] are compatible with the XPS data and at least one empirical threshold exponent.

Summarizing our discussion for Mg, the $L_{2,3}$-absorption and -emission exponents are not in quantitative agreement with each other. A large part of the reason for this is due to the significant contribution of the peaked TDOS structure in the emission edge, placing a high demand on its required level of accuracy. TDOS structure is of little importance in the absorption edge. Phonon and lifetime broadenings are negligible (as in Na) and so is the magnitude of spin-orbit exchange. Thus, the peaking in the $L_{2,3}$-absorption edge is essentially all due to a many-body effect, while in the emission edge the TDOS makes a significant (though not dominant) contribution. Based on either a two or three phase shift analysis, the Mg K-emission and -absorption edges are *predicted* to be rounded due to lifetime broadening, with an additional small *peaking* due to a many-body response. An accurate determination of this latter effect should set more stringent limits on the acceptable threshold exponents for the $L_{2,3}$ edges.

5. *Aluminum*

In Sec. IV we analyzed the Al K- and $L_{2,3}$-edge data and obtained excellent fits in the near-threshold regions using values of $\alpha_1 = 0.095 \pm 0.015$ and $\alpha_0 = 0.18 \pm 0.02$ for the absorption edges[31,103] and

$\alpha_1 = 0.12 \pm 0.015$ and $\alpha_0 = 0.17 \pm 0.02$ for the emission edges.[31] The α_0 values were determined with the inclusion of the d-threshold exponent $\alpha_2 = -0.10$. Its contribution is determined by $|A_2/A_0|^2$ in Eq. (1.1), which was taken to be 0.52 (Ref. 96) (a value intermediate between several results[90,97] listed in Table I). Inclusion of the d contribution made about a 15% correction to the values of α_0, and this correction was not very sensitive to small changes in either α_2 or $|A_2|^2$ (see Fig. 7 and Sec. IV). Phonon broadening and spin-orbit exchange effects were included in the analyses and were found to contribute insignificantly to the threshold exponents. In the K-edge spectrum, lifetime broadening was by far the dominant source of rounding; in fact, the positive α_1 contributed a slight peaking to the data. The TDOS structure contributed a small rounding to the K-absorption and -emission edges (more in absorption), a small peaking to the $L_{2,3}$-absorption edge, and a sizeable peaking to the $L_{2,3}$-emission edge. This latter peaking, however, was significantly less than the contribution to the Mg $L_{2,3}$-emission spectrum.

The absence of *strong* complicating *non*-many-body effects in the Al $L_{2,3}$ data—such as TDOS structure (as in the Mg $L_{2,3}$-emission edge), spin-orbit exchange (as in the Na $L_{2,3}$-absorption edge), and incomplete phonon relaxation (as in the Na $L_{2,3}$-emission edge)—and the reasonable approximation (see Sec. II A) that the TDOS structure within the narrow and comparitively featureless near-threshold region is not greatly affected by the presence of a core hole allows for the important test of one of the MND theory's most basic predictions.[5,8] This states that the many-body response in the absorption process should simply be the time-reversed response in emission and should therefore be the same in magnitude. The extremely good consistency between the absorption and emission $L_{2,3}$-edge threshold exponents, 0.18 ± 0.02 and 0.17 ± 0.02, and even the absorption and emission K-edge exponents, 0.095 ± 0.015 and 0.12 ± 0.015, provides strong support for the theory's basic validity.

The XPS α value of 0.115 ± 0.015 (Ref. 37) is smaller than $\alpha_{\min} = 0.125$ determined from δ_0 and δ_1 alone [see Eq. (5.4)], so it is not possible to predict α_0 or α_1 using a two phase shift analysis as was done for Na or Mg. However, the availability of both the $L_{2,3}$- *and* the K-edge data for Al allows for the most rigorous test of compatibility using a three phase shift analysis: from any two empirical values in the set (α, α_0, α_1), the third is strictly defined by Eqs. (1.2), (1.3), and (1.4). Its comparison with the third empirical

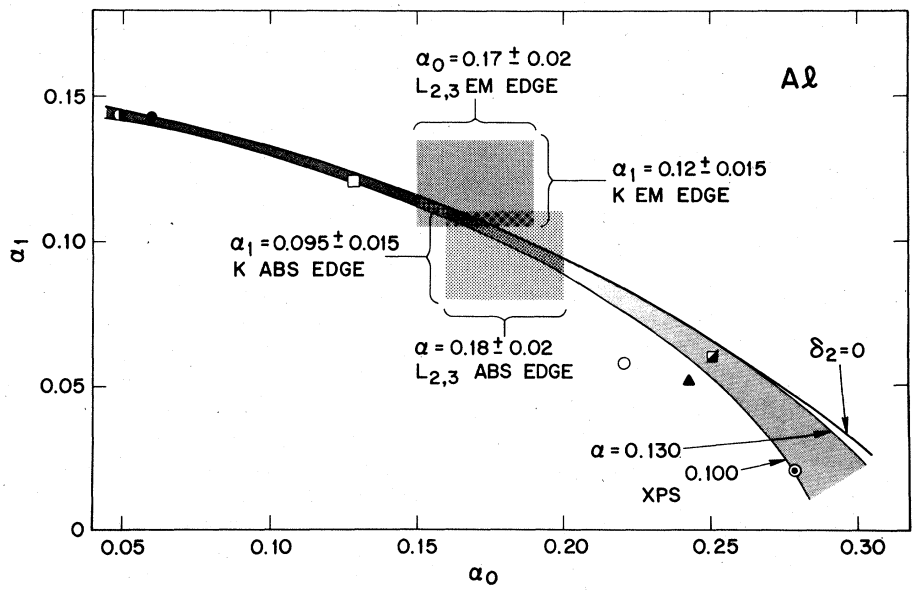

FIG. 20. Compatibility plot using three phase shifts for Al relating threshold exponents α_0 and α_1 with singularity index α. Range of compatibility indicated by intersection of α_0 and α_1 values (this work) and α values (Ref. 37). Solutions above $\delta_2 = 0$ contour are unphysical. Note that all five independent experiments are described by common set of compatible phase shifts. Solid and half-filled circles correspond to calculations of Almbladh and von Barth, Ref. 96, for L and K holes, respectively; open square to calculations of Bryant and Mahan, Ref. 57; filled triangle to Mahan, Ref. 42; half-filled square to Minnhagen, Ref. 98; open and dotted circles to Ohmura and Sano, Ref. 100, for L and K holes, respectively. EM: emission, ABS: absorption.

value, then, provides a direct check on compatibility without making any *a priori* assumptions about the relative magnitudes of δ_0, δ_1, and δ_2.

In Fig. 20 we show an expanded section of Fig. 17(a) appropriate for Al. The contours defined by the limits of α measured in the XPS experiment clearly pass through the shaded rectangles of uncertainty defined by the error limits of both α_0 and α_1 determined in the absorption and emission experiments. This indicates that the results of *all five* independent experiments are in fact compatible.

Having firmly established the necessary condition of compatibility, it is now important to examine in detail the magnitudes of the phase shifts defined by the set of empirical values (α, α_0, α_1). We can do this using a three phase shift analysis as was done for Na and Mg, i.e., from (α, α_0) and Eq. (1.4) we predict δ_0, δ_1, and δ_2 values that are all $\gtrsim 0$. The results of this are listed in Table V using the (α, α_0, α_1) set of (0.115, 0.18, 0.102) for absorption and (0.115, 0.17, 0.107) for emission. As mentioned for Na and Mg these values are only representative; other compatible δ_l's could be given that are also consistent with the overlapping shaded regions shown in Fig. 20.

Because we also have empirical α_1 values for Al, there is an alternative and even more demanding prescription for determining the δ_l's and, ultimately, for testing compatibility, namely, using *four* phase shifts in the analysis: the total set of empirical (α, α_0, α_1) values plus Eq. (1.4) uniquely define δ_0, δ_1, δ_2, *and* δ_3. This provides a virtually unconstrained test of the MND theory since the g phase shift δ_4 can certainly be ignored in Al. If the results are to be physically meaningful, not only the d phase shift, but the f phase shift is required to be small and positive. As an example, for the values (0.115, 0.18, 0.102) used in our three phase shift analysis above for the absorption data we find that although δ_2 is small and positive (see Fig. 20), δ_3 is negative, indicating that this is *not*, in fact, an acceptable set of values. δ_3 becomes positive when α_1 is increased to 0.103, a value compatible with the K-absorption spectrum. Similarly, δ_3 is negative for the values (0.115, 0.175, 0.104), and becomes positive when α_1 is increased to 0.105, a value compatible with both the K-absorption and -emission spectra. Therefore, we have been able to solve for a unique set of physically meaningful phase shifts which both satisfy all the requirements of compatibility and predict threshold exponents and singularity indices that quantitatively describe the data. As already emphasized, the lack of strongly complicating non-many-body effects in the edge spectra of Al and the use of four scattering phase shifts make this demonstration unusually powerful.

In Table V we have compared the experimental and predicted α, α_0, α_1, and δ_l values with various theoretical calculations.[42,58,96,98,100] The results are also shown in Fig. 20. As was the case for Mg, the theories generally predict α values in good agreement with experiment, but detailed agreement with the experimental threshold exponents is lacking. All calculated values straddle the region defined by the present study.

Summarizing our discussion for Al, the only simple metal for which both $L_{2,3}$- and K-absorption and -emission data exist, we have been able to draw unambiguous conclusions about the interpretation of its edge spectra. Phonons, lifetime broadening, and spin-orbit exchange were of negligible importance in the data. TDOS structure, while important in the quantitative evaluation of the fits, was sufficiently weak to allow for detailed analysis of the many-body effects. The K-edge spectra are rounded solely by lifetime broadening, while the $L_{2,3}$ spectra are peaked primarily as a result of the many-body response. Excellent fits were obtained using threshold exponents which were consistent for the absorption and emission experiments of the same edges and which were compatible with the sum rule, the XPS data, and the predictions of the MND theory for the different edges. This demonstration provides the strongest confirmation of the quantitative predictiveness and thus the essential validity of the MND theory.

C. Comparison between our results and those of other authors using the same x-ray edge data

The controversy over the ability of the MND theory to explain x-ray absorption and emission edge phenomena is documented by a wealth of conflicting analyses and interpretations. In this section we look at previous work in the light of the results reported here and elucidate the sources of agreement or disagreement. We primarily address x-ray edge data that we and other workers have analyzed. Conclusions based on electron energy loss data and other theoretical approaches are treated in Sec. V D.

The most thoroughly debated edge is the K edge of Li. Table VI gives a concise overview of the conflicting interpretations of its observed rounding. The initial calculations of Ausman and Glick[17] suggested the importance of a many-body explanation, which were subsequently supported by those of Mahan[19] and of Yue and Doniach.[99] None of these calculations included the effects of direct exchange, but even without them, Longe[18]

TABLE VI. History of explanations for the Li K-edge rounding.

Year	Many body		Phonons		Lifetime		Reference
	Expt.	Theory	Expt.	Theory	Expt.	Theory	
1969		yes					17
				yes			27
1970		yes					19
1971			no				116
				no			114
1973		no					18
		yes					99
				yes			28
1974	no		maybe		maybe		41
						yes	30
						no	117
			yes		maybe		40
1975		yes				yes	42
	no		no		yes		32
1976	no		yes		no		47
						no	110
		no					74
1977				yes			69 and 70
	no		yes		no		80

concluded from his calculations that the magnitude of α_1 was insufficiently negative to account for the rounding.

The first alternative explanation was made by McAlister,[27] who used a theory after Overhauser[113] to show that phonon broadening might be an important factor. His idea did not gain acceptance at that time primarily because of the experimental observation by Kunz which showed no temperature-dependent effect[116] and partly because of the theoretical work of Bergersen, McMullen, and Carbotte[114] which showed that Overhauser's model considerably overestimated the phonon broadening in both Li and Na.

Dow, Robinson, and Carver[28] attempted to revive the phonon explanation by proposing a model which claimed to predict a sufficiently large broadening in Li without also overestimating the size of the effect in Na (a calculation supporting this claim was not given). The model's predictions were further reported to be consistent with the *absence* of measurable temperature-dependent effects reported[116] at that time.

The electron energy loss measurements of Ritsko, Schnatterly, and Gibbons[41] provided the first definitive experimental evidence that the conventional MND theory could not explain the rounded edge. No alternative explanation was offered. The large Gaussian broadening found in the data analysis was stated to be consistent with either phonon or lifetime effects, although a Lorentzian fit was found to be less satisfactory. The *absence* of a temperature dependence of the edge was also reported in this work.

The lack of any experimental support for phonon broadening,[41,116] coupled with the arguments of Bergersen, Jena, and McMullen[117] that the model of Dow *et al.*[28] was in fact equivalent to the earlier conventional hole-phonon scheme of Overhauser,[113] left open the possibility for alternative explanations. Franceschetti and Dow[30] subsequently argued for lifetime broadening as the dominant cause for the observed rounding. Mahan presented similar reasonings shoftly thereafter,[42] maintaining that this was the explanation of the electron energy loss results.[41] Neither work tested for Lorentzian lifetime broadening of the data.

At about this time, new measurements by Kunz, Petersen, and Lynch[40] were reported which showed the long sought for temperature-dependent broadening. Although lattice excitations were clearly shown to be involved, those authors interpreted their results in terms of the model due to Dow *et al.*[28] and did not rule out the possibility of a temperature-dependent lifetime broadening as suggested by Dow.[118]

Following that experiment, Petersen[32] remeasured the Li K edge and argued that the rounding was primarily due to structure in the TDOS. From analysis of his data (using only Gaussian broadening) he suggested that the additional broadening of the K edge could be ex-

plained by a sizeable Li 1*s* lifetime with only a small phonon contribution.

Temperature-dependent XPS measurements[47] shortly thereafter cleared up the existing confusion about the relative importance of phonon, lifetime, and TDOS broadening. It was shown that phonon broadening of the TDOS was indeed the dominant rounding mechanism and that it was the lifetime broadening that was negligible. The phonon broadening models proposed by Overhauser,[113] Bergersen *et al.*,[114] Dow *et al.*,[28] and later by Hedin and Rosengren[112] were all shown to be inadequate. From the value of α, that work[47] also confirmed that α_1 was insufficiently negative to explain the observed edge data.

At about the same time the XPS work was published, calculations by Glick and Hagen[110] showed the Li 1*s* lifetime to be negligible. Also at about that time, Girvin and Hopfield[74] reconsidered an earlier suggestion by Kato *et al.*[73] that the scattering phase shifts in Li may be spin dependent due to direct exchange, thereby helping explain the small value of α_0 observed in the electron energy loss measurements.[41] Subsequent calculations by Kaga,[75] by Andereck and Iche,[76] by Yoshimori and Okiji,[76] and by Almbladh and von Barth[101] have recently shed additional light on this subject.

Finally, the detailed shape of the Li K-emission edge was theoretically predicted by Mahan[69] and by Almbladh[70] to be due to incomplete phonon relaxation. Subsequent analysis by Callcott, Arakawa, and Ederer[80] of their own Li K-emission edge data has convincingly supported this explanation. Those author's analysis of their absorption K-edge data has also come to support the conclusions reached in the XPS work.[47]

Explanations for the discrepancies between the Li K-edge results reported here and those of earlier works are now abundantly clear. Lifetime broadening cannot be represented by a Gaussian, absorption-edge analyses must first take into account the contribution from the Fermi-Dirac function and the Lorentzian lifetime contribution before phonon broadening magnitudes can be determined, emission-edge analyses must take into account the effects of incomplete phonon relaxation, and threshold exponents must include the effects of spin-dependent phase shifts resulting from direct exchange. It is gratifying that soon after these conclusions had been spelled out[47,69,70,74] there appeared reinterpretations[97,119] of previous work[28,41] in full agreement with the present understanding.

Prior to the present work the Al K-edge absorption data of Neddermeyer had been analyzed only by that author.[31] Although he did not include the Gaussian phonon and instrumental broadening in his analysis, the resultant Al 1*s* lifetime agrees very well with our result. Using a free-electron rather than a realistic TDOS he obtained $\alpha_1 = 0.0 \pm 0.1$. The limits are clearly conservative as judged by Fig. 3 in his work,[31] with $\alpha_1 = 0.1$ actually showing a considerably better fit. This agrees very well with our value of $\alpha_1 = 0.095 \pm 0.015$ using the calculated TDOS from Sec. III.

The high-resolution Na, Mg, and Al $L_{2,3}$-absorption edge data of Kunz *et al.*[103] have been analyzed and interpreted by several authors. Slowik[109] first subtracted a background from the data and then subtracted the L_2 component assuming that it had a shape identical to that of the L_3 component but with an adjustable intensity. He then plotted the logarithm of that result versus $\ln(\hbar\omega - \hbar\omega_0)$, where $\hbar\omega_0$ is the threshold energy. From the slope of the line he estimated the value of α_0 (α_2 was not considered). Applying this procedure to the Mg $L_{2,3}$ data[103] he found $\alpha_0 = 0.22 \pm 0.1$, in agreement with our results. Significantly, he also found from analyses of Mg-Bi and Mg-Sb alloy edge data that the theoretical $L_3 : L_2$ intensity ratio of 2 : 1 was realized only in Mg metal. The discrepancy was ascribed to the spin-orbit exchange interactions discussed earlier by Onodera and Toyozawa.[72] The complete set of Na, Mg, and Al $L_{2,3}$ data[103] were subsequently analyzed by Dow *et al.*[22] using Slowik's procedure[109] but without plotting the logarithm of the results. Instead, Dow *et al.* fit the results directly using Eq. (1.1) with α_0 and a Gaussian broadening as adjustable parameters (α_2 and spin-orbit exchange were not considered). The spin-orbit splitting and $L_3 : L$ intensity ratio were also allowed to vary. From their analysis they reported $\alpha_0 = 0.26 \pm 0.04$ for Na, 0.18 ± 0.04 for Mg, and 0.15 ± 0.04 for Al. The Mg value agrees favorably with our results, in spite of their neglect to include α_2, lifetime broadening, TDOS structure and exchange (these effects were shown in Sec. IV to be of secondary importance for Mg). For Al, the results overlap and differ primarily as a result of their having excluded α_2.[120] For Na, however, there is a marked disagreement with our results. As seen in Sec. IV, we found that no adjustment of the other non-MND-related parameters using $\alpha_0 = 0.26$ could give satisfactory fits to the data; a value of $\alpha_0 = 0.37 \pm 0.03$ was seen to be clearly superior. This lack of agreement is most significant because in many respects Na is the prototype free-electron metal in which the MND theory should be most applicable (contributions to the edge data from TDOS structure or from d-like conduction states are negligible).

In order to gain insight into the origin of the

disagreement between our Na $L_{2,3}$ results and those of Dow *et al.*[22] using the same data,[103] it is instructive to consider the recently published results of Callcott, Arakawa, and Ederer.[45,104] Those authors analyzed their own Na $L_{2,3}$-absorption data using a procedure similar to ours, namely, fitting the raw data with Eq. (1.1) and a broadening function. They ignored TDOS structure and lifetime broadening as had Dow *et al.*,[22] but our analysis has shown that these approximations do not introduce serious errors. Callcott *et al.* reported that $\alpha_0 = 0.24 \pm 0.04$ would fit their data using plausible values for the two other fitting parameters, namely, the Gaussian broadening and the $L_3 : L_2$ intensity ratio R. Their best fit was obtained with $R = 2.7$, instead of the theoretical value of 2. The authors do not justify this result, but do point out that it is consistent with the 3.3 ratio reported by Kunz *et al.*[103] in their discussion of their own Na $L_{2,3}$-edge measurements. (A direct comparison of these two different sets of Na $L_{2,3}$-absorption data is made in Sec. V D.) Callcott *et al.* further note that Onodera's fit[44] (using his own spin-orbit exchange formalism) to Kunz *et al.*'s data[103] gave an inconsistently large value of α_0, which Callcott *et al.* ascribed to difficulties in his fitting procedure[44] rather than to his formalism. Their opinion was based on Dow's communication[121] that he obtained a value of α_0 consistent with 0.26 ± 0.04 even after including Onodera's formalism.[122]

Apropos of Callcott *et al.*'s analysis, we note here that Slusky *et al.*[46] fit their Na $L_{2,3}$ electron energy loss data (discussed in Sec. V D) using either a variable R or using Onodera's theory.[44] They obtained $\alpha_0 = 0.24 \pm 0.01$ with $R = 1.92$ (ignoring spin-orbit exchange) and essentially the same result including exchange, with an exchange energy Δ of only 0.05 eV (the reason for this latter result is also discussed in Sec. V D).

Finally, turning back to Dow *et al.*'s initial analysis,[22] we note that in fitting the data of Kunz *et al.* they too used an adjustable $L_3 : L_2$ ratio. The ratio that was ultimately obtained was not reported nor were comparisons between results of their analyses and the data ever shown. As with Callcott *et al.*,[45,104] spin-orbit exchange was not considered, in spite of the previous work by Slowik[109] which showed that it should be.

Summarizing the above discussion, we have *three* different sets of Na $L_{2,3}$-edge data analyzed by *four* different methods: (a) that of Dow *et al.*[22] without spin-orbit exchange and using an unspecified R, giving $\alpha_0 = 0.26 \pm 0.04$, (b) that of Callcott *et al.*[45,104] without exchange and with $R = 2.7$, giving $\alpha_0 = 0.24 \pm 0.04$, (c) that of Slusky *et al.*[46] either including exchange with a negligible exchange energy or ignoring exchange with $R = 1.92$, giving $\alpha = 0.24 \pm 0.01$, and (d) that of Dow[121] with exchange (and unspecified R), giving a value for α_0 consistent with 0.26 ± 0.04. All these results should be contrasted with ours, which includes exchange and gives $\alpha_0 = 0.37 \pm 0.03$ and an exchange energy of 0.21 ± 0.04 eV.

What do these results for Na imply? A value of $\alpha_0 = 0.26$ leads (assuming only δ_0 and δ_1) to an XPS α value of 0.14, in sharp disagreement with the observed value of 0.20.[37] Furthermore, $\alpha_0 = 0.26$ disagrees with the majority[123] of all theoretical calculation performed to date[17,18,96,98,101] (see Table V), which show—not surprisingly—that $\delta_2 \ll 1$ in Na. This latter point is also seen in Fig. 16, where a value of $\alpha_0 = 0.26$ clearly indicates an unphysically large δ_2. Our value of $\alpha_0 = 0.37$, on the other hand, is consistent with the XPS predicted value (assuming only δ_0 and δ_1) of $\alpha_0 = 0.385 \pm 0.025$, with the theoretical values of the most reliable calculations[123] (see Table V), and with the physically reasonable result that $\delta_2 \ll 1$. In addition, the exchange energy of 0.21 eV is consistent with the two *a priori* calculations of Almbladh and von Barth.[101]

The origin of the incorrect value of $\alpha_0 = 0.26$ lies in the fact that in all previous analyses of the Na $L_{2,3}$-edge data the effect of spin-orbit exchange was omitted,[44] and/or R was allowed to vary arbitrarily in order to obtain a good fit. In the absence of exchange there is absolutely *no* justification for varying R from the value of 2, a constraint that has been violated in all previous analyses but has inexplicably gone unchallenged. (The need for a variable R is readily apparent in the data by the fact that $R \neq 2$. This fact in itself is looked at more closely for the three different Na $L_{2,3}$ data sets[45,46,103] in Sec. V D.) It appears to be a coincidence that the four analyses, two with[46,121] and two without[22,45] exchange, determined different values of R and still obtained virtually identical values of α_0. The reasons for this coincidence (see Sec. V D) are much less important here than the need for emphasizing that the results of all those analyses are fundamentally incorrect. Another analysis of the data of Kunz *et al.*[103] by Onodera[44] is also flawed because it used too large a Na $L_{2,3}$ lifetime width [see Fig. 10(a) and Table III]. Nonetheless, the essential result of his analysis, yielding a 0.23-eV spin-orbit exchange energy[44] with a value of $\alpha_0 = 0.41$,[18] is most definitely confirmed by our more detailed analysis. The final test of the magnitude of α_0 for Na will come from the measurement of its K-absorption or -emission edge. Our value of $\alpha_0 = 0.37 \pm 0.03$ (as well

as the XPS $\alpha = 0.20$ and a variety of theoretical calculations) clearly predicts a negative α_1; the value of $\alpha_0 = 0.24 - 0.26$ predicts α_1 to be positive (see Fig. 18).

For completeness, we mention the results of two other analyses of the Na, Mg, and Al $L_{2,3}$-absorption-edge data of Kunz *et al.*[103] Neddermeyer[31] analyzed the Mg and Al $L_{2,3}$ edges assuming only Lorentzian broadening, $|A_2|^2 = 0$, and a free-electron TDOS, and obtained $\alpha_0 = 0.3 \pm 0.07$ for Mg and $\alpha_0 = 0.2 \pm 0.05$ for Al. His values are both larger than our respective values of 0.23 ± 0.02 and 0.18 ± 0.02, but the uncertainty limits of his results allow them to overlap with ours. Mahan[42] compared the Na, Mg, and Al $L_{2,3}$-edge data[103] with theoretical spectra using his calculated values of α_0. The effects of phonons, lifetime, TDOS, and spin-orbit exchange were not considered. It is not possible to make any meaningful assessment of his calculated α_0 values without the inclusion of these effects.

The Mg and Al $L_{2,3}$-emission data of Neddermeyer[31] have been analyzed by Dow and coworkers[21,23] assuming a constant TDOS, $|A_2|^2 = 0$, and a Gaussian broadening to account for instrumental, lifetime, and phonon contributions. They obtained $\alpha_0 = 0.22 \pm 0.06$ for Mg and $\alpha_0 = 0.1 \pm 0.04$ for Al. Following that work Neddermeyer[31] reanalyzed his own data using both a free-electron TDOS and, for Al, a calculated TDOS after Smrčka.[90] He properly included separate Lorentzian lifetime and Gaussian instrumental broadenings as well. With $|A_2|^2$ also assumed to be zero, he obtained for Mg $\alpha_0 = 0.3 \pm 0.07$, and for Al $\alpha_0 = 0.2 \pm 0.07$ (free TDOS) and $\alpha_0 = 0.075 \pm 0.05$ (calculated TDOS). Our analysis of Neddermeyer's data,[31] which included the additional effects of nonzero $|A_2|^2$, phonon broadening, and our own calculated TDOS for both Mg and Al gave for Mg $\alpha_0 = 0.32 \pm 0.02$ (constant TDOS) and $\alpha_0 = 0.18 \pm 0.02$ (calculated TDOS), and for Al $\alpha_0 = 0.22 \pm 0.02$ (constant TDOS), $\alpha_0 = 0.17 \pm 0.02$ (calculated TDOS). The agreement between Neddermeyer's Mg results and ours using a free (~ constant) TDOS (0.3 vs 0.32) is gratifying, and the lack of agreement upon our including the calculated TDOS (0.18 vs 0.3) is expected because of the sharp structure introduced by it (the inclusion of phonons and a nonzero $|A_2|^2$ is important only on a quantitative level). There is no obvious explanation for Dow's[21] value of $\alpha_0 = 0.22$ from the same data using a constant TDOS (it should be somewhat larger; perhaps it results from his using a too small resolution function and zero phonon and lifetime widths). For the case of Al $L_{2,3}$-emission edges, our results again agree with Neddermeyer's[37] assuming a free (~ constant) TDOS (0.22 vs 0.2). As pointed out by Neddermeyer,[31] the disagreement with Dow *et al.*'s[23] α_0 value of 0.1 is likely due to their use of 0.08 eV for the instrumental function as opposed to its correct value of 0.19 eV. Interestingly, inclusion of our calculated TDOS reduces α_0 from 0.22 to 0.17, whereas Neddermeyer finds that Smrčka's TDOS[90] reduces α_0 from 0.2 to 0.075. Again as pointed out by Neddermeyer,[31] it is not clear to what extent Smrčka's calculations are quantitatively accurate. There is, of course, no absolute test of the reliability of a calculated TDOS; only comparison with experiment can address this question. On this basis, the compatibility obtained between the XPS data and the threshold exponents of four independent edge analyses (K and $L_{2,3}$ emission and absorption) using our calculated TDOS suggests that our TDOS for Al are indeed reliable.

The (somewhat smaller) discrepancies between our α_1 results and those of Neddermeyer[31] and of Dow *et al.*[23] from the analysis of Neddermeyer's Al K-emission data are similarly traceable (in part) to the different TDOS's that were used. Dow *et al.*, assuming a constant TDOS and a purely Gaussian broadening, obtained $\alpha_1 = 0.04 \pm 0.05$. Neddermeyer used a free TDOS and one calculated after Smrčka,[90] along with a purely Lorentzian broadening, to obtain values of $\alpha_1 = 0.0 \pm 0.05$ (free TDOS) and $\alpha_1 = 0.05 \pm 0.05$ (calculated TDOS). Our results of $\alpha_1 = 0.11 \pm 0.015$ (constant TDOS) and $\alpha_1 = 0.12 \pm 0.015$ (calculated TDOS) were obtained using the appropriate Lorentzian lifetime and Gaussian phonon and instrumental contributions. The effect of the TDOS is to require α_1 to be only slightly more positive. The remaining differences arise from the different broadening functions that were used.

Finally, and while on the subject of the importance of TDOS structure in the experimental x-ray absorption and emission edge spectra, we mention the work of Gupta and Freeman,[33] who argued that because the peaked structure near E_F in their calculated Mg $L_{2,3}$ TDOS looks very similar to the Mg $L_{2,3}$-emission-edge data, one-electron effects play a significant role in its interpretation. They then argued that such effects are also important in the Mg $L_{2,3}$-absorption-edge data as well. Similarly, Gupta and Freeman[34] calculated the $L_{2,3}$ TDOS for Na and maintained that band-structure corrections may effectively remove the need for invoking the MND theory to explain the spiked Na $L_{2,3}$-edge structure. We have shown in Sec. IV that even though the calculated TDOS does indeed resemble the Mg $L_{2,3}$-emission data, the inclusion of lifetime, phonon, and instrumental broadening effectively removes

such resemblances and that a strongly positive α_0 is required to fit the data. It is of course true that the TDOS for the Mg $L_{2,3}$-emission edge does play an important role in determining the appropriate value of α_0, but this does not at all imply some universal importance of one-electron TDOS as suggested by these authors.[33,34] Specifically, we have shown in Sec. III that in the Mg $L_{2,3}$-absorption edge the calculated structure just above E_F is an artifact of their model,[33] and that (see Sec. IV) even if such structure were real it would not effect the threshold behavior in the absorption data due to its extended dispersion. Furthermore, the suggestion[34] that TDOS structure in Na might be responsible for the observed spiked $L_{2,3}$-edge data has similarly been shown in Sec. IV to be unsubstantiated by our analyses. Even without our results, however, it is clear from the essentially identical Na $L_{2,3}$ edges in solid and liquid Na metal[124] that such a suggestion must be viewed as inappropriate.

Summarizing this section, we have seen that there are numerous edge analyses by other workers, which in some cases differ substantially from those reported here. The reasons for such discrepancies are invariably traceable to a neglect, overemphasis, or incorrect consideration of at least one of the following factors that enter into a complete analysis of an x-ray edge: phonon broadening, lifetime broadening, spin-orbit exchange, or one-electron TDOS structure. Which effect or effects that need be considered depends entirely on the particular edge under question. Conclusions regarding K or $L_{2,3}$ edges in general have only led to oversimplification and, invariably, confusion.

D. Comparison between our results and those of other authors using different data or other theoretical correlations

Up until now we have tested the validity of the MND theory by its ability to account quantitatively and consistently for x-ray photoemission, x-ray absorption, and x-ray emission edge data. In view of the number of factors that need be considered in a proper analysis of the x-ray absorption and emission data (see Sec. II) and the lack of success of previous analyses (see Sec. V C), it is not surprising that alternate approaches have been sought to assess the MND theory. In this section we look at these findings and compare them with our results.

The measurement of the energy loss of high-energy electrons as a function of angle was suggested[35] as an auxiliary means to test the MND theory. Electrons with sufficiently high energy and zero momentum transfer q should behave like photons, while at finite q they should also excite non-dipole-allowed transitions. This means that Eq. (1.1) for a core hole of l symmetry must be modified to include A_l as well and thus weight the threshold exponents α_l and $\alpha_{l\pm1}$ accordingly. As mentioned in Sec. V B this technique provided the first definitive evidence showing that the rounding of the Li K edge was not due to a strongly negative α_1 exponent because there is no peaking at $q \neq 0$ (corresponding to a positive α_0).[41] Following that experiment the Mg,[43] and more recently, the Na and K $L_{2,3}$ edges[46] have been studied by Slusky *et al.* with the electron energy loss technique. For all three metals it was found that the $q = 0$ edge data do indeed become rounded when the

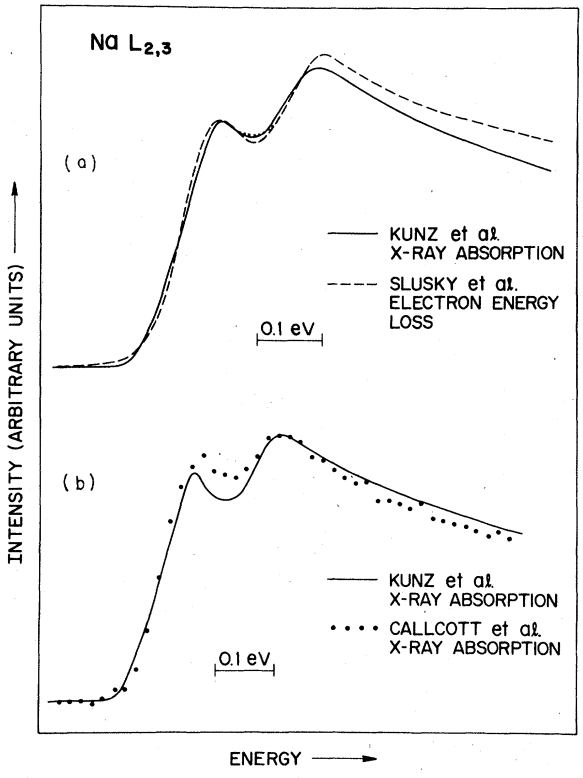

FIG. 21. (a) Comparison between Na $L_{2,3}$ x-ray absorption data of Kunz *et al.*, Ref. 103, and electron energy loss data of Slusky *et al.*, Ref. 46. The former, with 0.026-eV resolution, have been Gaussian broadened to match the latter, with 0.037-eV resolution. Note disagreement between data sets in L_3:L_2 intensity ratio. Also, note disagreement between near-threshold region of L_3-edge electron energy loss data, dashed line, and least-squares fit to it, indicated by closely spaced dots (from Ref. 46). (b) Comparison between Na $L_{2,3}$ x-ray absorption data of Kunz *et al.*, Ref. 103, and data of Callcott *et al.*, Ref. 45. No adjustment for different resolution was made. Again note disagreement of L_3:L_2 intensity ratios between data sets, but in opposite direction than in (a).

A_1 component (α_1 threshold exponent) contributes to the $q \neq 0$ spectra. Most significantly, the changes in edge shape were concluded to be in accord with the behavior predicted by the MND theory.[5,8] This is particularly gratifying in view of the improved data analysis[46] compared with those of other investigators. However, some of their results are in marked disagreement with earlier XPS work, with theoretical calculations, and with the results reported here. Specifically, for Na at $q = 0$ Slusky *et al.*[46] obtain (almost independent of the details of their analysis) an average α_0 of about 0.24 ± 0.01 and a spin-orbit exchange energy Δ of only ~0.05 eV. This should be contrasted with our values of $\alpha_0 = 0.37 \pm 0.03$ and $\Delta = 0.21 \pm 0.05$ eV. A clue to the source of this discrepancy is given by the $L_3 : L_2$ ratios of 1.92, 1.68 and 2.49 quoted for the Na, Mg, and K $L_{2,3}$ edges, respectively. These values are at odds with the theoretical value of 2 and with those determined from our analysis of the Na and Mg data of Kunz *et al.*[103] This suggests that as a first step the different data sets should be tested for consistency. Since the Mg electron energy-loss data[43] are of low resolution, we compare only the Na data.

In the upper half of Fig. 21 the Na $L_{2,3}$ x-ray absorption data of Kunz *et al.*[103] (solid line), taken with an instrumental resolution of 0.026 eV, are shown broadened to match the electron energy loss data[46] (dashed line), taken with a resolution of 0.037 eV. Note that while there is agreement in the overall shapes of the edges, there is appreciable disagreement in the $L_3 : L_2$ intensity ratios. One possible source of this discrepancy could be the background subtraction procedure in the electron energy loss data. It must remove the background from the supporting carbon film which has a broad plasmon in the region of the Na $L_{2,3}$ edge. This suggestion is, however, entirely conjectural. Moreover, the x-ray absorption edge data of Callcott *et al.*,[45] shown in the lower half of Fig. 21, also exhibit $L_3 : L_2$ intensity ratios that do not agree with the data of Kunz *et al.*[103] The disagreement in this case is in a direction opposite to that found for the electron energy loss data.[46] It is that much more surprising, then, that the independent analyses of the two different data sets gave α_0 values of comparable magnitude (Callcott *et al.*[45] also arbitrarily allowed the $L_3 : L_2$ intensity ratio to vary, obtaining a value of 2.7 and a value for α_0 of 0.24 ± 0.04). What is clear from these comparisons is that the different $L_3 : L_2$ intensity ratios in the raw data cannot possibly be reconciled by the same spin-orbit exchange energy, which is known to alter this quantity dramatically.[44] Since spin-orbit exchange is also known to effect of the value of α_0 (see Sec. IV and Fig. 10), the disagreement of the α_0 values can, in part, be understood from the inconsistency of the raw data.

There is an additional factor in the data analysis of Slusky *et al.*[46] which significantly affects α_0, that is, that the fits included many points well outside the near-threshold region. Since all the data points were given equal weighting, the small number of points in the near-threshold region carried proportionately little weight. In Fig. 21, the fit[46] to the electron energy loss data in this critical region (just between the L_3 and L_2 edges, see Sec. IV) is indicated by closely spaced dots (there is near perfect agreement with the data above and below this region). The fit is clearly unacceptable, and indicates that a more positive α_0 value is required.

Summarizing this discussion, then, we have pointed out that while the electron energy loss data of Na, Mg, and K do qualitatively support the predictions of the MND theory, the results of the analysis of the $q = 0$ Na $L_{2,3}$ data disagree quantitatively with the XPS results, the theoretical calculations, and our analysis of high-resolution x-ray absorption data. There are two important reasons for this. First, the electron energy loss data are not fit in the near-threshold region. This is the only region of the data in which the MND theory can be meaningfully assessed. Second, the data themselves do not agree with the x-ray absorption measurements,[103] showing a different $L_3 : L_2$ intensity ratio. The origin of this is not presently understood, but is clearly responsible for the differences in spin-orbit exchange energies quoted by us and by Slusky *et al.*[46] Before quantitative conclusions can be drawn about the MND theory using electron energy loss data it remains to be demonstrated that this technique does indeed yield results that are in all respects equivalent to x-ray absorption measurements.

From a theoretical point of view, Dow and coworkers have attempted to make a number of correlations of experimentally determined threshold exponents with each other and with other various parameters. We now examine each of these correlations critically.

One of the first parameters with which α_0 was correlated was the electron-gas radius parameter r_s. Dow and Sonntag[24] used their empirically determined threshold exponents[22,24] and found a linear relationship with r_s, viz., $\alpha_0(r_s) \approx 0.068\, r_s$. Their results are plotted in the upper half of Fig. 22. These authors argued that at $r_s = 0$, α_0 must also be equal to zero, but using a simple screening model could not reconcile their results with the principal result of the MND theory,

Eq. (1.1). They further argued that since any reasonable value of α_0—and thus α_1 from Eq. (1.4)—for Li is predicted to lie outside the empirical linear relationship with r_s, final-state interactions described by the MND theory must be unimportant.

There are a number of flaws in this chain of arguments. As we have shown in Sec. V C, the value of $\alpha_0 = 0.26$ for Na is incorrect. In the lower half of Fig. 22 we have plotted our results from Sec. IV as a function of r_s. Note that our values of α_0 also show a linear dependence with r_s, but with a significantly different slope. Dow and Sonntag's analysis is not only incorrect for Na (see Sec. V C), but for Mg and Al it also underestimates α_0 because of the neglect of α_2. Had we neglected α_2 for Mg and Al the differences between slopes and intercepts would be larger still.

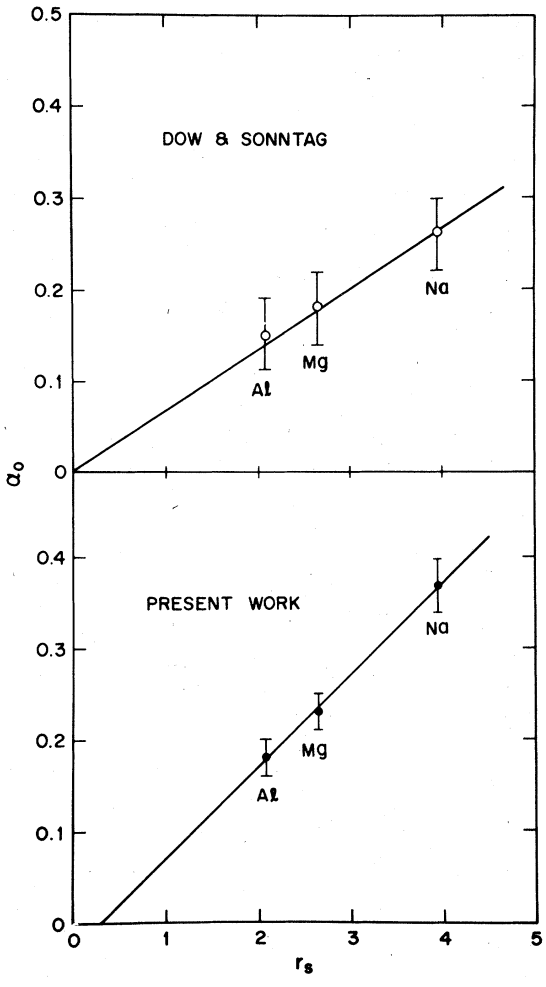

FIG. 22. Plots of x-ray edge threshold exponents α_0 for Na, Mg, and Al vs electron-gas radius parameter r_s. Top: Dow and Sonntag, Ref. 24, from their analysis of $L_{2,3}$ x-ray absorption data from Kunz *et al.*, Ref. 103. Bottom: this work, from analysis of same x-ray data. Note same linear dependence of α_0 vs r_s but different slopes in the two analyses. Nonzero (negative) intercept at $\alpha_0 = 0$ in present work is consistent with presence of core-core interactions (see text).

The reason for the observed linear behavior of α_0 vs r_s is clear.[37,39,48] Within the isochoric series Na, Mg, Al the free-electron s density varies proportionately with r_s. The s density, in turn, determines the magnitude of δ_0, which is the leading term in α_0. The second term in α_0 is α, and in I (Ref. 37) this too was shown to vary linearly with r_s because of its dependence on the contribution of δ_0 (s density).[125] Thus, it must follow that α_0 itself must also vary linearly with δ_0 (s density).

It is important to note that δ_0 is only a linear function of r_s. A value of $r_s = 0$ does not at all imply, contrary to Dow and Sonntag's arguments,[24] an infinite free-electron density because core-core interactions remove the physical significance of zero r_s. It is also for this reason that only metals within an isochoric series can be correlated with r_s since their core-core interactions are approximately the same. Lithium is in a different period than Na, Mg, and Al, so it clearly cannot follow the same r_s dependence. Similar conclusions have recently been reached by Bryant[126] in explaining the reported[127] negative slope in the linear dependence of α_0 vs r_s for K, Rb, and Cs.

Another parameter with which α_0 has been correlated is the singularity index α. Dow and Franceschetti[38] plotted the α values for Al and Mg determined by Ley *et al.*[128] against the α_0 values obtained by Dow *et al.*[22] Their results are reproduced in the upper half of Fig. 23. The dotted line drawn by Dow and Franceschetti[38] is meant to suggest the existence of some general trend of the experimental data. The solid line is the theoretical correlation according to those authors' calculations.[38] It was stated that only an unusual or pathological electron-hole scattering potential would cause significant corrections to the calculated relationship of α_0 vs α. This fact, coupled with the observation that the solid and dashed lines have opposite correlations, was taken as evidence of either inconsistencies in the data or in the MND theory. We now know[37] that the α values of Ley *et al.*[128] were in error because they were obtained with a procedure that neglected the instrumental broadening. Moreover, and independent of the data analysis of Ley *et al.*, the conclusions of Dow and Franceschetti[38] are misleading for two additional reasons. First, to suggest a trend on the basis of two data points

whose error bars overlap is itself a questionable procedure. Second, the calculated solid line assumes an *infinite* number of geometrically related phase shifts in Mg and Al. This is not only unphysical for the simple *sp* metals in general, but contradicts existing experimental and theoretical results for these metals in particular. A variety of theoretical calculations (see Table V) for Na, Mg, and Al all suggest a reasonable upper limit of $\delta_2/\delta_1 \sim 0.2$. In the lower half of Fig. 23 we show the theoretical α_0 vs α curves for the upper and lower limits of $\delta_2/\delta_1 = 0.2$ and 0, respectively (this is just a slightly modified version of Fig. 16). Note that at $\alpha = 0$, α_0 is not zero. Note also that this result, which is simply a consequence of Eqs. (1.2)–(1.4), is anything but unusual or pathological. In the bottom of Fig. 23 we have indicated the XPS results for α from I,[37] and the x-ray absorption edge results for α_0 from this work. Excellent agreement between all three experimental values and theory is obtained, as discussed in Sec. V B.

Another correlation of α_0 has been made with α_1. Dow[20] introduced the use of compatibility to check for consistency of phase shifts in explaining two different edges from the same metal. With only two equations, (1.2) and (1.4), Dow argues that in the simple *sp* metals, $\delta_l = 0$ for $l \geq 2$, leaving just δ_0 and δ_1 as the two unknowns. At one point Mahan[42] contested this assumption, but it is now recognized (see above and Sec. V B) that a reasonable upper limit for δ_2/δ_1 is 0.2, making Dow's initial assumption adequate to test for at least qualitative compatibility. In a series of subsequent papers, Dow and co-workers[21-23] set out to show that the MND theory did not even qualitatively explain the x-ray edge data in Mg and Al because the phase shifts used to analyze the peaked $L_{2,3}$-edge data produced insufficiently negative α_1 threshold exponents to account for their rounding in the K edges. Although lifetime broadening was discussed in these works and was shown to produce qualitatively good fits with the slightly positive α_1 values predicted from the $L_{2,3}$-edge analyses, the conclusions were that because the α_1 threshold exponents did not account for the K-edge rounding *exclusively*, the MND theory appeared to be inadequate. We have shown in Sec. V B, however, that the threshold exponents for the K and $L_{2,3}$ edges are indeed compatible and that the existence of other well-known phenomena in the x-ray edge data, viz., lifetime broadening, does not at all invalidate the applicability of the MND theory.

On the basis of the $L_{2,3}$-edge analyses by Dow *et al.*,[22] the α_1 exponents were predicted to be slightly positive. Moreover, Dow and co-workers

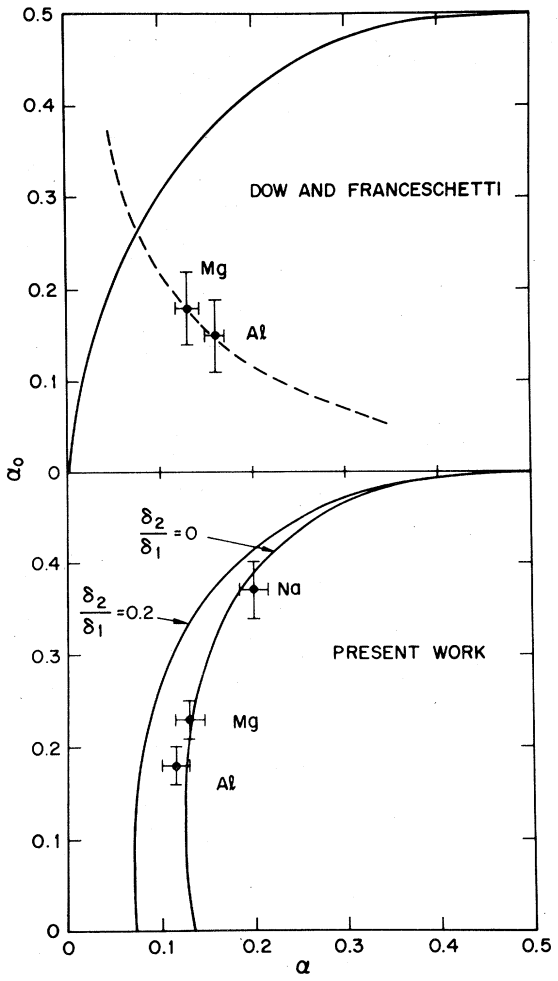

FIG. 23. Plots of x-ray edge threshold exponents α_0 vs x-ray photoemission (XPS) singularity indices α. Top: Dow and Franceschetti, Ref. 38, from earlier edge analyses (Ref. 22) of $L_{2,3}$ x-ray absorption data from Kunz *et al.*, Ref. 103, and from XPS analyses of Ley *et al.*, Ref. 128. Dashed line from Ref. 38 drawn to suggest trend from two data points. Solid line from Ref. 38 based on compatibility relation assuming infinite number of phase shifts. Note disagreement between dashed and solid lines. Bottom: this work, from analysis of same x-ray edge data and from XPS analysis of Ref. 37. Solid lines correspond to physically reasonable limits of *d*-phase shift contribution in Na, Mg, and Al (higher-order phase shifts are negligible, see Fig. 16 and Table V). Note excellent agreement between data and compatibility curves.

calculated that α_1 must *always* be *positive* for the simple metals.[21,25,26] It was further calculated that for $L_{2,3}$ emission edges $0 \lesssim \alpha_0 \lesssim 0.15$.[26] Our analyses of the $L_{2,3}$ edges in Na, Mg, and Al all require $\alpha_0 > 0.15$, in clear disagreement with this latter result. Furthermore, from Sec. V B we saw that the compatibility relations predict a *negative* α_1 value for Na using either the α value

from the XPS data[37] or the α_0 value from the $L_{2,3}$ x-ray absorption edge measurements. Our prediction of a negative α_1 for Na therefore contradicts Dow *et al.*'s general conclusion of its being positive. Analysis of Na K-edge absorption or emission data should settle this question conclusively.

VI. CONCLUSIONS

The development of the MND theory[5,8] a decade ago opened up the possibility for interpreting x-ray edges of simple metals in an entirely new way, in the many-body rather than the one-electron approach. The ease with which the theory could be applied, its novelty, and its apparently qualitative success, encouraged a great deal of enthusiasm. The claim of understanding the x-ray edges soon became generalized to the statement that K edges are rounded and $L_{2,3}$ edges are peaked as a result of a many-body effect. The simplicity of the statement, the ease by which it could be tested, and the eventual demonstration that the K edges are, in fact, not rounded by a many-body effect provoked the equally simple and general counterclaim that it is primarily one-electron, not many-body effects that are responsible for the shapes of x-ray edges and that the MND theory is either incorrect or in need of substantial modification. We now know that both statements represent extreme points of view and that either one- or many-body phenomena may dominate in a particular case. The mistake has been to argue from the particular to the general, to deny (or inflate) the importance of a phenomenon in general because it happens to be unimportant (or significant) in a particular example. Invariably this came about from the exclusion or incorrect treatment of those factors that did not support the particular point of view being stressed. With the advantageous perspective of hindsight, it is illuminating to see how this happened for each edge.

The rounding of the Li K edge had been attributed to either many-body effects,[15,17,19,99] phonons,[27,28] lifetime broadening,[30,42] or TDOS structure.[32] In all cases the importance of only one effect was sought, so all the others were ignored. The rounded K edges of Al and Mg were interpreted solely in terms of either a many-body rounding[15] or a lifetime broadening.[20] The two effects were initially not treated jointly. In the analysis of the Na, Mg, and Al $L_{2,3}$ edges the d phase shift was either very much overemphasized[42] or ignored completely.[22] The fact that it may be important for Al and negligible for Na was never considered. Spin-orbit exchange[44] was not taken seriously until quite recently, even though the $L_3 : L_2$ intensity ratio in Na was observed[103] to be clearly at odds with the theoretical value of 2. Instead, the spin-orbit intensity ratio was arbitrarily treated as an adjustable parameter.[22,45,46,121] TDOS structure was calculated for Mg,[33] and found to resemble its observed $L_{2,3}$ emission spectrum. Lifetime, phonon, instrumental, and thermal broadening effects were ignored in this assessment. General arguments about the importance of TDOS structure were extended[33,34,95] to other edges in other materials without any comparisons with experiment. In all of the cases cited the particular phenomenon being emphasized did indeed make *some* contribution to the measured spectrum under question, but the degree to which it contributed was simply not considered.

It is with this background that the present work was undertaken to analyze the x-ray absorption and emission edge data from Li, Na, Mg, and Al. Both the many-body response described by the MND theory and the more conventional phenomena of TDOS structure, exchange, and the broadenings due to thermal, instrumental, phonon, and lifetime effects were considered for each edge. The non-MND-related parameters were thoroughly compared and found to agree excellently with theoretical calculations and with other experiments. The parameters of the MND theory, the Friedel phase shifts, were rigorously tested for compatibility, i.e., they were required to obey Friedel's sum rule and be consistent with x-ray photoemission data and with x-ray absorption and emission data for both K and $L_{2,3}$ edges. They were also compared with calculated phase shifts. In all cases where comparison between experimental and theoretical or predicted and theoretical values were possible the agreement was generally very good to excellent. Comparisons between experimental and predicted values were in all cases excellent. Only for Li, which is suggested to be anomalous because of direct exchange effects in its edge spectra, are there discrepancies.

Following these general conclusions we now address the two questions posed in the introductory section of this work, viz., (a) what are the dominant factors that determine the shapes of the x-ray edges in each of the simple metals, and (b) is the MND theory quantitatively predictive in understanding these edges. The results of our analyses can be succintly summarized as follows. The $L_{2,3}$ edges of Na, Mg, and Al are dominantly peaked by the many-body interactions which are described *quantitatively* by the MND theory. By contrast, the K edges of these metals are rounded primarily because of lifetime broad-

ening, the many-body effect actually causing a slight peaking. In Li, on the other hand, lifetime broadening is negligible; the rounding is due to phonons. The lack of significant rounding due to a many-body effect is entirely consistent with detailed calculations of the phase shifts described by the MND theory and is in no way an invalidation of its applicability or usefulness. On the basis of this work we believe that the essential validity of the MND theory is confirmed.

An account of the importance of the other phenomena considered in our analyses is as follows. TDOS structure contributes the most peaking in the Mg $L_{2,3}$-emission edge, followed by the Al $L_{2,3}$-emission edge. The Al K-absorption and -emission edges are actually somewhat rounded by the TDOS. The "break" in the Li K-absorption edge is also a TDOS effect, while the similarly (and fortuitously) shaped break in the Li K-emission edge is due to incomplete phonon relaxation. This latter phenomenon complicates determination of the many-body contribution in the Na $L_{2,3}$-emission edge data. TDOS structure has little effect on the shapes of the other edges. Phonons and lifetime broadening contribute only a small rounding to the shapes of the $L_{2,3}$ edges of Na, Mg, and Al. The d contribution to the TDOS in the $L_{2,3}$ edges of these metals affect the s-threshold exponent by about 15% for Al, 10% for Mg, and only 2% for Na. Spin-orbit exchange is quite significant for Na but below experimental detectability for Mg and Al. Direct exchange appears to be important only for Li, although a quantitative theoretical description is presently lacking. A similar statement applies to the theoretical description of the large phonon broadening in Li. The most general statement that can be made about the importance of these other non-MND-related phenomena (save phonon broadening in Li and lifetime broadening in the K edges of Na, Mg, and Al) is that while they are small on an absolute scale and do not determine the qualitative shape of the observed x-ray edge data in the simple metals, their collective inclusion in the data analysis is nonetheless essential for the quantitative evaluation of the MND theory.

In considering the overall success of the MND theory so far, it is appropriate to look into future areas of development and testing of that theory. Before doing this, it is necessary to emphasize several fundamental and practical points. First, despite the apparent simplicity of the many-body formalism, its application (as with any theory) will require the consideration of all the other factors that ordinarily enter into the proper analysis of an experimental x-ray edge spectrum. Second, the theory is readily applicable only to those metals containing a small number of phase shifts and whose TDOS structure is within the capabilities of realistic calculations. Third, the theory is expected to be valid only within a small fraction of the Fermi energy, i.e., generally within about 0.5 eV from the edge. Finally (and because the applicable range of data is so small and the materials amenable for study are so limited), it is essential that the data be of the highest quality and resolution.

With the above qualifications in mind, there appear to be three experimental areas for testing the MND theory beyond those presented here. The first and most immediate concerns the absorption and emission K edges of Mg and Na. For emission, the effects of self-absorption must be scrupulously checked and, if present, removed. Our analyses of the $L_{2,3}$ and XPS data of these metals make definitive predictions about the sign and magnitude of the many-body threshold exponents. The measurement of these edges are eagerly anticipated. The second area involves the simple metals K, Rb, and Cs. Their least bound core level absorption edges have been recently measured by Ishii *et al.*,[127] although a detailed analysis has yet to be performed. The corresponding core level emission edges, the next least bound absorption and emission edges, and the x-ray photoemission data of these metals all remain to be measured. These experiments will ultimately test the compatibility of the phase shifts determined from their analysis. The third experimental testing ground of the MND theory involves high-resolution electron energy loss measurements of Al, Rb, and Cs. As pointed out in Sec. V D it presently needs to be demonstrated that that technique itself produces $q = 0$ spectra identical to those measured with x-ray absorption. Following the successful demonstration of that, however, the $q \neq 0$ spectra and their careful analysis should provide an important check on our understanding of x-ray threshold phenomena.

The above experimental developments are, of course, contingent upon the theoretical progress in those areas. This involves not only reliable TDOS calculations of K, Rb, and Cs, but a careful look at the validity of using ground-state band-structure techniques in the interpretation of the "final-state" systems produced in the x-ray absorption process (see Sec. II A). Similarly, the need is imposed for carefully considering the relative magnitudes of the $l \pm 1$ transition probabilities which enter into a proper analysis of an edge of l symmetry. The effects of both spin-orbit and direct exchange will require further refinements, the former so that it can incorporate the effects of energy and l-symmetry de-

pendence, the latter so that it can finally account for Li on a more quantitative level. Lastly, the fundamental question of formally extending the MND theory beyond the immediate vicinity of the edge remains a problem whose solution will greatly enhance the usefulness and applicability of the MND theory.

[1]D. H. Tomboulian, in *Handbuch der Physik*, edited by S. Flügge (Springer, Berlin, 1957), Vol. 30, pp. 246–304.
[2]L. G. Parratt, Rev. Mod. Phys. 31, 616 (1959).
[3]F. Seitz, *Modern Theory of Solids* (McGraw-Hill, New York, 1970).
[4]*Soft X-Ray Band Spectra and the Electronic Structure of Metals and Materials*, edited by D. J. Fabian (Academic, New York, 1969).
[5]G. D. Mahan, Phys. Rev. 163, 612 (1967).
[6]J. J. Hopfield, Comments Solid State Phys. 2, 40 (1969).
[7]P. W. Anderson, Phys. Rev. Lett. 18, 1049 (1967); Phys. Rev. 164, 352 (1968).
[8]P. Nozières and C. T. De Dominicis, Phys. Rev. 178, 1097 (1969).
[9]J. Friedel, Comm. Solid State Phys. 2, 21 (1969).
[10]N. H. March, in *Band Structure Spectroscopy of Metals and Alloys*, edited by D. J. Fabian and L. M. Watson (Academic, London, 1973), p. 297.
[11]J. Friedel, Philos. Mag. 43, 153 (1952).
[12]K. D. Schotte and U. Schotte, Phys. Rev. 185, 479 (1969); 185, 509 (1969).
[13]D. C. Langreth, Phys. Rev. 182, 973 (1969).
[14]M. Combescot and P. Nozières, J. Phys. 32, 913 (1971).
[15]G. D. Mahan, in *Solid State Physics*, edited by H. Ehrenreich, F. Seitz, and D. Turnbull (Academic, New York, 1974), Vol. 29, p. 75.
[16]L. Hedin, in *X-Ray Spectroscopy*, edited by L. V. Azároff (McGraw-Hill, New York, 1974), p. 226.
[17]G. A. Ausman, Jr. and A. J. Glick, Phys. Rev. 183, 687 (1969).
[18]P. Longe, Phys. Rev. B 8, 2572 (1973).
[19]G. D. Mahan, J. Res. Natl. Bur. Stand., Sect. A 74, 267 (1970).
[20]J. D. Dow, Phys. Rev. Lett. 31, 1132 (1973).
[21]J. D. Dow, Phys. Rev. B 9, 4165 (1974).
[22]J. D. Dow, J. E. Robinson, J. H. Slowik, and B. F. Sonntag, Phys. Rev. B 10, 432 (1974).
[23]J. D. Dow, D. L. Smith, and B. F. Sonntag, Phys. Rev. B 10, 3092 (1974).
[24]J. D. Dow and B. F. Sonntag, Phys. Rev. Lett. 31, 1461 (1973).
[25]J. D. Dow, L. N. Watson, and D. J. Fabian, J. Phys. F 4, L76 (1974).
[26]J. D. Dow, J. Phys. F 5, 1113 (1975).
[27]A. J. McAlister, Phys. Rev. 186, 595 (1969).
[28]J. D. Dow, J. E. Robinson, and T. R. Carver, Phys. Rev. Lett. 31, 759 (1973).
[29]H. Neddermeyer, Phys. Lett. A 44, 181 (1973).
[30]D. R. Franceschetti and J. D. Dow, J. Phys. F 4, L151 (1974).
[31]H. Neddermeyer, Phys. Rev. B 13, 2411 (1976).
[32]H. Petersen, Phys. Rev. Lett. 35, 1363 (1975).
[33]R. P. Gupta and A. J. Freeman, Phys. Rev. Lett. 36, 1194 (1976).
[34]R. P. Gupta and A. J. Freeman, Phys. Lett. A 59, 223 (1976).
[35]S. Doniach, P. M. Platzman, and J. T. Yue, Phys. Rev. B 4, 3345 (1971).
[36]S. Doniach and M. Šunjić, J. Phys. C 3, 285 (1970).
[37]P. H. Citrin, G. K. Wertheim, and Y. Baer, Phys. Rev. B 16, 4256 (1977).
[38]J. D. Dow and D. R. Franceschetti, Phys. Rev. Lett. 34, 1320 (1975).
[39]P. H. Citrin, G. K. Wertheim, and Y. Baer, Phys. Rev. Lett. 35, 885 (1975).
[40]C. Kunz, H. Petersen, and D. W. Lynch, Phys. Rev. Lett. 33, 1556 (1974).
[41]J. J. Ritsko, S. E. Schnatterly, and P. C. Gibbons, Phys. Rev. B 10, 5017 (1974).
[42]G. D. Mahan, Phys. Rev. B 11, 4814 (1975).
[43]S. G. Slusky, P. C. Gibbons, S. E. Schnatterly, and J. R. Fields, Phys. Rev. Lett. 36, 326 (1976).
[44]Y. Onodera, J. Phys. Soc. Jpn. 39, 1482 (1975).
[45]T. A. Callcott, E. T. Arakawa, and D. L. Ederer, Phys. Rev. B 18, 6622 (1978).
[46]S. G. Slusky, S. E. Schnatterly, and P. C. Gibbons, Phys. Rev. B 20, 379 (1979).
[47]Y. Baer, P. H. Citrin, and G. K. Wertheim, Phys. Rev. Lett. 37, 49 (1976).
[48]G. K. Wertheim and P. H. Citrin, in *Topics in Applied Physics*, edited by M. Cardona and L. Ley (Springer, Heidelberg, 1978), Vol. 26, p. 197.
[49]P. H. Citrin, G. K. Wertheim, and M. Schlüter, Solid State Commun. 32, 429 (1979).
[50]B. Bergersen, F. Brouers, and P. Longe, J. Phys. F 1, 945 (1971),
[51]P. Longe, Phys. Rev. B 14, 3699 (1976).
[52]G. D. Mahan, Phys. Rev. B 14, 3702 (1976).
[53]Y. Ohmura, K. Ishikawa, and Y. Mizuno, J. Phys. Soc. Jpn. 36, 370 (1974).
[54]S. M. Bose and A. J. Glick, Phys. Rev. B 17, 2073 (1978).
[55]L. Hedin, J. Phys. 39, C4-103 (1978) and references therein.
[56]U. von Barth and G. Grossman in Ref. 55 and private communication.
[57]G. W. Bryant and G. D. Mahan, Phys. Rev. B 17, 1744 (1977).
[58]W. Bambynek, B. Crasemann, R. W. Fink, H.-U. Freund, H. Mark, C. D. Swift, R. E. Price, and P. V. Rao, Rev. Mod. Phys. 44, 716 (1972).
[59]R. A. Ferrell, Phys. Rev. 186, 399 (1969).
[60]C.-O. Almbladh and P. Minnhagen, Phys. Status Solidi B 85, 135 (1978).
[61]M. H. L. Pryce, in *Phonons in Perfect Lattices and in Lattices with Point Imperfections*, edited by R. W. H. Stevenson (Oliver and Boyd, Edinburgh, 1966), p. 403.
[62]J. J. Markham, Rev. Mod. Phys. 31, 956 (1959).
[63]T. H. Keil, Phys. Rev. 140, A601 (1965).
[64]G. D. Mahan, Ref. 15, p. 107.
[65]C. P. Flynn, Phys. Rev. Lett. 37, 1445 (1975).
[66]M. Šunjić and A. Lucas, Chem. Phys. Lett. 42, 462 (1976).

[67]P. H. Citrin and D. R. Hamann, Phys. Rev. B 15, 2923 (1977).
[68]C.-O. Almbladh and P. Minnhagen, Phys. Rev. B 17, 929 (1978).
[69]G. D. Mahan, Phys. Rev. B 15, 4587 (1977).
[70]C.-O. Almbladh, Solid State Commun. 22, 339 (1977); Phys. Rev. B 16, 4343 (1977).
[71]S. Abraham-Ibrahim, B. Caroli, C. Caroli, and B. Roulet, Phys. Rev. B 18, 6702 (1978).
[72]Y. Onodera and Y. Toyozawa, J. Phys. Soc. Jpn. 22, 833 (1967).
[73]A. Kato, A. Okiji, and Y. Ôsaka, Prog. Theor. Phys. 44, 287 (1970).
[74]S. M. Girvin and J. J. Hopfield, Phys. Rev. Lett. 34, 1320 (1975).
[75]H. Kaga, J. Phys. Soc. Jpn. 43, 1144 (1977).
[76]B. S. Andereck and G. Iche, Phys. Rev. B 16, 639 (1977); A. Yoshimori and A. Okiji, *ibid.* 16, 3838 (1977).
[77]C. E. Moore, *Atomic Energy Levels*, U.S. Natl. Bur. Stand. Circ. No. 467 (U.S. GPO, Washington, D.C., 1949), Vol. 76.
[78]See, for example, J. S. Thomsen, in *X-Ray Spectroscopy*, edited by L. V. Azároff (McGraw-Hill, New York, 1974), p. 26; J. R. Cuthill, *ibid.*, p. 133.
[79]R. S. Crisp, Philos. Mag. 36, 609 (1977).
[80]T. A. Callcott, E. T. Arakawa, and D. L. Ederer, Phys. Rev. B 16, 5185 (1977).
[81]H. Neddermeyer, Z. Phys. 271, 329 (1974).
[82]M. L. Cohen and V. Heine, in *Solid State Physics*, edited by H. Ehrenreich, F. Seitz, and D. Turnbull (Academic, New York, 1970), Vol. 24, p. 37.
[83]G. Martinez, M. Schülter, and M. L. Cohen, Phys. Rev. B 11, 660 (1975).
[84]W. A. Harrison, in *Soft X-Ray Band Spectra*, edited by D. J. Fabian (Academic, New York, 1968), p. 227; N. W. Aschroft, *ibid.*, p. 249.
[85]F. Herman and S. Skillman, *Atomic Structure Calculations* (Prentice-Hall, Englewood Cliffs, N. J., 1963).
[86]M. J. G. Lee, Proc. R. Soc. A 285, 440 (1966); Phys. Rev. 178, 853 (1968).
[87]J. C. Kimball, R. W. Stark, and F. M. Mueller, Phys. Rev. 162, 600 (1967).
[88]N. W. Ashcroft, Phys. Lett. 13, 1 (1966); Philos. Mag. 8, 2055 (1963).
[89]G. Gilat and L. J. Raubenheimer, Phys. Rev. 144, 390 (1966).
[90]L. Smrčka, Czech. J. Phys. B 21, 683 (1971).
[91]G. A. Rooke, J. Phys. C 2, 767 (1968).
[92]B. Segall, Phys. Rev. 124, 1797 (1961).
[93]R. W. Shaw and N. V. Smith, Phys. Rev. 178, 985 (1969).
[94]G. D. Mahan, in *Electronic Density of States*, edited by L. H. Bennett, U. S. Natl. Bur. Stand. Spec. Publ. No. 323 (U.S. GPO, Washington, D.C., 1971), p. 253.
[95]R. P. Gupta, A. J. Freeman, and J. D. Dow, Phys. Lett. A 59, 226 (1976).
[96]C.-O. Almbladh and U. von Barth, Phys. Rev. B 13, 3307 (1976).
[97]J. D. Dow, D. L. Smith, D. R. Franceschetti, J. E. Robinson, and T. R. Carver, Phys. Rev. B 16, 4707 (1977).
[98]P. Minnhagen, Phys. Lett. A 56, 327 (1976); J. Phys. F 7, 2441 (1977).
[99]J. T. Yue and S. Doniach, Phys. Rev. B 8, 4578 (1973).
[100]Y. Ohmura and H. Sano, J. Phys. Soc. Jpn. 43, 875 (1977).
[101]C.-O. Almbladh and U. von Barth (unpublished).
[102]Assuming $\Gamma_{1s}=0.47$ eV (Lorentzian) for Al from this work and $\Gamma_{2p}\sim 0$, convolution with $\Gamma_{sp}\sim 0.13$ eV should give a measured Al $K\alpha_1(=K\alpha_2)$ width of 0.52 eV, in agreement with that measured by K. Läuger, J. Phys. Chem. Solids 32, 609 (1971) using a similar instrumental resolution.
[103]C. Kunz, R. Haensel, G. Keitel, P. Schreiber, and B. Sonntag, in Ref. 94, p. 275.
[104]T. A. Callcott, E. T. Arakawa, and D. L. Ederer, Jpn. J. Appl. Phys. (52) 17, 149 (1978).
[105]E. J. McGuire, Phys. Rev. A 2, 273 (1970).
[106]V. D. Kostroun, M. H. Chen, and B. Crasemann, Phys. Rev. A 3, 533 (1971).
[107]D. L. Walters and C. P. Bhalla, Phys. Rev. A 4, 2164 (1971).
[108]J. D. Dow and D. L. Smith, J. Phys. F 3, L170 (1973).
[109]J. H. Slowik, Phys. Rev. B 10, 416 (1974).
[110]A. J. Glick and A. L. Hagen, Phys. Rev. B 15, 1950 (1977).
[111]T. Kobayasi and A. Morita, J. Phys. Soc. Jpn. 28, 457 (1970).
[112]L. Hedin and A. Rosengren, J. Phys. F 7, 1339 (1977).
[113]A. W. Overhauser, quoted in Ref. 27.
[114]B. Bergersen, T. McMullen, and J. P. Carbotte, Can. J. Phys. 49, 3155 (1971).
[115]This figure also appeared in Ref. 48, p. 223, in which the α_0 scale was mislabeled a factor of 2 too small.
[116]C. Kunz, J. Phys. (Paris) 10, C4-180 (1971).
[117]B. Bergersen, P. Jena, and T. McMullen, J. Phys. F 4, L219 (1974).
[118]J. D. Dow, quoted in Ref. 40.
[119]S. E. Schnatterly, Comments Solid State Phys. 7, 99 (1976).
[120]In Ref. 97, Dow *et al.* maintain that exclusion of α_2 in their analysis does not change their value of $\alpha_0=0.15$ within their quoted error limits of ± 0.04. Although our analysis confirms this to be the case, we have found (see Sec. IIB) that such large limits effectively preclude meaningful testing of the MND theory's quantitative predictiveness.
[121]J. D. Dow, quoted in Ref. 45.
[122]In Ref. 104, M. A. Kolber and J. D. Dow are quoted as having extended the theory of Onodera, Ref. 44, to include an energy dependent exchange interaction.
[123]The authors of Ref. 57 discuss the unreliability of their results for Na, while the authors of Ref. 74 cite theirs for Na as being in significant disagreement with the XPS measurements. The authors of Ref. 100, as those of Refs. 57 and 74, calculate *d* phase shifts which are too large (e.g., they are comparable to those calculated in Ref. 100 for Mg).
[124]H. Petersen and C. Kunz, Phys. Rev. Lett. 35, 863 (1975).
[125]In Refs. 37 and 48 a similar plot of α vs r_s appeared mislabeled with the reversed ordering of Na, Mg, and Al.
[126]G. W. Bryant, Phys. Rev. B 19, 2801 (1979).
[127]T. Ishii, Y. Sakisaka, S. Yamaguchi, T. Hanyu, and H. Ishii, J. Phys. Soc. Jpn. 42, 876 (1977).
[128]L. Ley, F. R. McFeely, S. P. Kowalczyk, J. G. Jenkin, and D. A. Shirley, Phys. Rev. B 11, 600 (1975).

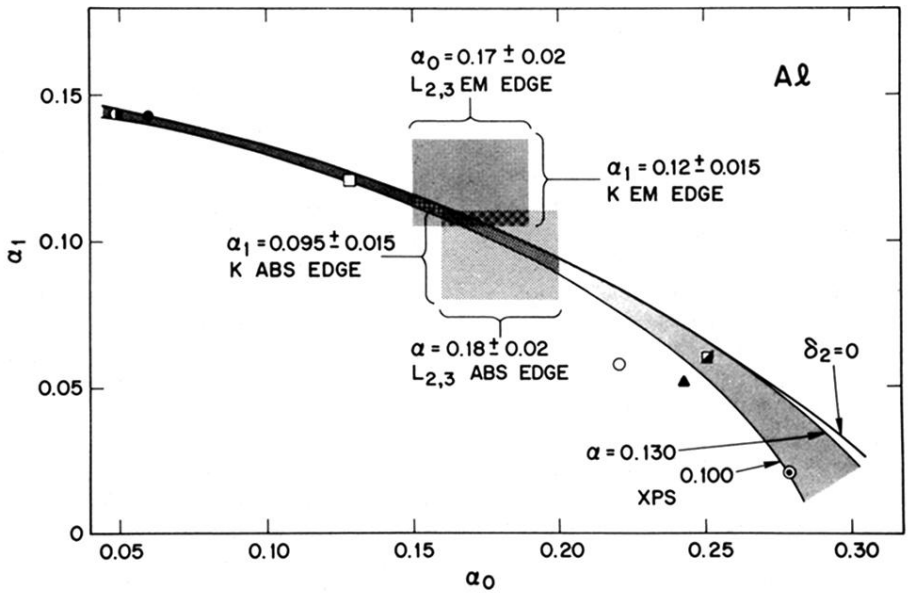

FIG. 20. Compatibility plot using three phase shifts for Al relating threshold exponents α_0 and α_1 with singularity index α. Range of compatibility indicated by intersection of α_0 and α_1 values (this work) and α values (Ref. 37). Solutions above $\delta_2 = 0$ contour are unphysical. Note that all five independent experiments are described by common set of compatible phase shifts. Solid and half-filled circles correspond to calculations of Almbladh and von Barth, Ref. 96, for L and K holes, respectively; open square to calculations of Bryant and Mahan, Ref. 57; filled triangle to Mahan, Ref. 42; half-filled square to Minnhagen, Ref. 98; open and dotted circles to Ohmura and Sano, Ref. 100, for L and K holes, respectively. EM: emission, ABS: absorption.